

**IZMIR KATIP CELEBI UNIVERSITY
GRADUATE SCHOOL OF NATURAL AND APPLIED
SCIENCES**

**EVALUATING STEADY-STATE VISUALLY-EVOKED
POTENTIALS USING ENSEMBLE LEARNING METHODS**

**PhD THESIS
Ebru SAYILGAN**

Department of Biomedical Technologies

**Thesis Advisor: Assoc. Prof. Dr. Yalcin ISLER
Thesis Co-Advisor: Assist. Prof. Dr. Yilmaz Kemal YUCE**

AUGUST 2020

**IZMIR KATIP CELEBI UNIVERSITY
GRADUATE SCHOOL OF NATURAL AND APPLIED
SCIENCES**

**EVALUATING STEADY-STATE VISUALLY-EVOKED
POTENTIALS USING ENSEMBLE LEARNING METHODS**

PhD THESIS

Ebru SAYILGAN

(D160203002)

ORCID: 0000-0001-5059-3201

Department of Biomedical Technologies

Thesis Advisor: Assoc. Prof. Dr. Yalcin ISLER

Thesis Co-Advisor: Assist. Prof. Dr. Yilmaz Kemal YUCE

AUGUST 2020

İZMİR KATİP ÇELEBİ ÜNİVERSİTESİ
FEN BİLİMLERİ ENSTİTÜSÜ

DURAĞAN HAL GÖRSEL UYARILMIŞ POTANSİYELLERİN
TOPLULUK ÖĞRENMESİ YÖNTEMLERİYLE
DEĞERLENDİRİLMESİ

DOKTORA TEZİ

Ebru SAYILGAN

(D160203002)

ORCID: 0000-0001-5059-3201

Biyomedikal Teknolojiler Ana Bilim Dalı

Tez Danışmanı: Doç. Dr. Yalçın İŞLER

Tez Eş Danışmanı: Dr. Öğr. Üyesi Yılmaz Kemal YÜCE

AĞUSTOS 2020

Ebru SAYILGAN, a **PhD** student of **IKCU Graduate School Of Natural And Applied Sciences**, successfully defended the thesis entitled “**EVALUATING STEADY-STATE VISUALLY-EVOKED POTENTIALS USING ENSEMBLE LEARNING METHODS**”, which she prepared after fulfilling the requirements specified in the associated legislations, before the jury whose signatures are below.

Thesis Advisor:

Assoc. Prof. Dr. Yalcin ISLER
Izmir Katip Celebi University

Thesis Co-Advisor:

Assist. Prof. Dr. Yilmaz Kemal YUCE
Alanya Alaaddin Keykubat University

Jury Members:

Assoc. Prof. Dr. Erkin GEZGIN
Izmir Katip Celebi University

Assoc. Prof. Dr. Savaş SAHİN
Izmir Katip Celebi University

Assist. Prof. Dr. Nalan OZKURT
Yasar University

Assist. Prof. Dr. Mustafa Berkant SELEK
Ege University

Date of Defense : 17.08.2020

To my family

FOREWORD

First and foremost, I am sincerely thankful to my Ph.D. supervisor Assoc. Prof. Dr. Yalcin Isler, for his support, supervision, patience, and critical scientific insights, guide me to the completion of this dissertation. Whenever I lost track of how to proceed, he ordered useful recommendations. Besides this, he emboldened me to widen my horizon. I am lucky to have Assoc. Prof. Dr. Yalcin Isler as my advisor.

I am also grateful to my worthy co-advisor Yilmaz Kemal Yuce, for his valuable advice and support.

Finally, I would like to thank you from the deep of my heart to my whole family. Thanks to their trust in me and their endless support. I dedicate my dissertation to them. They deserve to read my appreciation in Turkish:

“Hayattaki en değerli varlıklarım olan canım ailem,

Doktora eğitimimin sonuna geldim ve tezimi tamamlayarak umuyorum ki mutlu son ve başlangıçlarım olacak. Sizin bana verdiğiniz emeklerin, desteğin ve sonsuz sevginin hakkını kesinlikle ödeyemem ama tezimi size ithaf edebilirim. Her zaman yanımda olduğunuz için çok teşekkür ederim. Hepinizi çok seviyorum.

Kızınız, Kardeşiniz, Eşin, Annen,

Ebru”.

August 2020

Ebru SAYILGAN

TABLE OF CONTENTS

	<u>Page</u>
FOREWORD.....	vi
TABLE OF CONTENTS.....	vii
LIST OF TABLES	ix
LIST OF FIGURES	x
ABBREVIATIONS	xiii
ABSTRACT	xv
ÖZET.....	xvi
1. INTRODUCTION.....	1
1.1 Problem Statement	4
1.2 Motivation	8
1.3 Hypothesis	8
1.4 Objectives of the Thesis	9
1.5 Contributions of the Thesis	10
1.6 Organization of the Thesis	10
2. OVERVIEW OF BRAIN COMPUTER INTERFACE.....	13
2.1 Brain Architecture	14
2.2 Components of Brain Computer Interface	17
2.3 Brain Computer Interface Classifications	19
2.3.1 Synchronous and asynchronous (self-paced) Brain Computer Interface	19
2.3.2 Dependent and independent Brain Computer Interface	20
2.3.3 Invasive and non-invasive Brain Computer Interface	20
2.4 Neuroimaging Methods of Brain Computer Interface	21
2.4.1 Intra-cortical	21
2.4.2 Electrocorticography (ECoG)	22
2.4.3 Magnetoencephalography (MEG).....	22
2.4.4 Functional magnetic resonance imaging (fMRI)	23
2.4.5 Functional near-infrared spectroscopy (fNIRS).....	23
2.4.6 Positron emission tomography (PET)	23
2.4.7 Electroencephalography (EEG).....	24
2.5 Control Signals Types in Brain Computer Interfaces	25
2.5.1 Spontaneous signals	26
2.5.1.1 Sensorimotor rhythms (SMRs).....	26
2.5.1.2 Slow cortical potentials (SCPs).....	27
2.5.1.3 Non-motor cognitive signals	28
2.5.2 Hybrid Signals.....	28
2.5.3 Evoked Potentials.....	28
2.5.3.1 P300 signals.....	29
2.5.3.2 Visual Evoked Potentials (VEPs).....	29
2.6 Steady-State Visual Evoked Potential (SSVEP) Based BCI.....	33

2.6.1	Vision physiology	35
2.6.2	Visual stimulus.....	38
2.6.3	Signal acquisition and preprocessing	42
2.6.4	Feature extractions	43
2.6.4.1	Temporal methods	44
2.6.4.2	Frequential methods	44
2.6.4.3	Time-frequency representations	45
2.6.4.4	Other feature extraction methods	45
2.6.5	Classification.....	46
2.6.6	Evaluation of classification	46
3.	MATERIAL AND METHODS.....	49
3.1	Data Set Description and Preprocessing	49
3.2	Feature Extraction	51
3.2.1	Time-domain based feature extraction.....	51
3.2.2	Frequency-domain based feature extraction	54
3.2.3	Wavelet transform based feature extraction.....	55
3.2.3.1	Wavelet decomposition	57
3.2.3.2	Parameters for feature extraction.....	59
3.3	Feature Selection with Statistical Evidence of ANOVA	60
3.4	Machine Learning Classification Algorithms	61
3.4.1	Decision trees	62
3.4.2	Discriminant analysis	63
3.4.3	Logistic regression	64
3.4.4	Support vector machines (SVM).....	65
3.4.5	K-nearest neighbor classifier (KNN)	66
3.4.6	Naive bayes classifier.....	67
3.4.7	Ensemble learning	68
3.5	Evaluation of Machine Learning Algorithms.....	71
3.5.1	k-fold cross-validation.....	71
3.5.2	Confusion matrix.....	72
4.	RESULTS AND DISCUSSION.....	73
4.1	Time-domain Features Results	73
4.1.1	Multiple classification results.....	73
4.1.2	Binary classification results	74
4.2	Frequency-domain Features Results	78
4.2.1	Multiple classification results.....	78
4.2.2	Selected three class classification results	79
4.2.3	Binary classification results	81
4.3	Wavelet Transform Features Results	85
4.3.1	Multiple classification results (for 8 frequencies).....	85
4.3.2	Multiple classification results (for 7 frequencies).....	92
4.3.3	Classification results for three selected frequencies	93
4.3.4	Binary classification results	100
5.	CONCLUSION.....	114
	REFERENCES.....	117
	CURRICULUM VITAE.....	128

LIST OF TABLES

	<u>Page</u>
Table 1.1 Studies in the literature comparing the EEG signal for different mother wavelets.....	5
Table 2.1 Brain rhythms with their frequency ranges and characteristics.	17
Table 2.2 Comparison of neuroimaging methods	25
Table 2.3 Characteristics of VEP modulations	32
Table 2.4 Control signals summary.....	33
Table 3.1 List of participants for single target flickering (Male (M), Female (F)) ...	50
Table 3.2 EEG time-domain features (EEG signal is represented by x , and $F_i^{(t)}$ stands for the EEG features computed from x).....	52
Table 3.3 Wavelet families in the literature used for mother wavelet comparisons of the EEG signal.....	56
Table 3.4 Wavelet families used in this study	57
Table 3.5 Speed and memory value definitions of classifiers	70
Table 3.6 Confusion matrix	72
Table 4.1 Results of multiple classification for time-domain features.....	74
Table 4.2 Results of classification performances in terms of classifiers for time-domain features	76
Table 4.3 Results of multiple classification for frequency-domain features.....	79
Table 4.4 Results of classification performances in terms of classifiers for frequency-domain features.....	83
Table 4.5 Normality test results of features extracted from SSVEP data	86
Table 4.6 Variance homogeneity test of normally distributed data.....	86
Table 4.7 Selected features from EEG frequency bands. The selected features via significance values ($p \leq 0,05$) obtained by ANOVA are indicated by “✓”.....	87
Table 4.8 Multiple classification results of wavelet transform features before the feature selection. (for 8 frequencies).....	88
Table 4.9 Multiple classification results of wavelet transform features after the feature selection. (for 8 frequencies).....	90
Table 4.10 Average success of classifiers before and after feature selection (*).....	91
Table 4.11 Multiple classification results of wavelet transform features (for 7 frequencies).....	92
Table 4.12 Classification performance of energy, entropy, and variance as separate features for selected three frequencies	96
Table 4.13 Classification performance of energy, entropy, and variance as a feature set for selected three frequencies	99
Table 4.14 Classification results of the most successful frequency pairs of the Haar mother wavelet.....	108
Table 4.15 Classification performance of energy, entropy, and variance as a feature set (All features together) for Haar wavelet.....	112

LIST OF FIGURES

	<u>Page</u>
Figure 1.1 Fundamental components of communications	1
Figure 1.2 Chronological development of the thesis indicating objectives and achieved contributions	12
Figure 2.1 Functional areas of the cerebral cortex [78]..	16
Figure 2.2 Components of BCI	18
Figure 2.3 Classification of BCI systems	19
Figure 2.4 Types of neuroimaging methods	21
Figure 2.5 International 10-20 electrode layout [93]	24
Figure 2.6 Classification of control signals.....	26
Figure 2.7 Independent stimulus sequences of the targets of a t-VEP based BCI. b) A single t-VEP response [102].....	30
Figure 2.8 Stimulation sequences of the targets of c-VEP based BCI [102]. a) Target sequences of a stimulation cycle. b) A waveform of the evoked response.....	31
Figure 2.9 a) Stimulating sequences of targets of f-VEP based BCI (SSVEP based BCI) [102]. b) Power spectrum of the evoked frequency at a frequency of 10 Hz ...	32
Figure 2.10 a) SSVEP raw signal b) Power spectrum of the 10 Hz stimulated SSVEP signal	34
Figure 2.11 a) Human eye structure b) Location of the fovea [127].....	36
Figure 2.12 Different stimuli (color, pattern, size) designed to generate SSVEP responses [124].....	38
Figure 2.13 Main colors used in stimulus design [124]	39
Figure 2.14 Simple stimulus examples used for visual stimulus design [110]	40
Figure 2.15 The complex stimulus designed for the SSVEP response is a) initial version b) inverted version [110] c) 4 x 4 dimension and d) 2 x 2 dimension [124].	40
Figure 2.16 Feature extraction methods.....	44
Figure 3.1 Electrode placement throughout experiments using 10-20 system (left), and electrodes used in this study (right) [149]	49
Figure 3.2 Hardware installation for experiments [149]	50
Figure 3.3 Components of wavelet coefficients and decomposition of subbands for 512 Hz sampling frequency	58
Figure 3.4 Relationship between DWT frequency bands and EEG rhythms.....	59
Figure 3.5 Basic structure of a decision tree classifier.....	63
Figure 3.6 Linear vs. quadratic discriminant analysis classifiers.....	64
Figure 3.7 Logistic regression model.....	65
Figure 3.8 Model of SVM algorithm	66
Figure 3.9 KNN step-by-step running scheme.....	67
Figure 3.10 The basic model of ensemble learning classification	69

Figure 3.11 Summary and some important properties of classifiers used in this thesis.....	70
Figure 3.12 k-fold cross-validation model used in the classification of this study with k=5	71
Figure 4.1 Binary classification performance of the time-domain features.....	75
Figure 4.2 Three selected frequencies (6Hz - 8.2Hz - 10 Hz) among the seven frequencies	79
Figure 4.3 Results of selected 3-class classifications for frequency-domain features	80
Figure 4.4 Binary classification performance of the frequency-domain features	82
Figure 4.5 Classification performance of energy, entropy, and variance as separate features	94
Figure 4.6 Classification performance of energy, entropy, and variance together as a feature set	95
Figure 4.7 Percentage of classifier where the best result is the most often obtained as a result of running the algorithms 240 times in total. (Energy, entropy, and variance as separate features)	98
Figure 4.8 Percentage of classifier where the best result is the most often obtained as a result of running the algorithms 240 times in total. (Energy, entropy, and variance as a feature set).....	100
Figure 4.9 Binary classification performance of the features for Bior 3.5 mother wavelet function	102
Figure 4.10 Binary classification performance of the features for Coif 1 mother wavelet function	103
Figure 4.11 Binary classification performance of the features for Db 4 mother wavelet function	104
Figure 4.12 Binary classification performance of the features for Haar mother wavelet function	105
Figure 4.13 Binary classification performance of the features for Rbio 2.8 mother wavelet function	106
Figure 4.14 Binary classification performance of the features for Sym 4 mother wavelet function	107
Figure 4.15 Change of accuracy value according to the differences between frequencies for Bior 3.5 mother wavelet.....	108
Figure 4.16 Change of accuracy value according to the differences between frequencies for Coif 1 mother wavelet.....	109
Figure 4.17 Change of accuracy value according to the differences between frequencies for Db 4 mother wavelet	109
Figure 4.18 Change of accuracy value according to the differences between frequencies for Haar mother wavelet	110
Figure 4.19 Change of accuracy value according to the differences between frequencies for Rbio 2.8 mother wavelet	110
Figure 4.20 Change of accuracy value according to the differences between frequencies for Sym 4 mother wavelet.....	111

Figure 4.21 Percentage of classifier where the best result is the most often obtained as a result of running the algorithms 240 times in total. (Energy, entropy, and variance as a feature set) 113

ABBREVIATIONS

ALS	: Amyotrophic Lateral Sclerosis
BCI	: Brain-Computer Interface
CMT	: Charcot-Marie-Tooth
CRT	: Cathode Ray Tube
CV	: Cross-validation
CWT	: Continuous Wavelet Transform
DWT	: Discrete Wavelet Transform
ECG	: Electrocardiography
ECoG	: Electrocorticography
EEG	: Electroencephalography
EMG	: Electromyography
EOG	: Electrooculography
EP	: Evoked Potential
ERD	: Event-Related Desynchronization
ERP	: Event-Related Potentials
ERS	: Event-Related Synchronization
FFT	: Fast Fourier Transform
fMRI	: Functional Magnetic Resonance Imaging
fNIRS	: Functional Near-Infrared Spectroscopy
HMI	: Human-Machine Interface
HRV	: Heart Rate Variability
ITR	: Information Transfer Rate
KNN	: K-Nearest Neighbor
LCD	: Liquid Crystal Display
LDA	: Linear Discriminant Analysis
LED	: Light Emitting Diodes
MEG	: Magnetoencephalography
PET	: Positron Emission Tomography
QDA	: Quadratic Discriminant Analysis
RBF	: Radial Basic Function
SCP	: Slow Cortical Potentials
SMR	: Sensorimotor Rhythm

SNR	: Signal to Noise Ratio
SSVEP	: Steady-State Visual Evoked Potential
SVM	: Support Vector Machines
VEP	: Visual Evoked Potential
WT	: Wavelet Transform

EVALUATING STEADY-STATE VISUALLY-EVOKED POTENTIALS USING ENSEMBLE LEARNING METHODS

ABSTRACT

Steady-state visual evoked potentials (SSVEPs) have been designated to be appropriate and useful for many areas in clinical neuroscience, cognitive, and in engineering. SSVEPs have become popular recently, due to their advantages such as high bit rate, simple system structure, and short training time, etc. To design SSVEP based BCI system, signal processing methods appropriate to the signal structure should be applied. One of the most appropriate signal processing methods of these non-stationary signals is the Wavelet Transform. After literature searched, we noticed that there was no study on the mother wavelet type selection by applying Discrete Wavelet Transform of SSVEP signals.

SSVEP signal were recorded at seven different stimulus frequencies (6 – 6.5 – 7 – 7.5 – 8.2 – 9.3 – 10 Hz). A total of 115 features were extracted: time-domain, frequency-domain and time-frequency domain. These features were classified by a total of 25 different classification processes. Classification evaluation was presented with the 5-fold cross-validation method and accuracy values obtained from the confusion matrix.

According to the results, (I) the most successful wavelet function was Haar wavelet, and (II) the most successful classifier was Ensemble Learning classifier. (III) Instead of the energy, entropy, and variance features were used alone, the feature vector, which was a feature set, gave better results. (IV) As a result of the feature selection made with the one-way ANOVA test, it reduces the classification accuracy. (V) By conducting detailed research on stimulation frequencies, the highest performances were obtained in the frequency pairs with "6-10", "6.5-10", "7-10", and "7.5-10" Hz.

DURAĞAN HAL GÖRSEL UYARILMIŞ POTANSİYELLERİN TOPLULUK ÖĞRENMESİ YÖNTEMLERİYLE DEĞERLENDİRİLMESİ

ÖZET

Durağan Durum Görsel Uyarılmış Potansiyeller (DDGUP), klinik sinirbilim, bilişsel ve mühendislikteki birçok alan için uygun ve yararlı olarak belirlenmiştir. DDGUP yüksek bilgi aktarım hızı, basit sistem yapısı ve kısa eğitim süresi gibi avantajları nedeniyle son zamanlarda popüler hale gelmiştir. DDGUP tabanlı BBA sisteminin tasarımı için sinyal yapısına uygun sinyal işleme yöntemleri uygulanmalıdır. Bu sabit olmayan sinyallerin en uygun sinyal işleme yöntemlerinden biri Dalgacık Dönüşümüdür. Literatür araştırmasından sonra, DDGUP sinyallerine Ayrık Dalgacık Dönüşümü uygulanarak, ana dalgacık tipi seçimi üzerinde bir çalışma olmadığını tespit edildi.

DDGUP sinyalleri yedi farklı uyaran frekansında (6 – 6,5 - 7 – 7,5 – 8,2 – 9,3 – 10 Hz) kaydedilmiştir. Zaman alanı, frekans alanı ve zaman-frekans alanı olmak üzere toplamda 115 öznitelik çıkarılmıştır. Bu öznitelikler, yedi temel makine öğrenme algoritmasının alt parametreleri nedeniyle toplam 25 farklı sınıflandırma sürecine göre sınıflandırılmıştır. Sınıflandırma değerlendirmesi, 5-kat çapraz validasyon yöntemi ve hata matrisinden elde edilen doğruluk değerleri ile sunulmuştur.

Elde edilen sonuçlara göre, (I) en başarılı dalgacık fonksiyonu Haar dalgacığı olarak ve (II) en başarılı sınıflandırıcı Topluluk Öğrenimi sınıflandırıcısı olarak elde edilmiştir. (III) Tek başına kullanılan enerji, entropi ve varyans öznitelikleri yerine, bir öznitelik kümesi olan öznitelik vektörü daha iyi sonuçlar vermiştir. (IV) Tek yönlü ANOVA testi ile yapılan öznitelik seçimi sonucunda, sınıflandırma doğruluğunu azalttığı görülmüştür. (V) Stimülasyon frekansları hakkında ayrıntılı araştırmalar yapıldığında, en yüksek performanslar "6-10", "6,5-10", "7-10" ve "7,5-10" Hz frekans çiftlerinde elde edilmiştir.

1. INTRODUCTION

The concept of communication is an essential focus for different fields. Such as linguistics, ethology, cell biology, computer science, biomedical engineering, genetic engineering, sociology, anthropology, philosophy, semiotics, and literary theory, and each uses the term uniquely. The communication, another definition of information transfer [1], can be realized in different ways. The connection has been used in many ways and so many contexts that it means almost everything for all living things. So what is the communication that has a great place, and importance in our lives, and has been developing for centuries? The connection can be expressed as the transfer of emotions, thoughts, and information from one place to another [1]. Figure 1 shows the essential components of communication.

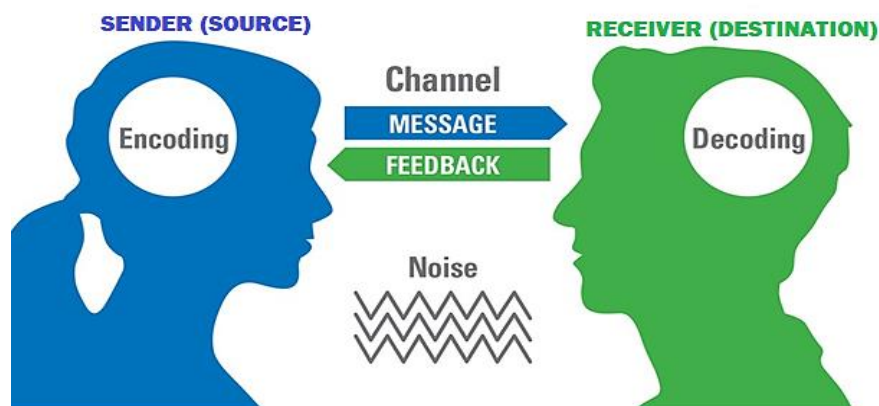


Figure 1.1 Fundamental components of communications.

These components can be briefly described as follows [2]:

Sender (Source): The sender is the subject who creates the message and transmits it to the other party through a channel.

Receiver (Destination): The subject or group to whom the message is intended to be delivered is the recipient component in communication.

Message: The message is the information that the sender wants to transmit to the destination or receiver. And here, not only words but also everything used to describe an emotion thought to express the message.

Channel (Sending Format): The way the message reaches the destination from the source is the channel. Channel; There may be tools such as speech, writing, numbers, body language movements, and even thoughts taken with brain signals, i.e., biosignals.

Since bio-signals are a natural and spontaneous form of communication, they are an excellent option, especially for people who cannot communicate in traditional ways. For many years now, people have been thinking that electrophysiological measurements of brain function can provide a channel that does not need the muscular system to send messages or commands to the outside world [3], and are researching for it. Over the last 25 years, productive human-machine interface (HMI) research programs or applications have emerged [4, 5]. Our focus is on improving communication and control technologies that address the needs and potentials of people with neuromuscular disorders (Amyotrophic lateral sclerosis (ALS), multiple sclerosis, brainstem stroke, Charcot-Marie-Tooth (CMT) and spinal cord injury, etc.). By understanding the function of the brain, robust and low-cost computer equipment emerged. The primary purpose of the existing systems in the literature is to provide word processing programs, or neuroprosthesis to express their wishes for these users who are entirely or semi-paralyzed [3-16].

For HMI applications, different types of biomedical signals including electrooculography (EOG), electromyography (EMG), electrocardiography (ECG) and electroencephalography (EEG) or a mix of them have been used since these signals can be acquired more quickly by comparing to other types of signals [5, 16]. Besides, only brain activities are used as input signals of the support system frequently in cases of limited use of people's eye and muscle activities or not working at all. This type of HMI systems is called the brain-computer interface (BCI) [10, 14-16]. Communication with this technology occurs roughly as follows: biomedical signals of temporal resolution produced by neuronal dynamics from the scalp are received and recorded [3, 12]. The properties of the recorded brain signals

are extracted, and these properties are converted to outputs, commands, scripts, or similar applications in the real world [3-16].

Various methods are available to monitor brain activity [4]. These include electrocorticography (ECoG), intra-cortical, EEG, functional magnetic resonance imaging (fMRI), magnetoencephalography (MEG), positron emission tomography (PET), and optical imaging. However, intra-cortical, ECoG, fMRI, PET, MEG, and optical imaging are not preferred because they are technically challenging, more invasive, and expensive [4, 6, 10, 11]. Also, fMRI, PET, and optical imaging methods, which depend on blood flow, are less suitable for fast communication as they take a long time [4]. Among these monitoring methods, only EEG methods offer a practical BCI possibility. It is relatively non-invasive to other methods, requires a short time, is workable in most environments, and has the advantages of more straightforward and cheaper equipment [4, 5, 10].

Commonly used control signals in EEG-based BCIs are slow cortical potentials (SCP), sensorimotor rhythms (μ and β rhythms), event-related potentials (ERP), event-related synchronization (ERS) and desynchronization (ERD), and visual evoked potentials (VEP) [14, 15, 17-19]. VEP-based BCI is considered to be a dependent BCI, unlike other systems [20]. Because the production of VEP depends on the control of the outflow pathways and eye movements of the cranial nerves and extraocular muscles, therefore, this method cannot be applied to a small number of people with severe neuromuscular barriers that may lack the exit channel of extraocular muscle control. However, for most people, VEP-based BCI is more suitable than other systems. It has advantages such as high information transfer rate (ITR), simple system structure, short user training, and short time requirement [20-23]. Apart from these, the eye muscles' health is sufficient for the user to use this system.

VEPs are the brain's response to visual stimulation [20, 21]. They reflect the visual information processing mechanism in the brain. VEPs that appear with short stimuli are usually transient responses of the optical system [22]. Transient evoked potentials are the responses of the system under study to sudden changes in the input [23, 24].

Approximately 60 years ago, Regan began experimenting with long stimulus trains. This stimuli produced a stable VEP of small amplitude, which can be extracted by averaging over multiple trials, and these EEG waves were named as "Steady-State" Visually Evoked Potentials (SSVEPs) of the visual system [25-29].

SSVEP is a resonance phenomenon that occurs mainly in the visual cortex when an individual's visual attention focuses on a light source that flickers with a frequency above 6 Hz [20, 22]. Also, SSVEP consists of a periodic component of the same frequency as the flickering light source, likewise of many harmonic frequencies [26, 27]. Since SSVEP is an intrinsic neuronal response relatively independent of higher-level cognitive processes, it is widely used to study low-level processing in the brain and perform clinical assessments of visual pathways [20, 22, 29, 30]. SSVEP could be recorded on the visual cortex from the scalp with maximum amplitude in the occipital region [24-27, 29]. The interest in SSVEP based BCI studies is mainly owing to the robustness of the SSVEP phenomenon.

1.1 Problem Statement

The analysis of EEG signals using machine learning methods is developed for precise diagnosis to doctors and provides fast and accurate tools in assistive applications designed for individuals. Among the various approaches available in the literature, the Wavelet Transform (WT) has proven to be an effective time-frequency analysis tool for analyzing transient signals [31-49]. Feature extraction and classification from SSVEP signal processing stages are used to evaluate various transient events in biological signals. Various wavelet families are available to define and adapt signal characteristics. However, choosing an appropriate mother wavelet is very important for the analysis of these signals. There are studies comparing different mother wavelet types for ECG [49, 50, 51], EMG [49, 51], EEG [31-49] and SSVEP [32, 37]. Research studies to date for EEG-signal classification using the wavelet technique have mostly been done using the Daubechies (Db) family. Besides, there is only one study in the literature, although the SSVEP-based BCI study designed using wavelet families is almost nonexistent. The maximum accuracy achieved in this study is 95.00% [32]. However, in this study, although the signal is suitable for Discrete Wavelet Transformation (DWT), it has made analysis using the Continuous

Wavelet Transformation (CWT) method. Also, in reference [37], the SSVEP signal was used for a single wavelet type (Db40), but no mother wavelet selection was made. Thus, the mother wavelet selection for SSVEP is still an unanswered question. In the same study, analyzes were made for a single frequency. In this thesis, a detailed analysis was performed using multiple frequencies.

Table 1.1 Studies in the literature comparing the EEG signal for different mother wavelets.

WAVELET FAMILY	TASKS	CLASSIFIER	SUCCESSFUL WAVELET	NUMBER OF COMMANDS	REF.
Db2, Db4, Sym4, Sym5	Left- and right-hand movement and also forward imagery used for analysis	Bayes Net, SVM, RBFN	Sym4	3	[31]
Cmor, Mey, Mex Hat, Bior	Users in this study are required to gaze at one stimulus according to his or her control intention	SVM	Cmor	1	[32]
Db, Haar, Bior	This study is aimed at image compression of the gray scale	–	Db	–	[33]
Db4	BCI system is recognizing isolated spoken words	MLP	Db4	–	[34]
Haar, Db (2–10), Coif (1–10), Bior (1.1, 2.4, 3.5, 4.4)	EEGs belong to both normal and abnormal (epileptic) signals	Probabilistic Neural Network (PNN), SVM	Coif1	2	[35]
Haar	This study purposed controlling cursor movements for ALS patients	MLP, PNN (RBF), SVM	Haar	2	[36]
Db40	It is intended to control the movement of a small ball	Fisher Classifier	Db40		[37]
Db10, Db7, Sym7	Graz data set II-B was analyzed on a two-class data set for motor imagery - Left and right hand	Hidden Markov Model	Db10	4	[38]
Mor	This study is aimed to compare two signals for decoding finger movements	LDA	Mor	2	[39]

Table 1.1 Studies in the literature comparing the EEG signal for different mother wavelets. **Continued, page 2 of 3.**

WAVELET FAMILY	TASKS	CLASSIFIER	SUCCESSFUL WAVELET	NUMBER OF COMMANDS	REF.
Db6	Study aims at analyzing and classifying the eye blinks obtained from EEG signals for control applications	k-NN and ANN	Db6	2	[40]
Db (2-20), Sym(2-20), Coif(1-5)	Carried out three experimental runs of imagining the motion (both fists and / or both feet) for classification	NN	Coif4	2	[41]
Sym (4 and 10), Coif (2 and 4), Db (2 and 6)	The used dataset in this study is BCI-IIIa from the BCI competition 2005	k-NN, SVM, AdaBoost	Db2	2	[42]
Haar, Db (2-20), Sym(2-8), Coif (1-5)	In this study, a speech recognition system has been developed to recognize speaker in isolated words spoken in Malayalam independently	MLP	Db4	4	[43]
Db (2 and 8), Bior(1.5 and 2.8), Haar	Classification of EEG signals obtained from normal, interictal, and seizure people	SVM	Bior2.8	—	[44]
Bior3.7, Coif5, Db8, Haar, Sym18,	Analyzed data in this study consists of 20 numbers of normal meditators and 20 non-meditators	The Pearson correlation coefficient	Db8	3	[45]
Db4, Sym4, Cmor3-3, Haar	The time-frequency images of three (C3, Cz, C4) channels used to extract feature of motor imagery, it is known as dataset III from BCI competition II	CNN	Cmor 3-3	2	[46]
Haar, Coif1, Bior 6.8, Rbior6.8, Db2, Db4	Four different mental tasks used for EEG classification problem	ANN	Coif1	4	[47]

Table 1.1 Studies in the literature comparing the EEG signal for different mother wavelets. **Continued, page 3 of 3.**

WAVELET FAMILY	TASKS	CLASSIFIER	SUCCESSFUL WAVELET	NUMBER OF COMMANDS	REF.
Bior2.2, Coif2, Db8, DMeyer2, Haar, Rbior2.2, Sym2	This study includes a mask image displaying the osseous information and a digital subtraction angiography image containing the vascular details to test the performance of various wavelet families	–	Db8	4	[48]
Db (1-15), Sym(1-15), Bior(1.1-6.8), Rbio(1.1-6.8)	Six different data sets were used. These include two EEG, EMG and ECG data. The study aimed to evaluation the performance of an adaptive selection algorithm for the mother wavelet selection	–	Db8	–	[49]

When a wavelet transform is applied to any pattern recognition system, a feature or features must first be extracted for it [53]. Thus, energy and/or entropy and/or variance are calculated by heart rate variability (HRV) [54-57], ECG [58, 59], EMG [60, 61], EOG [62, 63], EEG [64-68], SSVEP [68-70]. However, in most of these studies, all of these features are used together. When the mathematical formulas are examined, which of these similar features might be more successful or their superiority to each other has not been discussed before. Besides, in these studies summarized in the table above, examined in the literature, these features have never been used before. This presented thesis aims at filling this lack.

The research presented in this thesis is especially about selecting the most suitable wavelet function for signal analysis of SSVEP signals, detailed investigation of energy, entropy, and variance attributes, and examining the appropriate frequency(s) for SSVEP based BCI design.

There is also no in-depth study on the selection of stimulation frequencies. It was thought that higher accuracy rates would be obtained for pattern recognition by examining the frequency selection and the differences between the frequencies. The frequency or frequencies that give the best results are thought to help design a user-

friendly BCI system by providing higher accuracy rates and time advantages. Due to the shortcomings in the literature mentioned above, this study was considered to be conducted.

1.2 Motivation

There are two situations in which I am particularly motivated when doing this study:

My first source of motivation was my grandmother, although she did not get ALS disease at an early age, she suffered for a long time. She had a hard time, both physically and psychologically. Life was very difficult for her since we did not have an easily accessible (affordable, portable, and user-friendly) BCI technology at that time and even today.

Another motivation is the biography of the famous scientist Prof. Dr. Stephen Hawking, whose life energy should be a model for everyone. Despite his illness, he embraced science and life more tightly. Using different interfaces to communicate with the outside world, physicist Prof. Dr. Stephen Hawking has a exceptional early-onset and slow-moving ALS form. This form is known as motor neuron disease, which has been slowly paralyzed over the years. Prof. Dr. Stephen Hawking used a communication channel, a state-of-the-art application, consisting of a cheek muscle dependent to a speech-producing device. Prof. Hawking is a famous model that motivates developing these and similar technologies that help mentally healthy people.

1.3 Hypothesis

In general, the main problem of BCI systems is that they require high accuracy and custom-designed systems that can be customized easily. When it comes to SSVEP based BCI design, it is crucial to meet these criteria with the minimum channel, frequency, and classifier. These components are vital in terms of both time and system accuracy, easy applicability, and comfort.

In this thesis, it is aimed to design the SSVEP-based BCI system with the features listed above and a hypothesis, including the following steps is established:

- Using SSVEP signals from a single channel (since the most prosperous region in the visual cortex in the occipital lobe, it will be time-consuming to examine others)
- Analysis with the most appropriate feature extraction method for signal type (between time domain, frequency domain, and time-frequency domain),
- What would be the results of the frequencies and classifiers tested in this case?
- At the same time, what would be the results if the ones that gave maximum accuracy in the classification techniques with multiple, triple (with maximum difference frequencies) and binary classification?
- And finally, does system performance increase as the difference between frequencies increases?

Based on this hypothesis, analyzes and evaluations were made.

1.4 Objectives of the Thesis

The study presented in this thesis aimed to achieve significant optimization of cortical visual responses, signal processing methods, and machine learning algorithms, as well as the accuracy and reliability of the superior multi-command SSVEP-based BCI system, which is lacking in the literature. New approaches have been explored using existing methods to develop an accurate, reliable, comfortable SSVEP-based BCI. That can offer severe motor neuron diseases a communication alternative using attention modulation without requiring neuromuscular activities or eye movements. As a result, the following research objectives were achieved in this study:

1. For SSVEP detection, the performances of the feature extractors and classifiers were investigated from the literature, methods that were not used before were identified, examined, and compared with each other.
2. For the SSVEP detection, a reconstructed existing feature extraction method with high accuracy results was proposed,
3. By conducting detailed research on stimulation frequencies, the highest accuracy frequencies were determined,

4. Performances of the classifier types, which have not been compared before, concerning SSVEP detection were evaluated in the literature.
5. The mother wavelet selection that best reflects the SSVEP signal was performed,
6. Multiple, triple and binary classification performances were analyzed, and their superiority was compared for SSVEP detection,
7. In parallel with the differences between stimulation frequencies, an increase in system performance was observed and detected.

1.5 Contribution of the Thesis

All the objectives listed above have been achieved, and contributions have been made during the studies. In some cases, different studies have been carried out in parallel. The main contributions of this thesis are listed as follows:

1. This thesis is a detailed study of the selection of stimulation frequencies.
2. To the author's best knowledge, this is the first study on in-depth research and evaluation of mother wavelet selection using the DWT method in SSVEP-based BCI.
3. To the author's best knowledge, this is the first study about the combination of energy, entropy, and variance features. It was determined which combination had a higher discrimination power on BCI studies.
4. This thesis is the first study about the evaluation and comparison of the used classifiers to the author's best knowledge.
5. To the author's best knowledge, this is the first study to examine the differences between stimulation frequencies and their effects on the system.

1.6 Organization of the Thesis

Within the scope of the thesis, from general to specific information about BCI and SSVEP based BCI studies are given. The materials and methods used are explained, and the results are analyzed in detail.

The rest of this thesis is organized as follows:

In Chapter 2, a review of the theoretical background is made to define the concepts of BCI and SSVEP based BCI systems. From the structure of the brain to the construction of the eye to which the SSVEP signals are related, physiological information is also briefly mentioned.

Chapter 3 is a section that introduces the materials and methodologies used in the thesis. Initially, an explanation was made regarding the acquisition and recording of the EEG signal used. Then, in the scope of this thesis, all the pattern recognition (preprocessing, feature extraction, feature selection, classification, evaluation) steps and methods in order are explained detail.

In Chapter 4, the results of the methods applied in the previous section are examined, and the findings obtained are evaluated in detail.

In Chapter 5, a summary of all the work done in this thesis, the contributions obtained are presented. The development of this thesis was carried out in chronological order, as shown in Figure 1.2. All objectives mentioned above, and contributions have been made during the studies. In some cases, different studies have been carried out in parallel.

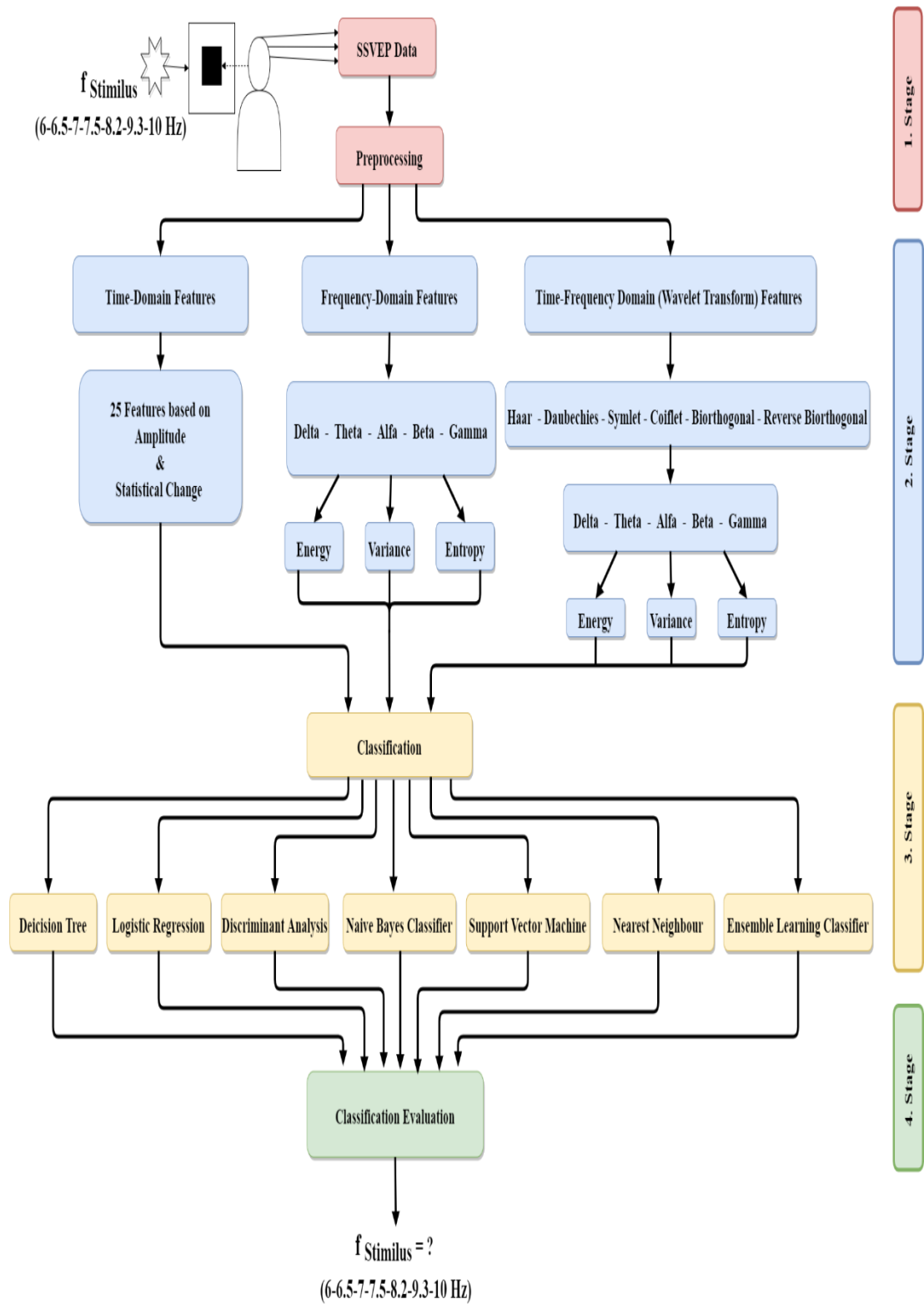


Figure 1.2 Chronological progress of the thesis pointing out objectives and achieved contributions.

2. OVERVIEW OF BRAIN COMPUTER INTERFACE

Technology is an area that starts with the invention of the wheel and extends to the advancement of artificial intelligence and affects every aspect of society. Revolutionary changes continue in the healthcare delivery system with the advancement of technology and the increasing speed of technology to meet changing healthcare needs [71]. These technological advances have significantly changed medical practices. The use of electronic health records, humanoid robots used in almost every area of health care, automated dispensing robots that apply drugs combined with highly specialized artificial intelligence is generally a few examples in this regard, and the brain-computer interface (BCI) is also one of the advances in neuroscience [72].

An artificial intelligence based BCI is a rapidly growing technology that means direct communication between a quietly speaking brain and bio-monitoring devices, electric chairs, robots, smartphones, and other external devices [73,74]. BCI can be seen as a set of systems that allow the direct transmission of electrical signals from neurons in the brain to an external device and/or system, such as a computer or robotic arm, without requiring any muscular system [3-19, 73,74].

BCI's initial release objective was developed for biomedical applications, which led to the production of auxiliary devices for the restoration of motion and communication power to rehabilitate lost motor abilities for physically semi- or fully-disabled patients [5]. However, researchers' horizons have been used not only for people with disabilities for medical applications but also for the development of non-medical applications such as prototypes of hand-free devices in many sectors such as the game and entertainment industry [17].

While real-time BCI applications exist worldwide, they are still in the global experimental stage. However, BCI applications have great potential and may become

clinically relevant soon [10]. The inclusion of these highly advanced technologies, especially in neuroscience healthcare, will change the medical profession. For this reason, healthcare providers face increasing difficulties integrating the continuous development of technology into medical practices. These challenges ask doctors and all healthcare providers to learn about recent technological advances and even implement what is available.

BCI is a technology that analyzes signals generated from the brain and transmits it to output commands in the real world to perform a specific task [3]. In doing so, they are unique because they do not contain normal neuromuscular pathways of peripheral nerves and muscles in paralyzed patients [9].

2.1 Brain Architecture

Some parts of human physiology need to be understood to understand and create BCI applications. This section provides essential and brief information about the physiological structure of the brain, which forms the basis of a BCI application.

Thanks to the brain, nerves, and spinal cord, it controls the central nervous system, manages the peripheral nervous system and regulates almost all functions of the body. Involuntary actions such as breathing, heartbeat, and digestion, without being noticed through the autonomic nervous system; More complex mental activities, such as thought, logic, and abstraction, are consciously managed by the brain [75].

All the stimuli coming from the sensory organs in the brain are evaluated, problems and events are considered and resolved, learning activity and memory are provided, hunger, thirst, sleep, wakefulness activities, blood pressure, and body temperature are regulated, and the time of hormones secretion is determined [76].

The human brain weighs an average of 1.5 kg. [75] It has a volume ranging from person to person, ranging from 1130 to 1260 cm³. There are about 86 billion neurons in the human brain. [77] When the mind is alive, it has blood circulation, it is very soft. It consists of gray matter.

The brain has three parts: the brainstem, the limbic system, and the neocortex [75-77]:

Brain Stem: It is the part surrounding the top of the spinal cord. It controls stereotyped responses, such as breathing, heartbeat, reflexes in distress situations, and essential functions related to life. No thinking and new learning take place in this section. It is a pre-programmed organizer that manages the responses necessary for our life. In other words, it is the center of our instinctive behavior.

Limbic System: It is the part surrounding the brain stem and controls our emotions. The amygdala and the hypothalamus are two critical parts of this part. The limbic system regulates an essential part of long-term memory. Therefore, we can remember the events that we have emotional connections more easily.

Neocortex: It is the center of thought. It manages high-level mental functions such as seeing, hearing, speaking, creating, thinking. It is the center where we bring together what we perceive through the senses and produce meaning. There are separate sections in the neocortex where the senses are hidden. The signals of speech, hearing, vision, and tactile senses are recorded separately in these lobes.

There are five main lobes [75] in the human brain. These:

1. Frontal lobe - conscious thinking; If it is damaged, there may be a change in mood or mood.
2. Parietal lobe - plays a vital role in combining information from various sensory organs. Besides, some parts of the parietal lobe are involved in the use of objects and some spatial processing (visuospatial processing).
3. Occipital lobe - the lobe where information about the sense of sight is processed. Slight damage causes hallucinations.
4. Temporal lobe - the perception of sound and smell and the processing of complex stimuli such as faces and spaces- are provided by this lobe.

5. Cerebellum - relates movement with information from the sense organs.
This lobe plays a vital role in ensuring balance.

Each lobe listed above is located in both hemispheres of the brain [75-77].

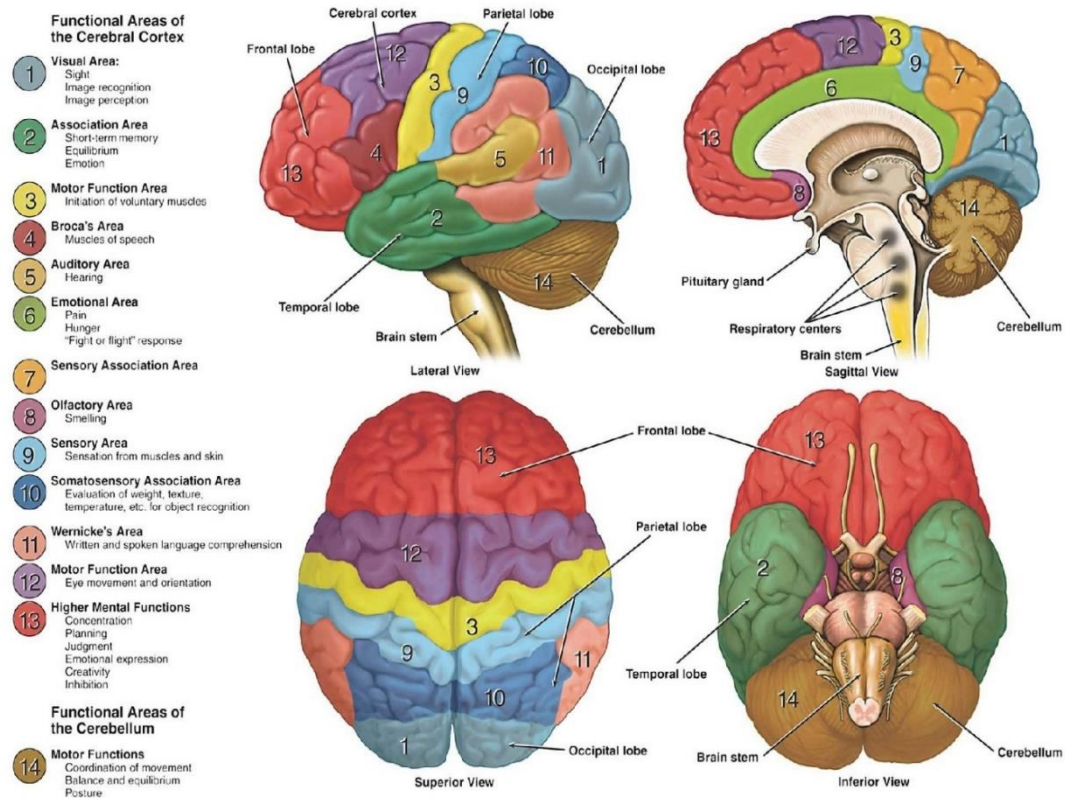







Figure 2.1 Functional Areas of the Cerebral Cortex [78].

Due to the extremely complex nature of the eighty-six million neurons fired, the signals consist of a mixture of varied frequencies. Scientists have divided distinct frequency ranges into some subgroups known as frequency bands (waves) as a result of researches. Each of these waves represents a different cognitive or non-cognitive state of the brain, and they first discovered in 1924 by Hans Berger by measuring EEG. In 1929, the German psychiatrist introduced the terms "alpha" and "beta" [12]. Other frequency bands, respectively, in 1936, Walter introduced the term "delta" for all frequencies below the alpha band. Also, he defined the "theta" band for the frequency range of 4–7.5 Hz. In 1938, the term 'gamma' was introduced by Jasper and Andrews for frequencies higher than 30–35 Hz [24, 79]. In the literature, different upper and lower frequency limits are available for these waves. Therefore,

brain rhythms, frequency ranges, and their characteristics are generalized in Table 2.1.

Table 2.1 Brain rhythms with their frequency ranges and characteristics.

RHYTHM	FREQUENCY RANGE	BRAIN WAVE	ASSOCIATED MENTAL ACTIVITY
Delta (δ)	0.1 – 3.5 Hz		<ul style="list-style-type: none"> • Sleep / Therapy for sleep disorders • Accelerated physical healing • Deep relaxation
Theta (θ)	4 – 7.5 Hz		<ul style="list-style-type: none"> • REM sleep • Access to unconscious mind • Healing of trauma and addiction • Deep meditation
Alpha (α)	8 – 13 Hz		<ul style="list-style-type: none"> • Relaxation • Creativity • Light meditative / Trance state • Increased serotonin production • Threshold to unconscious mind
Beta (β)	14 – 30 Hz		<ul style="list-style-type: none"> • Cognition • Focus • Analytical thinking • Stress / Anxiety • Fight / Flight response
Gamma (γ)	>30		<ul style="list-style-type: none"> • Whole-brain activity • Super-learning • Sudden insight

2.2 Components of Brain-Computer Interface

The primary purpose of designing a brain-computer interface is to detect, analyze, and evaluate the properties of the signals that show the intent of the user [4-10]. Also, it is to send these signal characters to an external device that works to fulfill the user's intent. The system created for this purpose generally includes four connected components: signal acquisition, processing (feature extraction), translation (feature

translation/classification), and device output (application) and/or feedback [16, 53]. Figure 2.2 shows these components and their various applications that serve their primary purpose (restore, replace, improve, supplement, enhance).

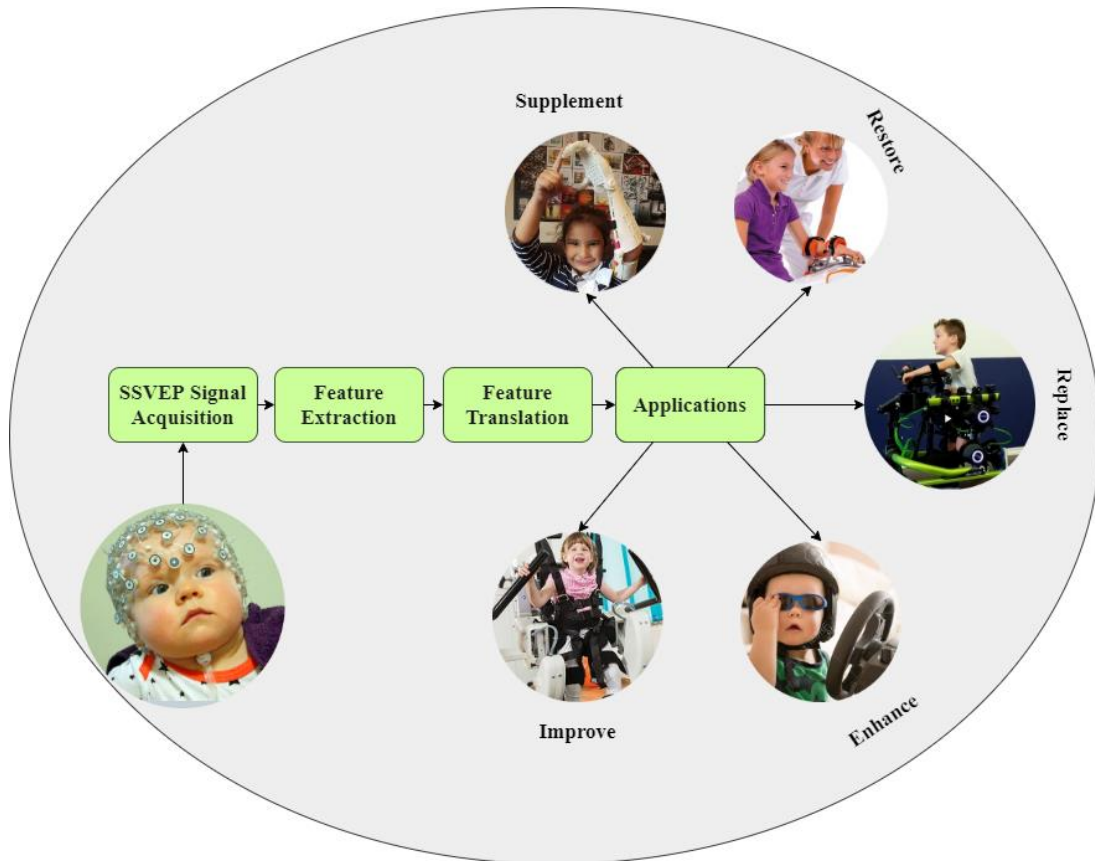


Figure 2.2 Components of BCI.

The main steps of a BCI system are briefly outlined below:

Signal acquisition: The signal acquisition step, which is the first step of the BCI system, involves measuring the activities in the brain and digitizing them to be processed on the computer [53].

Feature extraction: The process of obtaining the characteristic features of the signal corresponding to the brain activity captured by the signal acquisition step [16].

Translation (Feature translation / Classification): Which brain activity corresponds to the features obtained in this step is determined by using classification (machine

learning) algorithms, and commands to be used in the application step are generated [16].

Application: With the command obtained in the classification step, many applications can be developed to improve the life quality of partially or entirely disabled people [16].

2.3 Brain-Computer Interface Classifications

BCI systems are classified in three different ways according to the working principles of the methods used in system design [10, 11, 18, 80]. These classes are defined as invasiveness, dependency, and synchronization, as shown in Figure 2.3. In terms of dependability, the BCI could be categorized as dependent and independent BCI, while in terms of invasiveness, it could be divided into invasive and non-invasive BCI. In the final category, the BCI could be synchronous or asynchronous (self-paced).

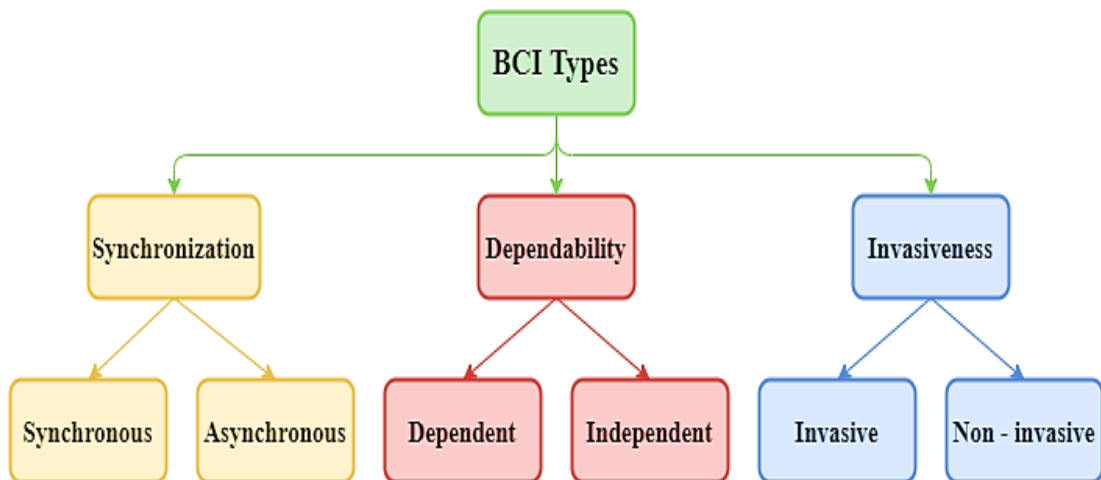


Figure 2.3 Classification of BCI systems.

2.3.1 Synchronous and asynchronous (self-paced) Brain-Computer Interface

In the classification of BCI systems according to the synchronization status, when user interaction with the system is done at a specific time, this type of BCI system is called synchronous BCI. In other words, the synchronous BCI system must interact with the user within a particular time frame. If there is no interaction during this

period, the system cannot receive the user's signals. On the contrary, in asynchronous BCI [81], also called "self-paced," the user can perform his mental tasks at any time, and the system will react to his mental activities. Therefore, the user can do his activity at any time.

2.3.2 Dependent and independent Brain-Computer Interface

In a dependent BCI, the user must have a certain level of motor control, while in an independent BCI, no motor control is required. The BCI system needs to be designed as independent BCI to help people without motor control [80]. An example of an independent BCI system is the SSVEP-based BCI system. In this system, the system can only control the gaze of the user. However, dependent BCI is more suitable for people who can partially or fully use the motor control system [18]. For example, it is ideal for the control of the rehabilitation robot or to use video games.

2.3.3 Invasive and non-invasive Brain-Computer Interface

A BCI system is classified as invasive and non-invasive based on where the brain activity is measured. In invasive recording methods, microelectrodes are placed under the brain's scalp, and neural activity is measured inside the motor cortex or cortical surface (electrocorticography (ECoG)). Their most important advantage is that they provide high temporal and spatial resolution by increasing the quality of the signal obtained and the signal to noise ratio.

On the other hand, these techniques have many disadvantages. Although it requires risky surgical procedures, there are usability problems. The small size of the brain regions monitored by implants placed in the brain can create problems with the system's output. Implanted microelectrodes cannot be shifted to measure brain activity in another area. There may also be problems with the stability of implants and infection prevention. For these reasons, the use of the invasive recording in the real world is generally limited to monkey experiments.

Unlike invasive methods, non-invasive methods do not require implanting electrodes or external objects to the brain. Therefore, it prevents the surgical procedures needed by invasive techniques. In this case, the signals may be of more inferior quality; however, it is the most preferred method due to the many advantages of non-invasive

BCI. For example, it does not require any surgical intervention, easy applicability, and portability, relatively low cost, etc.

In the next section, neuroimaging BCI methods, sub-methods used in invasive and non-invasive techniques, will be explained in detail.

2.4 Neuroimaging Methods of Brain-Computer Interface

In the signal acquisition step, which is the first part of the BCI system, two basic methods detect, measure, and display the brain's signals produced by the brain's neuronal activities: invasive and non-invasive techniques. These methods are responsible for the acquisition and recording of signals and their transfer to the next BCI component. These methods, which are categorized according to where the signals are measured in the brain, are subdivided. They differ according to the external sensors, devices, and procedures used within themselves. These methods are summarized in Figure 2.4.

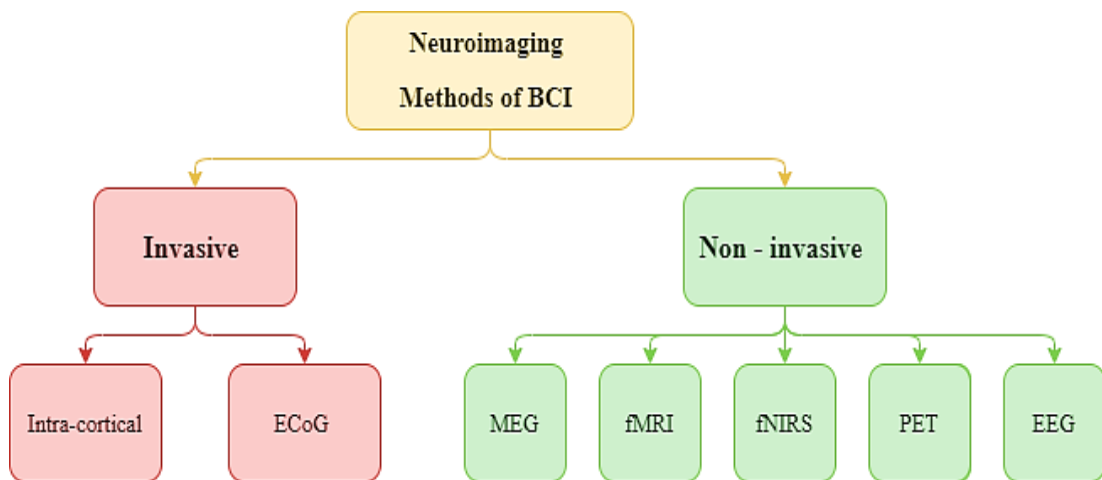


Figure 2.4 Types of neuroimaging methods.

2.4.1 Intra-cortical

The intracortical acquisition technique represents the most invasive method shown in Figure 2.4. This method, which is penetrated under the cortex surface of the brain, is obtained using a single electrode or a series of electrodes that measure individual neurons' movement activities. Since the electrode tips are placed very close to the signal source, they provide a relatively high spatial resolution. However, the

intracortical acquisition may show signal variability or signal loss in long-term use. This may be the result of neuronal cell death or increased tissue resistance. If the system contains a stimulus to activate the limb of individuals with disabilities, this additional stimulus can also create a significant noise effect, and this noise reduces system performance [82].

Studies using intra-cortical recording techniques with human subjects have been limited to some severely disabled people. However, intra-cortical signal acquisition on monkeys and rats has significantly contributed to BCI research studies. The movement of the BCI-based robot system was analyzed on animals using implanted electrodes. At the same time, monkeys managed to move a cursor to eight targets located in the corners of an imaginary cube in research to minimize the number of electrodes used in these systems. In light of the information obtained, an adaptive motion prediction algorithm has been developed. Moreover, the monkeys managed to move a brain-controlled robot arm using virtual reality and helped them eat with a real robot arm [83].

2.4.2 Cortical surface (ECoG)

Although ECoG is a recording method that requires less invasiveness than the intra-cortical process, it provides the advantages of the intra-cortical approach. It is performed surgically by implanting the electrode grids or strips onto the cortex surface [84]. Compared to non-invasive methods, it is less affected by the noise and artifacts caused by muscle connection to achieve a high signal to noise ratio. This method, which provides a substantial advantage, especially for seizure localization problems of epilepsy patients, is used by patients before surgery.

2.4.3 Magnetoencephalography (MEG)

It is a non-invasive method that measures magnetic fields produced by naturally occurring electrical currents from the chemical structure of the brain [85]. MEG signals can affect and be affected by other magnetic signals, such as the earth's magnetic field. Thus, this recording method requires a laboratory environment with protective, concealing, and specialized equipment. Despite its portability and cost issues, MEG signals are less distorted than methods received by the cortical surface.

However, this advantage does not significantly improve system performance or training times compared to other non-invasive signal acquisition methods [86].

2.4.4 Functional magnetic resonance imaging (fMRI)

Functional magnetic resonance imaging (fMRI) detects changes in blood flow due to neural activity in the brain [87]. These changes are offered as solutions to resource localization problems. Because in case of using any brain part, the blood flow is expected to increase in that part. This method helps to map brain areas that correspond to blood flow. Although the relatively temporal resolution of fMRI is low, it provides a high spatial resolution. The most important advantage of this method is that it captures information that cannot be collected by electrical or magnetic measurements from the deep parts of the brain [87].

2.4.5 Functional near-infrared spectroscopy (fNIRS)

Functional near-infrared spectroscopy (fNIRS) is a non-invasive method that measures blood flow dynamics to detect neural activity. It uses near-infrared light to detect blood flow dynamics [88]. Providing high spatial resolution signals is advantageous due to its portability and relatively inexpensive system. However, concerning temporal resolution, it offers less imaging capability. The fNIRS signal recording is likely to be less effective than methods based on electromagnetic signals. fNIRS is more suitable for clinical studies and practical use [89].

2.4.6 Positron emission tomography (PET)

Positron Emission Tomography (PET) is a nuclear medicine imaging method that shows functional changes that occur in organs and tissues [90]. PET displays normal or pathological tissues in which metabolic radioactive substances injected into the user through the vein accumulate. It is generally used for metabolic or functional imaging. In this technique, the PET method is performed by injecting the positron irradiated fluorine-labeled fdg molecule through the vein into the user.

2.4.7 Electroencephalography (EEG)

Although the brain's electrical activity research was revealed in 1875 by neurophysiologist Ricard Caton, who recorded the electrical activity of rabbit and monkey brains directly from the brain tissue [91], the first human electroencephalography (EEG) was recorded by Hans Berger in 1924. He created the term "electroencephalogram" by characterizing and defining the wave models containing alpha (α) and beta (β) waves [92].

EEG is the recording of electrical activity to cover all regions of the brain by measuring the voltage fluctuations that occur during the neurotransmission activity in the brain. The electrodes are attached to a hat-like device (cap). EEG has unique usability advantages over other brain imaging methods recommended for clinical and commercial use. This user-friendly method is both portable and relatively affordable. At the same time, EEG recording provides high temporal resolution. However, the signal-to-noise ratio and spatial resolution are more limited than other neuroimaging methods. Various solutions are provided to improve spatial resolution and signal localization problems in EEG signals. One of them is the use of increasing electrodes up to 256.

Electrodes used for EEG acquisition are placed on the scalp according to the international 10-20 settlement system [93]. The layout is shown in Figure 2.5.

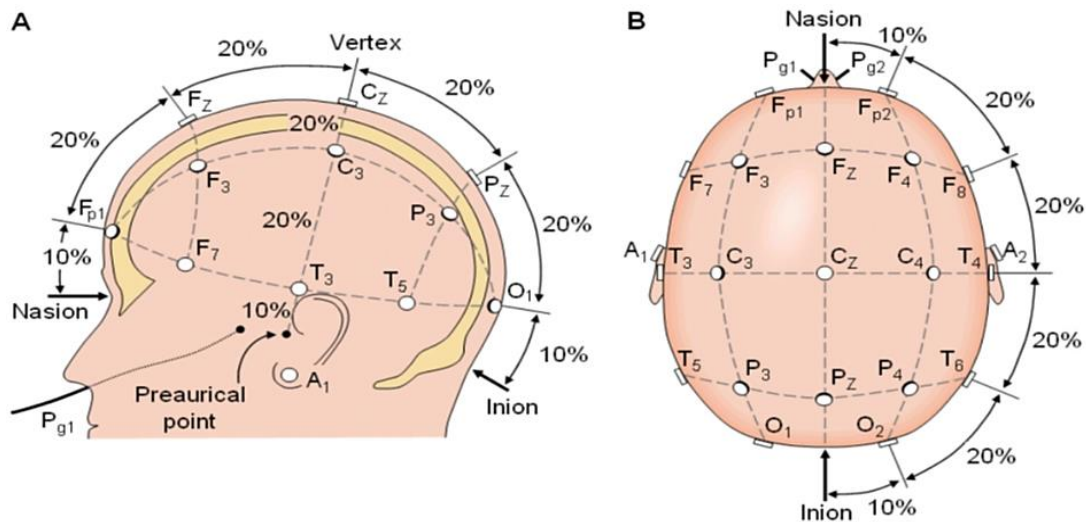


Figure 2.5 International 10-20 electrode layout [93].

Figure 2.5 shows the left portrait as indicated by A and the top view of the title as revealed by B. The notations in the claim that refer to each cortical region as reference are Pg: Nasopharyngeal, Fp: Frontal Polar, F: Frontal, A: Ear-lobe, T: Temporal, C: Center, P: Parietal and the last O: Occipital. Electrodes in the right hemisphere of the header are represented by even numbers, while the electrodes in the left region are identified by odd numbers [94]. As seen in Figure 2.5, the layout was created by dividing the skull's distance from the nasion level to the inion level by 10-20-20-20-10 percent.

When measuring EEG, two types of measurement criteria are usually used: Monopolar and bipolar. In a monopolar measurement, the voltage difference between each electrode and a common reference selected is measured. It is placed in a "neutral" zone (e.g., Mastoid, earlobe), which assumes that the chosen common reference's electrical activity is not affected by other brain activities. Besides, the reference signal may be the average of two or more electrodes. Moreover, the average of all electrodes can be selected as a reference, and this is called the common average reference (CAR). In a bipolar measurement, the voltage difference between all electrode pairs is measured [94].

Table 2.2 Comparison of neuroimaging methods.

NEUROIMAGING METHODS	SIGNAL TYPES	INVASIVE-NESS	PORTABILITY	SPATIAL RESOLUTION	TEMPORAL RESOLUTION
Intra-cortical	Electrical	Highly Invasive	Portable	Highest	Highest
ECoG	Electrical	Invasive	Portable	Higher	Higher
MEG	Magnetic	Non-invasive	Non-portable	High	High
fMRI	Metabolic	Non-invasive	Non-portable	High	Low
fNIRS	Metabolic	Non-invasive	Portable	High	Low
PET	Metabolic	Non-invasive	Non-portable	High	Low
EEG	Electrical	Non-invasive	Portable	Low	High

2.5 Control Signals Types in Brain-Computer Interfaces'

The primary purpose of BCI studies is to analyze and interpret user intentions by monitoring the cerebral region [14]. The electrical signals produced in the brain

contain many simultaneous phenomena related to cognitive tasks. Many of them are still not understood as their roots are unknown [14]. However, the physiological phenomena of some signals have been discovered in such a way that they can learn to modulate people at any time. In other words, a large number of BCI studies have been conducted that have managed to interpret users' intentions by finding out the effects and differences of various triggering conditions (e.g., evoked potentials (EP)) or spontaneous brain oscillations that are not necessarily associated with external stimulation (e.g., event-related synchronization (ERS) – desynchronization (ERD)). These signals are called control signals used in BCI systems [14]. These control signals can be divided into three basic categories [18]: 1) Spontaneous signals, 2) Hybrid signals, and 3) Evoked potentials. Figure 2.6 shows the classification of control signals. Also, a brief description of each is below.

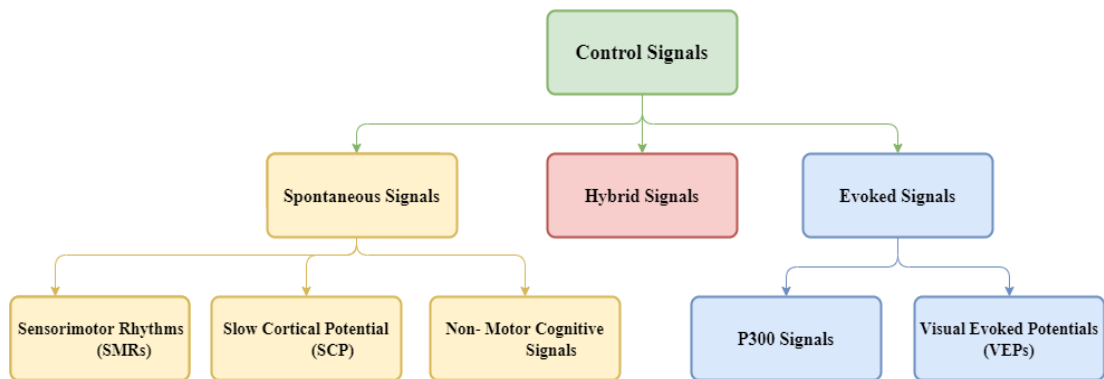


Figure 2.6 Classification of control signals.

2.5.1 Spontaneous signals

Spontaneous signals, one of the types of signals used in BCI, are signals produced without any external stimulation that affects the user. Spontaneous signals known in the literature are divided into Sensorimotor Rhythms (SMRs), Slow Cortical Potentials (SCPs), and Non-motor cognitive tasks.

2.5.1.1 Sensorimotor rhythms (SMRs)

Sensorimotor rhythms, also known as " μ and β rhythms," include brain activities localized in the μ band ($\approx 7-13$ Hz) and β band ($\approx 13-30$ Hz). Sensorimotor rhythms

are associated with motor images without any real movement [14]. Patterns of motor images are produced as a result of mental rehearsals of motor motion without any actual motor output [18]. However, sensorimotor rhythms are not easy to control, and often people have difficulty imagining motor images. To overcome this difficulty, long-term training is required. In this training, they ask users to imagine a particular motor image task in their minds. The sensorimotor rhythms obtained at the end of this task are obtained by comparison with a reference and then classified. As a result, the participant is provided with visual or audio feedback based on the classification success.

Sensorimotor rhythms can be based on two kinds of amplitude modulation known depending on the event: sensory stimulation, motor behavior, and synchronization (ERD) that creates mental images, and event-related synchronization (ERS). ERD includes an amplitude suppression of the rhythm, and ERS implies increasing amplitude.

2.5.1.2 Slow cortical potentials (SCPs)

Slow cortical potentials are slow, positive, and negative voltage changes in brain signals that last between milliseconds and a few seconds. SCPs are the part of the brain signals with a frequency below 1 Hz. SCPs are associated with changes in activity at the cortical level (detected in the frontal and middle cortex). Negative SCPs are associated with an increase in neuronal activity, while positive SCPs are assessed by a decrease in neuronal activity [15].

Success in the SCP signal training depends on many factors, such as the patient's psychological and physical condition. It is also known that the user's learning ability significantly affects SCP modulation training. Therefore, the value of SCPs as the appropriate control signal for each of the individual designs can only be determined by trials. At the same time, it is difficult to establish general rules in this regard, since personal effects are not the same for all users. SCPs have been extensively tested with ALS patients, and the accuracy rates obtained as a result of the SCP classification range from 70% to 80%. However, the information transfer rates provided by the real-time SCP-based BCI are relatively low. Also, longer training

times are required to use real-time SCP-based BCI. Due to these disadvantages, many researchers have not preferred SCP and is usually replaced by sensorimotor rhythms.

2.5.1.3 Non-motor cognitive signals

Non-motor cognitive tasks mean that the user uses cognitive tasks except the dream of motor movement, for example, to visualize the rotation of a letter in his mind, visual counting, mathematical calculations or neuronal activities have taken while listening to music. Ozmen et al. [95] and Sadreddini et al. [96] analyzed the differences between the imagination of motor movement and non - motor cognitive signals in their studies with pattern recognition methods and machine learning algorithms.

2.5.2 Hybrid signals

Hybrid signals are signal types in which a combination of electrical activities produced by the brain is used by BCI systems [97]. In the BCI system using this type of signal, only one input signal is measured and used, that is, a signal hybrid is used. The primary purpose of using two or more types of brain signals as input signals to the BCI system is to increase system performance and reliability [98]. It is also to avoid the disadvantages of each signal type.

2.5.3 Evoked potentials (EPs)

Evoked potentials (EPs) or evoked responses create an event-related activity that occurs as an electrical response to various sensory stimuli of the brain [24, 25]. Auditory and visual stimulation is widely used to produce this signal [23]. Evoked potentials typically show themselves as temporary waveforms, which depends on the type, power, and electrode positions on the scalp of the stimulus. The user's mental state, exemplified by attention, alertness, and anticipation, also affects the waveform morphology. The best-known EPs used in the literature are Visual Evoked Potentials (VEPs) and P300 signals [80].

2.5.3.1 P300 signals

P300 evoked potentials are positive peaks that occur approximately 300 ms after visual, auditory, or somatosensory stimuli. One of the essential advantages of using P300-based BCIs is that it requires little or no training. However, if the user rarely gets used to the stimulus, the P300 amplitude decreases, and system performance may decrease [99]. P300 is used for visual impairment in auditory stimuli, although visual stimuli are used in most applications based on their evoked potential, due to ease of application. The information transfer rates of P300 based BCIs are meager. At the same time, a lot of trials are required to capture the P300 potentials. Besides, some studies have shown that the detection accuracy of visual P300 potentials depends on their visual characteristics, such as the size or color of the symbols. Performance decreases when small symbol matrices are used, and performance increases when using the green and blue matrix compared to gray or black colors [100].

2.5.3.2 Visual evoked potentials (VEPs)

With the sensory stimulation of the visual field in the brain of a BCI user, visually evoked potentials produced in the visual cortex are formed [29]. That is, VEPs reflect the visual information-processing mechanisms in the brain. VEP-based BCI is a system where the user's EEG is recorded simultaneously when the user is visually focused on a target. In a VEP-based BCI, each target presented to the user is coded with a unique stimulus sequence that evokes a unique VEP pattern [102]. Therefore, when designing a target, the characteristics of VEP should be determined by analyzing. Thus, existing VEP-based BCI systems are divided into three categories based on the stimulus morphology used [102]:

1. Time-modulated VEP (t-VEP)
2. Code modulated VEP (Pseudorandom code) (c-VEP)
3. Frequency modulated VEP (f-VEP)

In the first modulation, t-VEP based BCI, the flash sequences of different targets are independent. Flash sequences for different targets should never overlap. To avoid overlapping two or more consecutive t-VEPs, t-VEP-based BCIs generally have low

stimulus rates (<4 Hz). Another method to prevent overlap of t-VEPs is that the target's flash sequence is dependent on each other. Still, the stimulus design can be made by randomly adjusting the duration. To make accurate target identification in t-VEP based BCI, it is necessary to average of many epochs. However, t-VEP based BCIs have a lower stimulus frequency (ITR) because they have a lower stimulus frequency (<30 bits/minute) [26, 27].

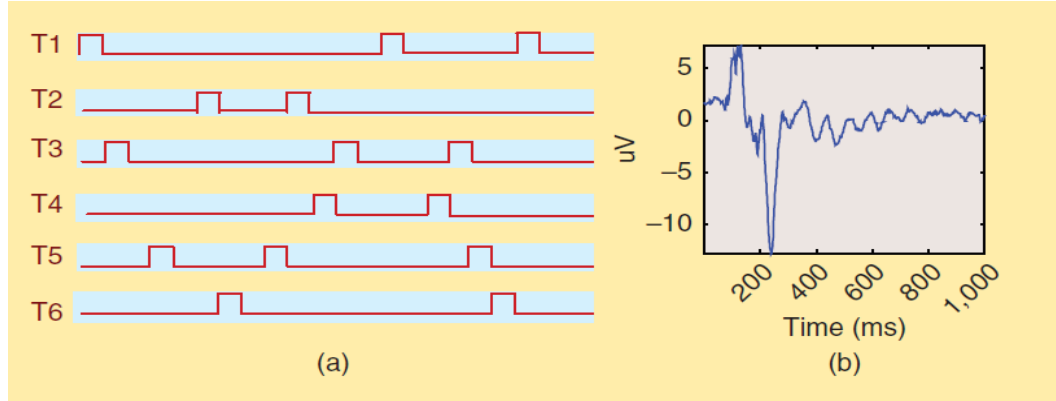


Figure 2.7 a) Independent stimulus sequences of the targets of a t-VEP based BCI. b) A single t-VEP response [102].

Although the first c-VEP based BCI was introduced by Sutter [29] in 1984, there is a minimal number of studies on the c-VEP signal until 2009. This is because the results of the proposed methods are not satisfactory. In 2009, Bin et al. [102] developed a 32-targeted c-VEP-based BCI with the highest ITR value among all BCI types designed in those years. Pseudorandom sequences are used in a c-VEP-based BCI, and the m sequence is the most used pseudorandom sequence [29]. A binary m-sequence is produced using linear and nonlinear system analysis, using maximum direct feedback and shifting records. An m-sequence has an autocorrelation function and is almost perpendicular to the time delay sequence [103]. Thus, an m-sequence and its delay sequence can be used for a c-VEP based BCI. Figure 2.9 shows the stimulation sequences of a c-VEP based BCI and the time streaming of the stimulation response.

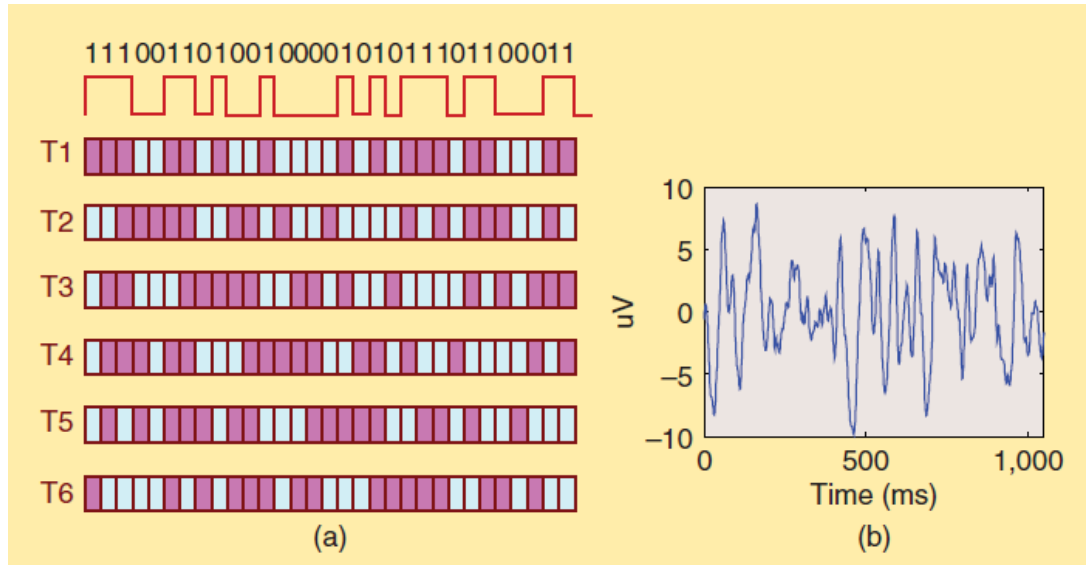


Figure 2.8 Stimulation sequences of the targets of c-VEP based BCI [102]. a) Target sequences of a stimulation cycle. b) A waveform of the evoked response.

In a final modulation f-VEP based BCI, each target generates a periodically evoked response sequence with the harmonics of the stimulus frequency, as well as the flashing stimulus at a different frequency [20, 21, 22, 26, 30, 104]. Power spectrum density is most commonly used for target identification of f-VEP based BCI [102]. So, figure 2.10 a) shows a stimulation sequence of an f-VEP based BCI and b) shows the power spectrum of the stimulated response. For the x segment of an EEG data obtained from an i-targeted f-VEP based BCI with flickering frequencies f_1, f_2, \dots, f_i , the target identification is implemented with the following steps:

- 1) Calculate the power spectrum ($P(f)$) of the EEG signal using a spectral analysis technique (e.g. Fast Fourier Transform (FFT)).
- 2) Calculate the signal-to-noise ratio (SNR) S_i of each stimulus frequency (f_i).
- 3) Determine the target of detection by selecting the target (I) corresponding to the maximum S_i .

The flicker frequency in f-VEP based BCI is generally higher than 6 Hz [104-110]. Stimulated responses caused by the repeated flashing of the target may overlap and form a periodic sequence of f-VEPs. This condition is called a frequency-locked steady-state visual evoked potential (SSVEP) [26, 27]. In this case, the name of f-VEP based BCIs is defined as SSVEP based BCI [104]. Over the past decades, the

robustness of SSVEP-based BCI systems has been credibly demonstrated in many laboratories, research groups, and clinical tests [101-122]. The advantages of an SSVEP-based BCI are, for example, simple system configuration, no user training, and a high ITR (30-60 bits/min) rate [18]. It is also among the advantages of being relatively less sensitive to artifacts produced by noise contamination, such as eye movements and electromyography [26].

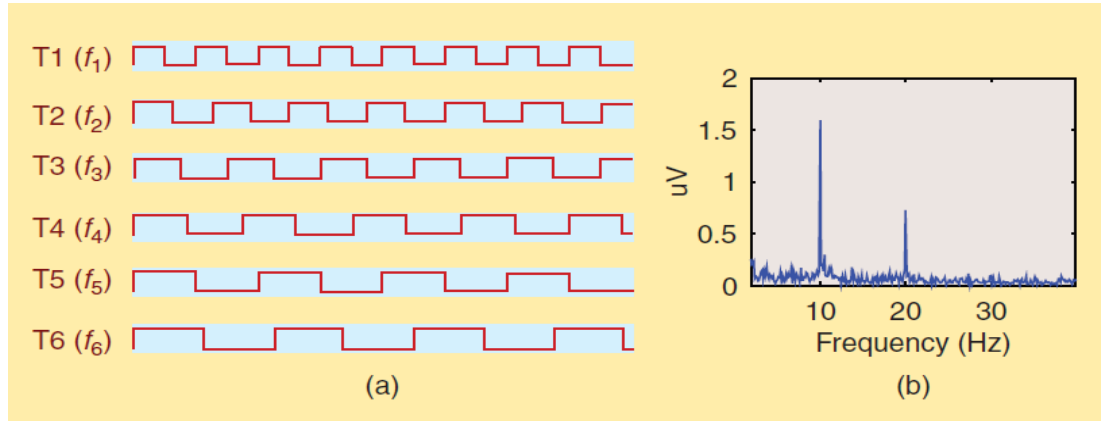


Figure 2.9 a) Stimulating sequences of targets of f-VEP based BCI (SSVEP based BCI) [102]. b) Power spectrum of the evoked frequency at a frequency of 10 Hz.

Modulation approaches differ due to different target identification methods used, as mentioned above, change in system performances. As a summary of these differences, the properties of the modulation are presented in Table 2.3.

Table 2.3 Characteristics of VEP modulations.

VEP MODULATION	CHARACTERISTICS
t-VEP	<ul style="list-style-type: none"> -Relatively low information transfer rate (<30 bits/min) -Synchronous signal is necessary -No user training required
c-VEP	<ul style="list-style-type: none"> -Very high information transfer rate (>100 bits/min) - Synchronous signal is necessary - User training required -More suitable for application with many options
f-VEP	<ul style="list-style-type: none"> -High information transfer rate (30-60 bits/min) -Simple system configuration -No user training required -More suitable for application with few options

As a result, the main features, advantages and disadvantages of all control signals used in the design of BCI systems described in section 2.5 are summarized in Table 2.4.

Table 2.4 Control signals summary.

SIGNAL	CHARACTERISTICS	TRANSFER RATE (BITS/MIN)	TRAINING	ADVANTAGES	DISADVANTAGES
Sensori-motor rhythms	It is based on modulations synchronized to motor activities	3-35	Yes	-Doesn't depend on any stimulation -Subject use it voluntarily	-Needs very long-time training - Some subjects might not be able to generate the signals
SCP	It is the slow voltages shift in brain signals	5-12	Yes	-Suitable for control applications	-Needs multiple EEG channels for recordings for good performance
P300	It is the positive peaks due to infrequent stimulus	20-25	No	-Need very little training or no training required	-Permanent attention to external stimuli -Some subjects might get tired
VEP	It is based on signal modulations in the visual cortex	60-100	No	-High bit rate -Single EEG channel is required	

2.6 Steady-State Visual Evoked Potential (SSVEP) Based Brain-Computer Interfaces

This thesis focuses mainly on SSVEP based BCI systems. Therefore, SSVEP based BCI system components will be detailed in this section.

SSVEP signals are continuous, periodic and also harmonic signals that emerge with an external visual stimulus frequency greater than 6 Hz and oscillate equal to or full times the frequency of the stimulus [26, 27, 29, 30]. In other words, SSVEP signals emerge by processing visual stimulus information in the visual (occipital) cortex in the brain [104]. As seen in Figure 2.10, SSVEP signals can be observed in frequency space and can be distinguished from EEG noises. In Figure 2.10 a), the raw signal of 10 Hz stimulated SSVEP used in the thesis, and b) the power spectrum and the first and second harmonics of the signal are seen.

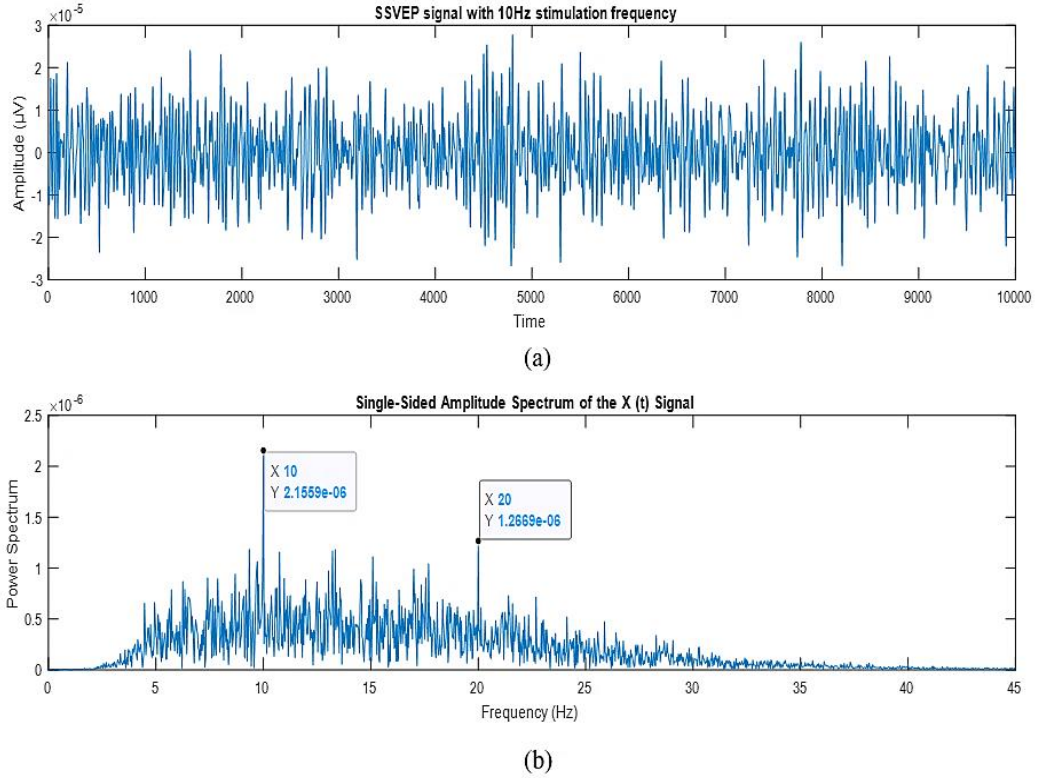


Figure 2.10 a) SSVEP raw signal b) Power spectrum of the 10 Hz stimulated SSVEP signal.

SSVEP signals are influenced by factors such as the user's focus status, the colour of the visual stimulus, its shape, the frequency of the stimulus's active/passive residence times, and the light source [123, 124]. These factors will be explained in detail in section 2.6.2. One of the characteristic features of the SSVEP signal is its amplitude and stability in phase [125] and the parallelism between the phase of the stimulus and the signal phase. Another characteristic feature that makes the SSVEP signal an ideal source is noise immunity. In SSVEP based BCI systems, the frequency of the visual stimulus used is generally chosen more significant than 6 Hz [104-110]. Because the frequency of noise caused by eye or body movements is less than 6 Hz. Therefore, SSVEP signals are relatively more immune to noise from these movements. Also, as explained in section 2.5.3.2, SSVEP based BCI systems are considered the ideal signal source for BCI systems due to their advantages such as no training required,

the stability of neuronal response, and high information transfer rate [20-23, 101-123].

2.6.1 Vision physiology

SSVEP signals emerge by recording neuronal activities obtained by the visual cortex through the eye organ. Therefore, one of the critical points when examining SSVEP based BCI is to understand the physiology of vision. In this section, an explanation will be given about the structure and working principle of the human eye. The eye consists of three different layers (tunic) [126]. The human vision process and the layers of the eye are as follows from the outermost to the innermost part [127]:

1. Outer fibrous layer: This layer consists of the cornea. This part of the eye provides support and protection of the shape and structure of the eye. It also provides a connection point for the extrinsic muscles, and the lights of objects first enter the eye through the cornea.
2. Middle vascular layer: This layer consists of the iris. This section provides pathways for blood vessels and lymphatics for eye tissue. Iris regulates the size of the pupil and controls the light entering the eyes. At the same time, the iris controls the watery humour (vitreous gel) that regulates the shape of the lens and travels through the chambers of the eyes.
3. Inner nerve layer: This layer consists of the retina. The retina is the innermost layer of the eye, consisting of a pigmented retina and a sensory retina, enhancing visual acuity and preventing the bounce of light and scattering from the sensory retina, transmitting light to electrical signals and sending visual information to the brain with optic nerves. Also, another essential point that should not be missed when talking about the inner nerve layer is fovea centralis. Fovea centralis is a small hole in the retina. When people focus on something, they are responsible for visual acuity. It is about 1 mm in diameter. Although it occupies less than one percent of the entire retina, it is responsible for half of the information transmitted to the primary visual cortex. Therefore, visual information passing through the fovea centralis reaches the visual cortex of the

occipital lobe. The neurons of the visual cortex transfer information to an image. Electrical impulses are sent to the brain by the optic nerve, and the image is formed [128].

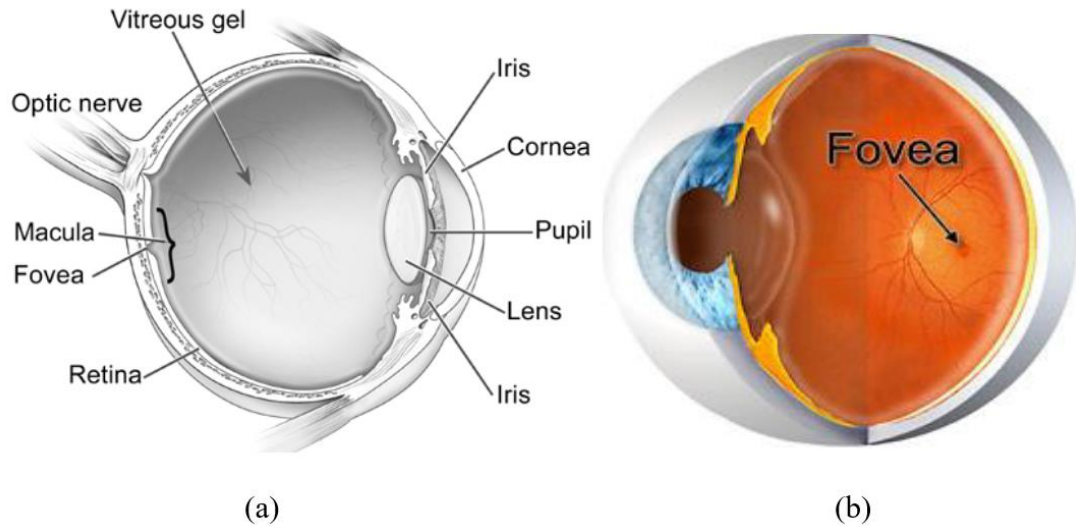


Figure 2.11 a) Human eye structure b) Location of the fovea [127].

It is not enough to know the physiology of human vision briefly to make visual stimulus design in SSVEP based BCI applications. Because of the cells in different areas of the human visual cortex for different visual characteristics such as shape, frequency and colour. Therefore, the structures responsible for the colour, shape and frequency of each object used in the design are different. Two types of photoreceptor cells sense light in the retina region of the eye. These cells are called rods and cones [126]. Rods are photoreceptors that do not include separation of colours and enable people to see in a reduced light environment. The rods work better in dim light because they are light sensitive. Cones, which are other receptors, are photoreceptors that enable people to see in colour. Three types of cones called R (red) -G (green) -B (blue) cones have different sensitivity curves according to the wavelength of the light. The peak sensitivity of the curves of the three cones does not precisely correspond to the colours of red, green and blue. Therefore, they are sometimes named in wavelength, corresponding to the peak sensitivity, in the following order and wavelengths [128]:

- Long (L): 564-580nm (L)
- Medium (M):
- 534-555nm (M)
- Short (S): 440-498nm (S)

The number of these three types of cones is not equal, and the ratios of R: G: B cones are 40: 20: 1. Besides, the perception of colour vision is subject to various dimensions of the three stimulated cone types. In the human eye, the maximum absorption for the R-G-B type cone is, respectively [128]:

- B: 498nm
- G: 534nm
- R: 564nm

Moreover, the human visual system consists of two main ways [101]. The first of these is called the Parvocellular (PC) path, and this path is colour sensitive, has lower contrast sensitivity, responds to higher spatial frequencies and lower temporal frequencies and continuous responses. The second is defined as the Magnocellular (MC) path and the MC path, known for its colour insensitivity, responds to lower spatial frequencies and higher temporal frequencies with higher contrast sensitivity when the brightness is balanced. MC and PC paths start from the retina. The PC path carries colour (red-green-blue), spatial contrast and shape information. The MC path determines frequency and depth [101]. The MC path has faster transmission speed, more rapid adaptation to the constant stimulus, larger receiving area compared to the PC path. Therefore, the contribution of paths to the SSVEP stimulus design largely depends on the characteristics of the stimuli. For example, black and white checkerboards with high temporal frequency and low spatial frequency can evoke greater SSVEP on the MC path. In contrast, coloured checkerboards on the low temporal frequency and high spatial frequency can produce more robust SSVEP responses on the PC path than the MC path [101].

2.6.2 Visual Stimulus

When designing an SSVEP-based BCI, several choices must be made about the properties of the visual stimuli the system will use for an SSVEP response. Visual stimulus design is a critical step in SSVEP-based BCI studies, since the size, colour, environmental lighting, spatial frequency, shape, the light source of the stimulus, the rate of active/passive duration of the stimulus, and frequency affect the generated signal [124]. The visual stimulus used can be designed with repeated shapes at a specific frequency on the computer screen, as well as external light sources such as Liquid Crystal Display (LCD) and Light Emitting Diodes (LED) [123]. In this section, the properties that determine the characteristics of the visual stimulus will be introduced.

- **Size:** The size of the stimulus is important in terms of being noticed. However, they should not be large enough to make it difficult to focus on the active stimulus on the screen with multiple stimuli. Because in this case, it is more challenging to ignore passive stimuli, and this is not the desired situation. At the same time, the stimulus size also affects the amount of light transmitted to the user [124]. Thus, size is an important criterion to determine how significant the stimulus should be or how much surface area remains for other stimuli.



Figure 2.12 Different stimuli (colour, pattern, size) designed to generate SSVEP responses [124].

- **Environmental lighting:** Generally, lighted environments are more useful for the comfort of the user. However, in short-term trials, a bright stimulus in

the dark may appear much more pronounced and make focusing easier. The concept of environmental lighting is closely related to the stimulus displayed and the contrast of ambient lighting. The pupil expansions caused by a dark environment can cause the eye to catch more of the stimuli. Therefore, it may be easier to capture the SSVEP response. As a result, it has been shown that based on all these observations, SSVEP based BCI performance can be increased in dark environments [27].

- **Contrast:** Contrast, also known as “modulation depth”, is defined as $(I_{\max} - I_{\min}) / (I_{\max} + I_{\min}) \times 100\%$. Here I_{\min} , I_{\max} denotes minimum and maximum brightness, respectively. The importance of contrast for the SSVEP response has been demonstrated by studies in which a higher contrast leads to stronger SSVEP responses, particularly for dark stimuli, as mentioned in the previous paragraph [129]. However, it has also been noted that higher contrast provides lower comfort for long-term trials.
- **Color:** Main colors used in stimulus design other than black, white, gray are red, green and blue. Colors differ in properties defined as hue, saturation and lightness, and these more perceptual terms are known to affect the SSVEP response [28].

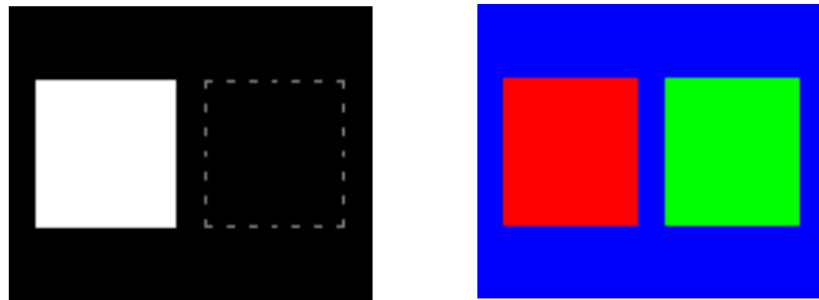


Figure 2.13 Main colors used in stimulus design [124].

- **Shape and Spatial Frequency:** In SSVEP research, the form of stimulus is divided into two classes as simple stimulus and complex stimulus. In this classification, the simple stimulus class consists of single light source flashing and / or single graphic (square, circle, rectangular, triangle, arrow,

etc.) stimuli that flash on the monitor. Simple stimulus examples are shown in Figure 2.14.

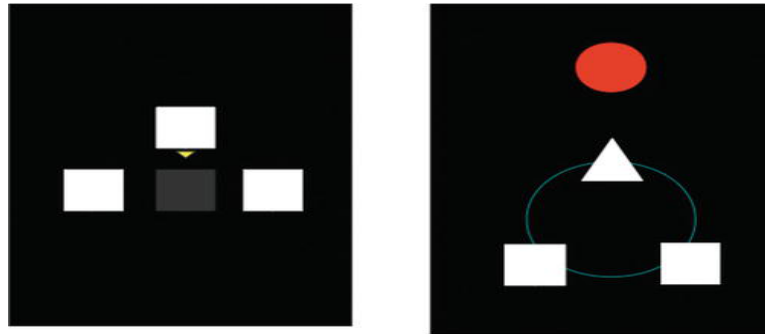


Figure 2.14 Simple stimulus examples used for visual stimulus design [110].

The complex stimuli class includes visual stimuli applied by periodic inversion of a shape, such as a checkerboard (chess) board, or a visual of a square graphic consisting of black and white stripes parallel to each other, at the desired frequency. Figure 2.15 shows the first case in a) and the inverse case in b). The spatial frequency is determined by the size and number of cells of the stimulus [124]. For example, Figure 2.15 c) shows a 6 cm chess board consisting of 4 x 4 pixels, while d) shows a 3 cm chess board consisting of 2 x 2 pixels.

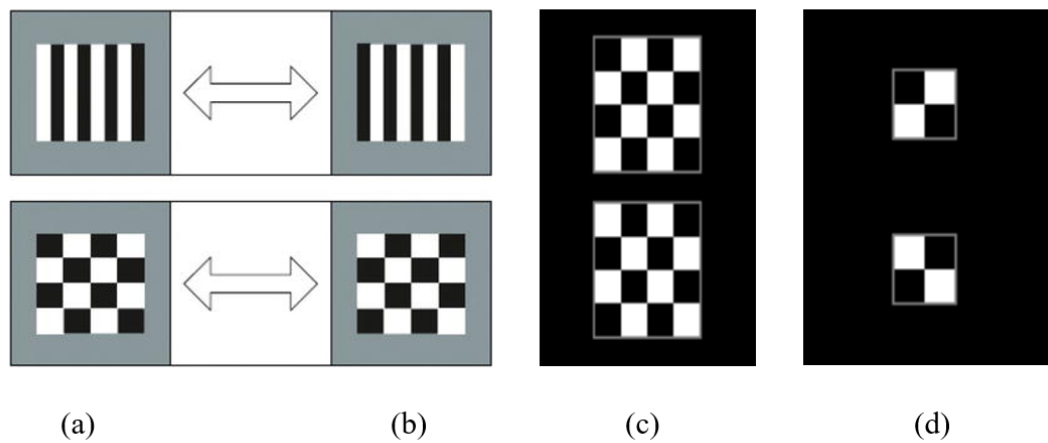


Figure 2.15 The complex stimulus designed for the SSVEP response is a) initial version b) inverted version [110] c) 4 x 4 dimension and d) 2 x 2 dimension [124].

- **Stimulation Source:** Another important factor affecting both comfort and performance is the stimulation source. There are two methods used as a source of stimulation [130]:

- Light / lamp
- Computer monitors

When the sources used to obtain visual stimuli are examined, Cathode Ray Tube (CRT), LCD and LED sources are frequently found [123]. In a study comparing the amplitudes of SSVEP signals resulting from visual stimuli obtained using LED light, CRT monitor and LCD monitor, it was observed that the amplitude of the SSVEP signal obtained when using LED light was significantly higher than the monitors [123]. Although high amplitude SSVEP signal is obtained by using LED light, external hardware is needed to use LED lights. Therefore, the flexibility and portability of the system decreases. On the other hand, when CRT and LCD are compared, it has been observed that CRT monitors have a constant vibration that can create an unwanted SSVEP response at the refresh rate [131]. In contrast, LCDs do not have this problem, but generally lower contrast and refresh rates have occurred. Still, computer monitor stimulation has the advantage that monitors can be found everywhere and can be easily integrated into a computer-based system. Therefore, when the monitor is used, the visual stimulus is controlled from the computer through software, and signal processing applications are also carried out on the same computer at the same time. This provides the system with flexibility by reducing the hardware dependency of the BCI system. In the vast majority of SSVEP based BCI studies, the monitor is used as a source of visual stimuli [123].

- **Frequency:** SSVEP-based BCIs often use the frequency feature distinctively to determine which target the user will focus on. For this reason, the system should use the same number of targets that can be distinguished from each other during the signal processing phase, as well as the number of targets it will use as a control signal. According to research, high frequencies are more comfortable and safe than low frequencies [130]. However, they produce a

smaller response and may not be produced by most computer monitors. Because computer monitors have refresh rates that determine which frequencies can be displayed correctly. A device with a refresh rate R can generate the R / k frequency set correctly, where $k \geq 2$. Other frequencies can only be generated approximately. It has been shown that using frequencies that the monitor can generate accurately can significantly improve performance [123].

2.6.3 Signal acquisition and preprocessing

Signal acquisition: Because the SSVEP signal is at low volts, it is first amplified, digitized, and preprocessed ready for processing and analysis then recorded [3].

Preprocessing: The purpose of the preprocessing step is to strengthen the SSVEP signal and increase the signal to noise ratio (SNR) [53, 132]. The low SNR value means that the information received by the brain remains behind other signals; in other words, it is challenging to detect valuable information. However, the high SNR value, on the contrary, makes it easier to obtain the desired information in the BCI system. Filtering techniques combined with transform techniques are used in the BCI system in the preprocessing step [133]. With these techniques, while the SNR value increases, unwanted signals are eliminated.

Since the amplitude of SSVEP signals is very low, it easily contains various physiological and electromagnetic sources [134]. It is affected by devices that emit electromagnetic waves during measurement and physiological artefacts such as muscle and eye movements. Besides, brain activities not associated with the SSVEP signal can also be included in the noise class [135]. Examples of electromagnetic artefacts that interfere with SSVEP signals are telephone, tablet and similar devices, electrodes, or city mains (power line) in the environment during measurement. To reduce the effects of these disruptors, all electronic devices that can be turned off and power line interference is reduced by applying a suitable spectral filter, for example, a 50Hz notch filter. On the other hand, it is challenging to avoid disruptors caused by physiological artefacts, ocular (EOG), muscles (EMG) cardiac activities (ECG), breathing and sweating. EOG and EMG are the most problematic artefacts affecting

SSVEP-based BCI, but these artefacts can be detected in the SSVEP signal and reduced by various methods.

The first step of preprocessing is usually filtering. The filters applied in the systems are divided into two groups as frequency-based filters and spatial filters [136]. Frequency-based filters are notch filters and band-pass filters. These filters can be applied to software or hardware. Some data acquisition units contain these filters. Using a band-pass filter, the signal is limited in a specific frequency band to include stimulus frequency and harmonics. Since the band-pass filter used in the studies uses visual stimulus in the low-frequency band, the frequency range is narrow and covers the low and mid-band frequencies. The notch filter is used to remove the mains frequency from the system [134].

2.6.4 Feature extraction

SSVEP signals are usually recorded with a series of electrodes ranging from 1 to 512 and a sampling frequency ranging from 100 Hz to 1000 Hz [80, 136]. Therefore, the number of data obtained is quite high. To get the best performance from the system, it is necessary to work with fewer data describing some relevant features of the signals. These data are defined as signal-specific "features". The features are usually collected in a vector known as the "feature vector" [80, 136]. Thus, feature extraction is defined as a process that receives one or more signals in a feature vector. Determining and removing useful features suitable for the signal structure from the signals is a crucial step in BCI design [53]. That is if the features extracted from SSVEP are not signal related or do not define the neurophysiological signals used well, the machine learning algorithms that make up the output of the system will have difficulty in determining the mental state of the user. Thus, the accuracy of recognition rates of the classification results will be very low [80]. Therefore, even if raw signals can be used as the input of the machine learning algorithm for some signals, it is essential and generally recommended to select and extract useful features to maximize the performance of the system by facilitating the task of the machine learning algorithm. Also, according to some studies, the selection of an excellent preprocessing and feature extraction method has been shown to have more

impact on the final performance than the choice of a good machine learning algorithm [80, 132, 134].

Numerous feature extraction techniques have been researched and proposed for EEG-based BCI systems [132, 134, 137]. These techniques can be divided into four main groups [80]:

- 1) methods that use temporal information embedded in signals,
- 2) methods using frequency information,
- 3) hybrid approaches based on time-frequency representations using both temporal and frequency information,
- 4) and other methods (e.g. spatial information, etc.).

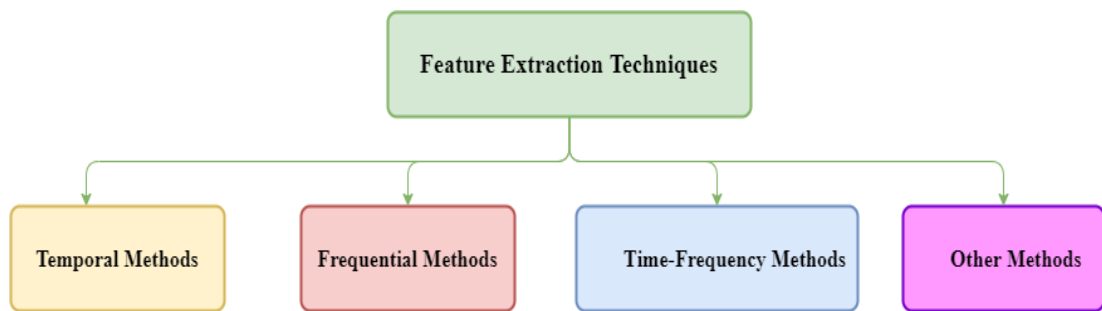


Figure 2.16 Feature extraction methods.

2.6.4.1 Temporal methods

Temporal methods use the temporal change characteristics of the signals as feature vectors. These methods are used primarily to identify neurophysiological signals with a precise and specific time signature, such as P300 or ERS - ERD, especially those triggered by motor images [80, 99, 100]. Among these temporal feature extraction methods, we can find the amplitude, statistical values, Mean Absolute Value, Slope Sign Changes, Zero Crossings, autoregressive parameters or Hjorth parameters of the raw EEG signals.

2.6.4.2 Frequential methods

EEG signals consist of a series of specific oscillations known as brain waves (rhythms) [138], which are also described in Brain Architecture in section 2.1. Performing a particular mental task that the BCI user focuses on changes the

amplitude of these different rhythms. Besides, in SSVEP signals, oscillations with frequencies synchronized with the stimulus frequency are expected [24, 25]. Therefore, it seems necessary to use frequently used frequency information embedded in EEG signals [139]. Two frequency-based methods and variations are often used in research. These are band power features and power spectral density features.

2.6.4.3 Time-frequency representations

Given that the neurophysiological signals (EEG, EMG, EOG, etc.) used in a BCI generally have specific properties in both temporal and frequency domains [53], time-frequency methods that can be seen as hybrid were used for the BCI design. These methods are based on various time-frequency representations and are extracted from signal information, both frequency and temporal [132]. The main advantage of these time-frequency displays is that they can capture relatively sudden temporal information. On the contrary, frequency methods assume that the signal is in a steady state.

2.6.4.4 Other feature extraction methods

Apart from the time domain, frequency domain and time-frequency features, other feature extraction methods were also used in BCI design [80]. Among these methods, methods based on interactions between signals can be mentioned. Because measuring the consistency of phase synchronization between sensors has proven to be effective for extracting EEG features in BCI [134]. Similarly, identification of EEG signals has made it possible to distinguish between different brain states thanks to brain link graphs. Using the interactions between the sensors, the fractal size of the signals or their multiple fractal spectrum has been used as features for BCI [134]. Finally, several studies have shown that using features extracted using different methods may result in increased system performance [80, 140, 141, 142].

Although many feature extraction methods have been proposed for BCI, it is challenging to identify the most efficient ones due to lack of comparison [80]. It is also essential to obtain a small number of features that represent context-specific information to achieve good performances. Therefore, it is vital to use adjustable

features (i.e. band power features in which frequency bands can be adapted to the subject) and dimensionality reduction or feature selection techniques to facilitate the subsequent operation of the classifier [143]. Although relatively many feature extraction techniques have been proposed, it is a fact that the BCI community should investigate and analyze new feature extraction methods and concepts. More precisely, it is crucial to have more interpretable BCI to find features that will lead to more efficient BCI design in terms of accurate recognition rates and to learn more about the mental processes that BCI users use to control the system.

2.6.5 Classification

The third important step in identifying neurophysiological signals in an SSVEP-based BCI is to convert features to desired outputs. This step is called "classification". The purpose of the classification step is to assign a class to the feature vector previously extracted automatically. This class represents the type of mental task performed by the BCI user. Classification is carried out using algorithms known as "machine learning". Machine learning algorithms can learn how to define the class of a feature vector through training sets. These sets consist of feature vectors labelled with their belonging classes [144, 145].

2.6.6 Evaluation of classification

While training machine learning algorithm to classify SSVEP signals is an important step, it is essential to consider how the algorithm is generalized on unprecedented data (test set) [145]. We need to know if the algorithm works correctly and whether we can trust its predictions. The machine learning algorithm can only memorize the training set. Therefore, it can make reasonable predictions about future examples or examples that it has not seen before. Thus, it is one of the essential steps for BCI systems to know and apply the techniques used to evaluate how well a machine learning model generalizes to new, unprecedented data [146].

Model Evaluation Techniques

The model assessment step is an integral part of the model development process. It helps to find the best model that represents our data and how well the chosen model will work in the future. Methods for evaluating the performance of a classification

model generally divided into two categories: Hold-out and Cross-validation (CV) [145]. Both methods use a test set to evaluate model performance. It is not recommended to use the previously used data to assess the model. Because our model will remember the entire training set and therefore, will always predict the right label for any data in the training set, this is called “overfitting” [144].

Hold-out technique

The purpose of the hold-out evaluation is, as mentioned earlier, to test a model on different data than it is trained. This method provides an unbiased estimate of learning performance [145].

In this method, the dataset is randomly divided into three subsets:

1. Training set: A subset of the data set used to create predictive models.
2. Validation set: It is a subset of the data set used to evaluate the performance of the model created during the training phase. It provides a testing platform to fine-tune the parameters of a model and choose the model that performs best.
3. Test set (Unprecedented data): It is a subset of the data set used to evaluate the possible future performance of a model. If a model fits the training set better than the test set, this is due to overfitting.

The hold-out approach is useful due to its speed, simplicity and flexibility. However, this technique is generally compatible with high variability because differences in the training and test dataset can cause significant differences in accuracy estimation [145].

Cross-validation technique

Cross-validation (CV) is a technique that includes dividing the original observation dataset into a training set used to train the model and an independent set used to evaluate the analysis [146].

The most common CV technique is k-fold cross-validation, where the original data set is subdivided into k equal-sized sub-samples called folds. k is a user-determined number, usually 5 or 10 as the preferred value, this is repeated k so that each time

one of the k subsets is used as the test set/validation set, and the other $k-1$ subsets are combined to form a training set. Error estimation is averaged in all k trials to obtain the total effectiveness of our model. If k is equal to the sample size, this is called "leave-one-out" [147].

For example, when performing 5-fold cross-validation, the data is first divided into five parts (approximately) of equal size. Many models are trained. The first model is trained using the first fold as the test set, and the remaining folds are used as the training set, this is repeated for each of these five folds of data, and the accuracy estimate is averaged in all five trials to obtain the total effectiveness of our model [148].

As can be seen, each data element is used precisely once in a test set and $k-1$ is used once in a training set, this significantly reduces bias as we use most of the data for the training set, and significantly reduces the variance as most of the data is also used in the test set. Changing training and test sets also contributes to the effectiveness of this method [145].

Model Evaluation Metrics

Model evaluation metrics are required to measure model performance. The choice of assessment metrics depends on a particular machine learning task (such as classification or regression) [145]. Also, some metrics, such as sensitive recall, are useful for multiple tasks. Supervised learning tasks such as classification and regression constitutes most of the machine learning applications, including this thesis study. Some of the most commonly used metrics for these two supervised learning models are confusion matrix, logarithmic loss, area under the curve (AUC).

The confusion matrix is used in this thesis, and it will be discussed in detail in section 3.5.2.

3. MATERIAL AND METHODS

3.1 Data Set Description and Preprocessing

In this thesis, the data set (AVI SSVEP Dataset) containing steady-state visual evoked potential signals designed and recorded by Adnan Vilic was used [149]. The data set contains data that include EEG measurements of healthy individuals looking at the repetitive flashing target to trigger responses of SSVEP signals at different frequencies, and the data set is free. All data were recorded using three electrodes (Oz, Fpz, Fz). Using the standard international 10-20 system for electrode placement, the reference electrode is positioned in Fz with the signal electrode in Oz and Fpz in the ground electrode. Impedances are kept at $5k\Omega$ or below. The amplifier used is g.USBamp from g.tec (Guger Technologies) set to a 512 Hz sampling rate. Figure 3.1 shows the electrode cap used for all experiments and the layout of the electrodes.

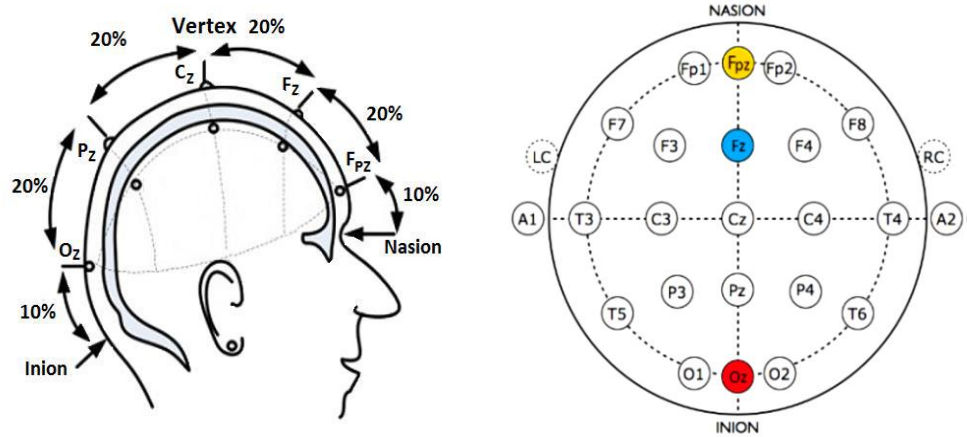


Figure 3.1 Electrode placement throughout experiments using 10-20 system (left), and electrodes used in this study (right) [149].

Subjects sat in front of an LCD computer display with a refresh rate of 120 Hz. Contrast and brightness are set to maximum. In addition, the screen resolution is 1680x1050 pixels. The targets presented to the subjects were arranged to have an area of 2.89 cm^2 . An application was developed in Microsoft Silverlight to display the visual stimulus to subjects and was run on a Windows 8-based computer. An analogue notch filter was applied to the data obtained at interference frequency (50Hz) [149]. The data were saved as .mat files opened using Matlab or Octave. As

an alternative file archive, raw EEG and target frequencies are created in .csv (comma-separated values) files that can be opened by any text editor. The difference between these two file types (.mat and .csv) is that .mat files contain more metadata about installation.

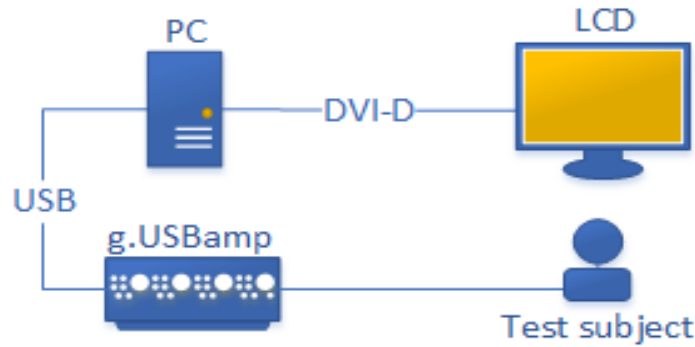


Figure 3.2 Hardware installation for experiments [149].

In this experiment, individuals have seated 60 cm away from a monitor staring at a single repetitive flashing target whose colour changed rapidly from black to white. The test stimulus is a flashing box at seven different frequencies (6 - 6.5 - 7 - 7.5 - 8.2 - 9.3 - 10 Hz) presented on the monitor. The data set consists of four sessions with four different participants. Each session in a session lasts 30 seconds and participants take a short break between trials. Experiments were repeated at least three times for each frequency. Table 3.1 presents a list of physiological knowledge (gender and age) of healthy individuals who participated in the experiment.

Table 3.1 List of participants for single target flickering (Male (M), Female (F)).

LIST OF PARTICIPANTS IN SINGLE TARGET STIMULATION				
Participant	1	2	3	4
Gender	M	M	M	F
Age	32	27	27	31

3.2 Feature Extraction

It is possible to define the neurophysiology of the human visual system, the neuronal activity of the visual cortex is replaced by visual stimulation, and variations of the brain response related to the features of the visual stimulus such as brightness, contrast and frequency [27, 28]. Neurons in the visual cortex synchronize their flickering to the frequency of blinking of the visual stimulus. Steady-state visually evoked potentials occur when visual stimuli are repeatedly presented, creating almost sinusoidal oscillations [26]. The SSVEP response shows an increase in energy at the same frequency of the blinking stimulus [26, 27, 28]. The strongest response occurs in the visual cortex of the brain (occipital), but other areas of the brain are also activated to different degrees [24, 25]. SSVEP marks can be detected even for narrow frequency bands around the visual stimulation frequency with signal processing methods that take advantage of the specific features of the signal such as timing, frequency and rhythm [23]. SSVEP-based BCI systems use visual stimulation as a way to evoke a particular electrical pattern in the visual (occipital) cortex [29]. Unlike independent EEG based BCI systems where the application is based on voluntary control of the subject's neural activity, the operation of SSVEP systems depends on the intended action, that is, the subject's ability to focus, fix (correct) and follow visual stimuli [20, 22, 23]. In addition, this thesis is on accepted signal processing strategies that validate the comprehensive scenarios analyzed.

Performance of SSVEP based BCI systems depends on the signal analysis used, feature extraction, and classification methods [23, 29, 30, 53]. For this purpose, analyzes were made by extracting features from three different domains (time, frequency and time-frequency) containing the signal's information.

3.2.1 Time-domain based feature extraction

The EEG time domain features are extracted from information in the original field (i.e. time-domain) of the EEG signal. Table 3.2 describes the relevant and distinctive EEG time-domain features we identified. These features are based on the amplitude (e.g. Average amplitude change value, root mean square, interquartile ranges, etc.)

and statistical changes of the EEG signal (e.g., mean, variance, skewness, and kurtosis, etc.) [150, 151, 152, 153].

Table 3.2 EEG time-domain features (EEG signal is represented by x , and $F_i^{(t)}$ stands for the EEG features computed from x).

EEG TIME-DOMAIN FEATURES ($F_i^{(t)}$)			
No.	Features	No.	Features
1.	EEG minimum value	14.	Kurtosis of EEG signal
2.	EEG maximum value	15.	Skewness of EEG signal
3.	EEG mean value	16.	Hjorth identifiers: 1) Activity
4.	EEG standard deviation value	17.	Hjorth identifiers: 2) Mobility
5.	Integrated EEG value	18.	Hjorth identifiers: 3) Complexity
6.	Mean absolute value	19.	Signal range (max-min.)
7.	Simple square integral value	20.	Inter-quarter intervals 1st Quartile
8.	EEG variance value	21.	Inter-quarter intervals 2nd Quartile (Median)
9.	Root mean square value	22.	Inter-quarter intervals 3rd Quartile
10.	Waveform length value	23.	Zero-crossing
11.	Average amplitude change value	24.	Slope-change value
12.	Absolute difference in standard deviation	25.	Mode value of the signal
13.	Maximum fractal length		

The formulas of the time-domain based features which are examined within the scope of this thesis and summarized in Table 3.2 are given below:

$$\text{Minimum value} \quad F_1^{(t)} = MIN = \min(x_n) \quad (3.1)$$

$$\text{Maximum value} \quad F_2^{(t)} = MAX = \max(x_n) \quad (3.2)$$

$$\text{Mean value} \quad F_3^{(t)} = MEAN(\bar{x}) = \frac{1}{N} \sum_{n=1}^N x_n \quad (3.3)$$

$$\text{Standart deviation value} \quad F_4^{(t)} = STD(\sigma) = \sqrt{\frac{1}{N} \sum_{n=1}^N (x_n - \bar{x})^2} \quad (3.4)$$

$$\text{Integrated EEG} \quad F_5^{(t)} = IEEG = \sum_{n=1}^N |x_n| \quad (3.5)$$

$$\text{Mean Absolute Value} \quad F_6^{(t)} = MAV = \frac{1}{N} \sum_{n=1}^N |x_n| \quad (3.6)$$

$$\text{Simple Square Integral} \quad F_7^{(t)} = SSI = \sum_{n=1}^N |x_n|^2 \quad (3.7)$$

$$\text{Variance of EEG} \quad F_8^{(t)} = VAR_t = \frac{1}{N-1} \sum_{n=1}^N (x_n - \bar{x})^2 \quad (3.8)$$

$$\text{Root mean square} \quad F_9^{(t)} = RMS = \sqrt{\frac{1}{N} \sum_{n=1}^N x_n^2} \quad (3.9)$$

$$\text{Waveform Length} \quad F_{10}^{(t)} = WL = \sum_{n=1}^{N-1} |x_{n+1} - x_n| \quad (3.10)$$

$$\text{Average amplitude change} \quad F_{11}^{(t)} = AAC = \frac{1}{N} \sum_{n=1}^{N-1} |x_{n+1} - x_n| \quad (3.11)$$

$$\text{Absolute differ. in std.} \quad F_{12}^{(t)} = DASDV = \sqrt{\frac{1}{N-1} \sum_{n=1}^{N-1} (x_{n+1} - x_n)^2} \quad (3.12)$$

$$\text{Maximum fractal length} \quad F_{13}^{(t)} = MFL = \log_{10} \left(\sqrt{\sum_{n=1}^{N-1} (x_n - x_{n+1})^2} \right) \quad (3.13)$$

$$\text{Kurtosis value} \quad F_{14}^{(t)} = K = \frac{1}{N} \sum_{n=1}^N \frac{(x_n - \bar{x})^4}{\sigma^4} \quad (3.14)$$

$$\text{Skewness value} \quad F_{15}^{(t)} = Sk = \frac{1}{N} \sum_{n=1}^N \frac{(x_n - \bar{x})^3}{\sigma^3} \quad (3.15)$$

$$\text{Hjorth (Activity)} \quad F_{16}^{(t)} = A = \text{Variance} (x(n)) = \frac{1}{N} \sum_{n=1}^N (x_n - \bar{x})^2 \quad (3.16)$$

$$\text{Hjorth (Mobility)} \quad F_{17}^{(t)} = M = \sqrt{\frac{A \left(\frac{dx(n)}{dn} \right)}{A(x(n))}} \quad (3.17)$$

$$\text{Hjorth (Complexity)} \quad F_{18}^{(t)} = C = \frac{M \left(\frac{dx(n)}{dn} \right)}{M(x(n))} \quad (3.18)$$

$$\text{Signal Range} \quad F_{19}^{(t)} = R = \max(x_n) - \min(x_n) \quad (3.19)$$

$$\text{First quartile} \quad F_{20}^{(t)} = Q_1 = x \left[\frac{(N+1)}{4} \right] \quad (3.20)$$

$$\text{Inter-quartile (median)} \quad F_{21}^{(t)} = Q_2 = Q_3 - Q_1 = x \left[\frac{3(N+1)}{4} \right] - x \left[\frac{(N+1)}{4} \right] \quad (3.21)$$

$$\text{Third quartile} \quad F_{22}^{(t)} = Q_3 = x \left[\frac{3(N+1)}{4} \right] \quad (3.22)$$

$$\text{Zero-crossing value} \quad F_{23}^{(t)} = \frac{1}{2N} \sum_{n=1}^{N-1} |\text{sign}[x_i(n)] - \text{sign}[x_i(n-1)]| \quad (3.23)$$

$$\text{sign}[x_i(n)] = \begin{cases} 1, & x_i(n) \geq 0, \\ -1, & x_i(n) < 0. \end{cases}$$

$$\text{Slope change value} \quad F_{24}^{(t)} = SC = \sum_{n=1}^{N-1} [f[(x_n - x_{n+1}) \cdot (x_n - x_{n+1})]] \quad (3.24)$$

$$f(x) = \begin{cases} 1, & \text{if } x \geq \text{threshold}, \\ 0, & \text{otherwise.} \end{cases}$$

$$\text{Mode value} \quad F_{25}^{(t)} = \text{Most frequent value in a data set} \quad (3.25)$$

3.2.2 Frequency-domain based feature extraction (EEG frequency-domain features)

EEG signals consist of a series of specific oscillations known as rhythms, as mentioned earlier. Performing a specific mental, sensory or visual task changes the amplitude of these rhythms [24, 138]. Moreover, signals such as SSVEP are identified by oscillations with frequencies synchronized with the stimulus frequency [25]. For this reason, many EEG-based BCI systems use frequency information embedded in the signal in the feature extraction process. In the literature, spectral estimation methods are generally used [21, 125, 132-137, 140-142, 153, 154]. Within the scope of this thesis, EEG frequency features were extracted from the frequency domain representation of the EEG signal using a Fourier transform. The relevant and distinctive EEG frequency characteristics we detected are based on the spectral information of EEG signals for each EEG rhythm, such as energy, variance and spectral entropy.

These features explain how power, variance, and irregularity (entropy) change in some related frequency bands. In practice, this means that these features will use their power in certain frequency bands [133, 151].

- 1) Features based on power spectrum, energy of each frequency band,

$$F_1^{(f)} = Energy_f = \sum_{k=1}^M y(k)^2 \quad (3.26)$$

Here is the Fourier transform of the analytic signal y of a real discrete time EEG signal x .

$F_1^{(f)} = E_f$ stands for the EEG features computed from y , and M corresponds to the maximum frequency.

- 2) Features based on variance of each EEG frequency band

$$F_2^{(f)} = Variance_f = \frac{1}{M-1} \sum_{k=1}^M (y_k - \bar{y})^2 \quad (3.27)$$

“ \bar{y} ” in the formula gives the average of the “ y ” signal.

- 3) Feature based on entropy of each EEG frequency band: Spectral entropy measures the regularity of the power spectrum of EEG signal

$$F_3^{(f)} = Entropy_f = \frac{1}{\log(M)} \sum_{k=1}^M P(y(k)) \log P(y(k)) \quad (3.28)$$

3.2.3 Wavelet transform based feature extraction

As the last feature extraction method, the features are extracted by using Discrete Wavelet Transform (DWT) including time-frequency domain properties [155]. Discrete wavelet decomposition was applied for the signal used, and the features were extracted from SSVEP signals using wavelet transform. In signal processing with wavelet transform, selecting a suitable mother wavelet is always the most important and the first step [35, 155, 156, 157]. Different mother wavelets give different wavelet transform coefficients in the same SSVEP segment. Thus, different results are obtained in each mother wavelet [156]. Wavelet families where mother wavelet types are compared for EEG signal in the literature, and which are used in the presented study are shown in Table 3.3 and Table 3.4 respectively.

Table 3.3 Wavelet families in the literature used for mother wavelet comparisons of the EEG signal.

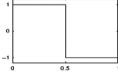
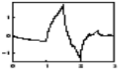
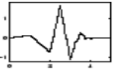
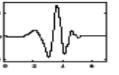
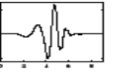
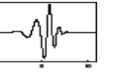
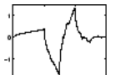
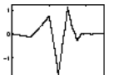
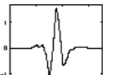
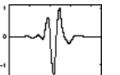
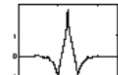


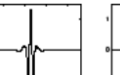

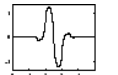

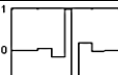

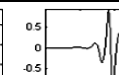

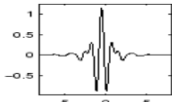
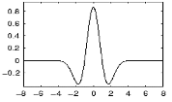
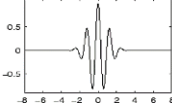
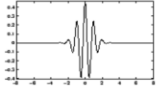
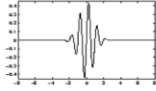
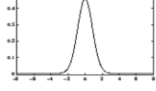
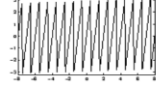
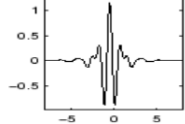
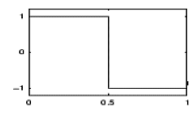
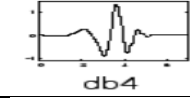
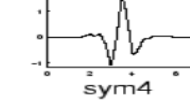
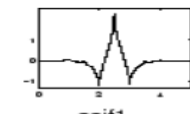
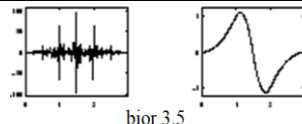
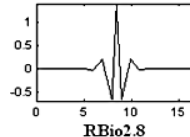
WAVELET FAMILY		
Name	Abbreviation	Representations
Haar wavelet	haar	
Daubechies wavelets	db	    
Symlets	sym	   
Coiflets	coif	    
Biorthogonal wavelets	bior	 
Reverse biorthogonal wavelets	rbio	   
Meyer wavelet	meyr	
Mexican hat wavelet (Ricker wavelet)	mexh	
Morlet wavelet	morl	
Complex Morlet wavelets	cmor	   
Discrete approximation of Meyer wavelet	dmey	

Table 3.4 Wavelet families used in this study.

WAVELET FAMILY		
Name	Abbreviation	Representations
Haar wavelet	haar	
Daubechies wavelets	db	
Symlets	sym	
Coiflets	coif	
Biorthogonal wavelets	bior	
Reverse biorthogonal wavelets	rbio	

3.2.3.1 Wavelet decomposition

EEG signal is non-stationary [12] [24], so Wavelet Transform has been used to examine not only spectral analysis of the signal but also the spectral behavior of the signal over time [157]. This method is a smooth and fast oscillating function that is well localized in frequency and time [155-157]. Wavelet transform (WT) can be applied as a specially designed dual FIR filter. The frequency responses of the FIR filters separate the high frequency and low-frequency components of the input signal [35, 155-157]. The point of dividing the signal frequency is usually between 0 Hz and half the data sampling rate (Nyquist frequency). In the multi-resolution algorithm (MRA) of the wavelet transform, the identical wavelet coefficients are used in both low-pass (LP) and high-pass (HP) filters [35]. The Low Pass filter coefficients are associated with the scaling parameter; the scale parameter will decide the oscillatory frequency and the length of the wavelet. At the same time, the High

Pass filter is associated with the wavelet function. Figure 3.3 shows the tree algorithm of an MRA of wavelet transforms for a discrete SSVEP signal sampled at 512 Hz. The outputs of the LP filters are called the approximations (a) coefficients, and the outputs of the HP filters are called the details (d) coefficients. In MRA of WT, any time-series signals can be entirely decomposed in terms of the a and d coefficients based on decomposition level, as presented in Figure 3.3. Implementation of DWT on raw signal produces an MRA of various statistical and non-statistical parameters across time and frequency. The subsets of the wavelet coefficients of the decomposition tree were selected as input vectors to the classifier. The SSVEP signals are decomposed into nine frequency, d_i is the detail band while a_i is the approximation band and $i = 1, 2, \dots, 9$ for 512 Hz sampling frequency.

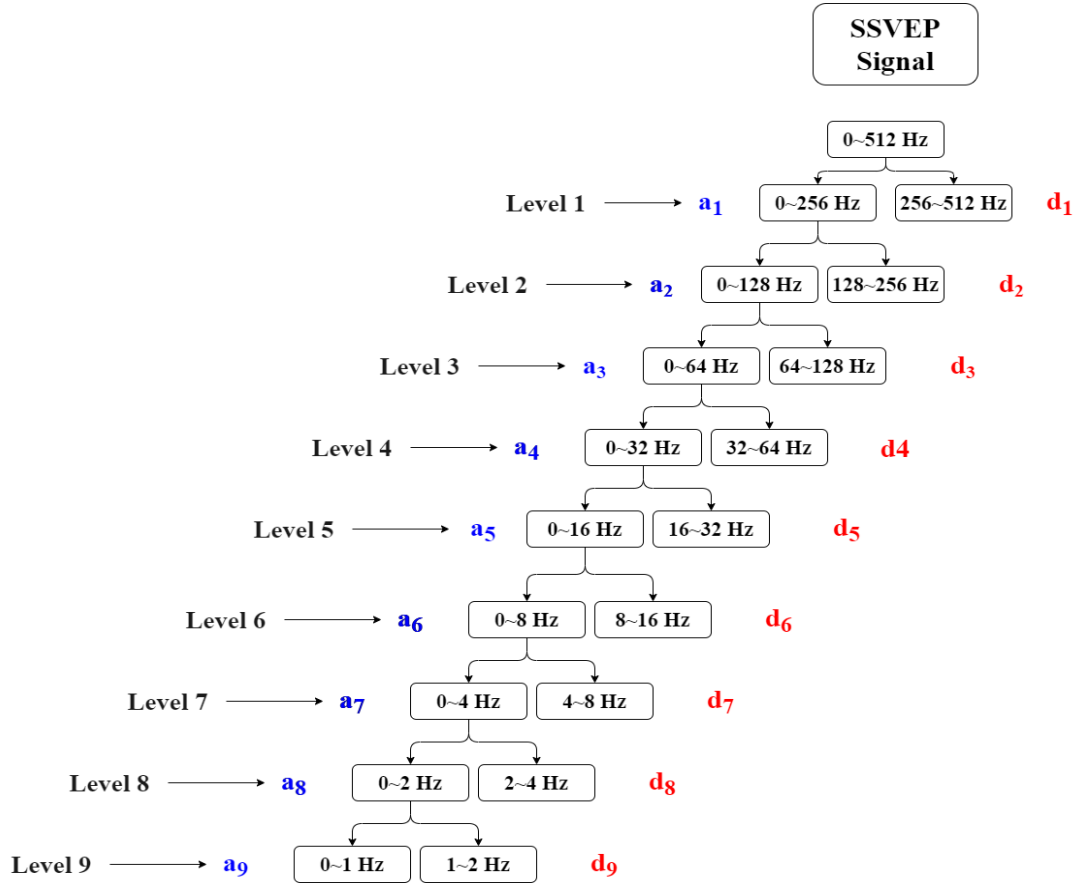


Figure 3.3 Components of wavelet coefficients and decomposition of subbands for 512 Hz sampling frequency.

3.2.3.2 Parameters for feature extraction

Using different DWT functions (Haar, Db2, Sym4, Coif1, Bior3.5, Rbior2.8), SSVEP signals are subdivided into frequency subbands (delta, theta, alpha, beta, gamma) showed in Figure 3.4, and the energy, entropy and variance values of each band calculated [35, 158-163]. As seen in Figure 3.4, each DWT frequency band is associated with one or two EEG rhythms. Thus, a number of features represented in the frequency bands were obtained.

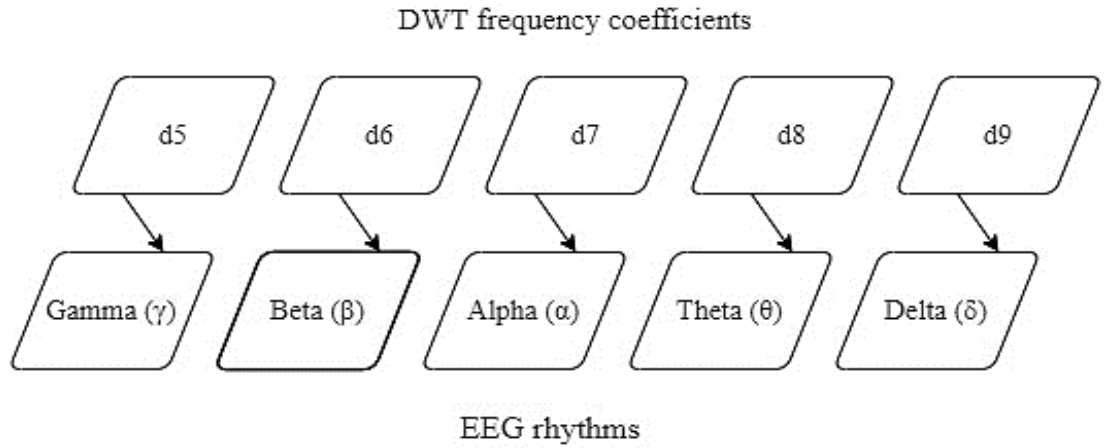


Figure 3.4 Relationship between DWT frequency coefficients and EEG rhythms.

Energy at each decomposition level was calculated using the following equations [35, 64-67, 158-163]:

$$F_1^{(w)} = Ed_i = \sum_{j=1}^N |d_{ij}|^2, \quad i = 1, 2, 3, \dots, l \quad (3.29)$$

$$F_1^{(w)} = Ea_i = \sum_{j=1}^N |a_{ij}|^2, \quad i = 1, 2, 3, \dots, l \quad (3.30)$$

where d_{ij} and a_{ij} , in the equations expresses each of the detail and approximate coefficients respectively, formed by the wavelet level corresponding to each EEG subband (delta, theta, alpha, beta, gamma). $i = 1, 2, 3, \dots, l$ is the wavelet decomposition level from levels 1 to l . Here N represents the number of detail and approximate coefficients at each decomposition level.

Another feature, the entropy at each decomposition level is calculated using the following equation [35, 44, 54, 64-67]:

$$F_2^{(w)} = Ent_i = -\sum_{j=1}^N d_{ij}^2 \log(d_{ij}^2) , \quad i = 1, 2, 3, \dots, l \quad (3.31)$$

The variance at each decomposition level was calculated using the following equation [35, 163]:

$$F_3^{(w)} = Var_i = \frac{1}{N-1} \sum_{j=1}^N (d_{ij} - \mu_i)^2 , \quad i = 1, 2, 3, \dots, l \quad (3.32)$$

Here μ_i represents the mean and is given by:

$$\mu_i = \frac{1}{N} \sum_{j=1}^N d_{ij} , \quad i = 1, 2, 3, \dots, l \quad (3.33)$$

Extracted features, which consist of different combinations, $(l + 1)$ dimensional are used as input vectors. That is to say for an ' l ' level decomposition, the feature vector of any parameter can be represented as Feature = $[xd_1, xd_2, \dots, xd_l, xa_l]$ here x is the parameter (energy, entropy and variance) [35, 163].

3.3 Feature Selection with Statistical Evidence of ANOVA

Feature selection is called the chosen or reduction of important features that will increase classifier performance and reduce our calculation time among the feature vectors after the feature extraction step [53, 143]. Since the data size decreases when the feature is selected, it does not guarantee to increase the estimation rate while it ensures to reduce the calculation load ratio [163].

In this study, wavelet features were created for the problem of distinguishing eight different frequencies, and the IBM SPSS 24 program [164] used in statistical analysis was used to see if there were significant differences between the features. One-way analysis of variance (ANOVA) was applied to see if there was a statistically significant difference between the features of the stimulation frequencies. To implement this test, it was first examined whether there was an outlier value in the data and whether it was suitable for normal distribution. No outlier data was found

during the visual inspection of the data. Then, normality tests, variance homogeneity tests, and one-way ANOVA tests were applied to the data with SPSS software. As a result of the normality test, if it was determined that the data were not suitable for normal distribution, normalization of the data was tried to be achieved by applying various transformations. The Levene test tested the variance homogeneity. Although this test will only be used in the selection of post-hoc tests to be applied according to the ANOVA test results, variance homogeneity was also tested. Finally, a one-way ANOVA test was used to check whether there was a statistically significant difference between the groups (stimulation frequencies). Although the ANOVA test shows that there is a difference between groups, it is not capable of showing which groups are separated. However, since the aim of this study was not to examine the differences in the groups with the post-hoc test, post-hoc tests were not performed. According to the selected statistical significance level (p), the features with a statistically significant difference between the measurements of stimulation frequencies were determined as the selected features. In this study, the statistical significance level (α) was chosen as 0.05.

3.4 Machine Learning Classification Algorithms

One of the most important sub-branches of supervised learning in machine learning is classification [80, 136, 139, 144, 145, 165, 166]. After feature extraction, classification is performed to recognize an SSVEP signal and convert it to command, that is, to use it as output [111]. For the classification process, the "datasets" formed by a certain number of feature vectors, of which class it belongs, are passed through the training period required by the classification type. As a result of this training, a decision mechanism algorithm is created, which is used to assign the unknown signal to the appropriate class [80, 134, 136].

In the classification phase, a single classifier was used in many EEG-based BCI systems [31-49, 80]. On the other hand, combinations of classifiers are very useful in synchronous experiments [42, 139, 152, 163, 167, 168]. In other words, measuring the performance of the system designed by looking at the performance of a single classifier may not always be the right way [80, 139, 165]. Therefore, in this thesis, feature vectors extracted from the SSVEP signal have been tested with seven basic

classifiers. The "Classifier Learner" application in the MATLAB software was used for the classification process, and the performances of all classifiers and their sub-parameters on the data were examined. These classifiers consist of the following algorithms: Decision Trees (*Fine, Medium, Coarse*), Discriminant Analysis (*Linear, Quadratic*), Logistic Regression, Naive Bayes (*Gaussian, Kernel-Based*), Support Vector Machines (*Linear, Quadratic, Cubic, Fine Gaussian, Medium Gaussian, Coarse Gaussian*), k-Nearest Neighbor (*Fine, Medium, Coarse, Cubic, Cosine, Weighted*) and Ensemble Classifiers (*Boosted, Bagged, Subspace Discriminant, Subspace KNN, RUSBoosted Trees*). Brief descriptions of each machine learning algorithm are presented below as subtitles.

3.4.1 Decision tree

The decision tree is a machine learning algorithm that separates the independent variables in the data into nodes according to information gain and gives the average in the range (learned during training) in response to a value from the relevant range during the prediction [144]. How to divide into nodes in decision tree algorithms is one factor that affects the accuracy of the tree. The creation of the lower nodes increases the homogeneity of the lower nodes. In other words, we can say that the node's purity increases according to the target variables. Therefore, decision trees use multiple algorithms to decide to split a node into two or more sub-nodes. The choice of algorithm depends on the type of target variable, but the most frequently used algorithms for categorical variables are Entropy, Gini, and Classification Error Method [80]. In this study, entropy was used. Entropy is a measure of randomness and irregularity in our data. Decision tree try to maximize information gain by making choices that reduce the entropy value (degree of randomness) of the current situation. It recalculates the error function in each node and selects the question/status with the lowest error.

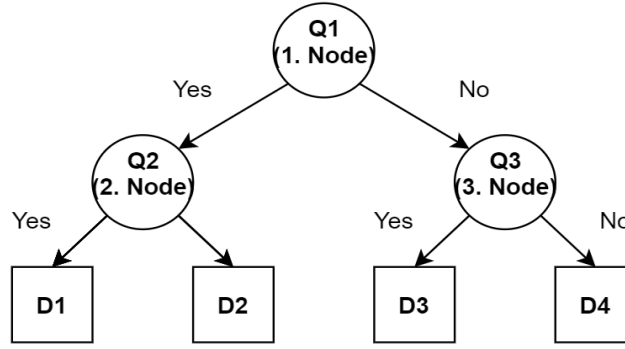


Figure 3.5 Basic structure of a decision tree classifier.

Entropy and information gain are calculated by the following equation, respectively [144]:

$$Entropy(S_i) = -\sum_{i=1}^m P_i \log_2 P_i \quad (3.34)$$

Here, p_i indicates the percentage of the group belonging to a particular class.

$$Gain(S, D) = Entropy(S) - \sum_{v \in D} \frac{|S_v|}{|S|} Entropy(S_v) \quad (3.35)$$

Here, S is the original dataset, and D is a divided part of the set. Her S_v , S 'nin bir alt kümesidir. Each S_v is a subset of S , that is, S_v is all discrete and constitutes S . In this case, information gain is defined as the difference between the entropy of the original data set before the split and the entropy value of each feature.

3.4.2 Discriminant analysis (Linear and Quadratic discriminant)

The purpose of discriminant analysis is to divide the independent variables in the data correctly into homogeneous groups [80]. Linear Discriminant Analysis (LDA) determines group elements and calculates the probability of belonging to different groups for each component. The element is then assigned to the group with the highest probability score. LDA creates a linear discriminatory function that assumes that predictors are normally distributed (Gauss distribution) and that different classes have class-specific elements and equal variance/covariance. Quadratic Discriminant Analysis (QDA) does not assume that variance/covariance is equal. So, the

covariance matrix for QDA can be different for each class. Thus it configures the discriminatory function to be of second-order [144, 145].

LDA gives better results than QDA when you have a small training set. In contrast, if the training set is too large, the classifier's variance will not be a significant problem, or if the common covariance matrix assumption for classes of data cannot be explicitly defended, QDA is recommended. Discriminatory functions of LDA and QDA are then used to classify observations. The overall fit is assessed by looking at what the group means and how well the model is classified [144].

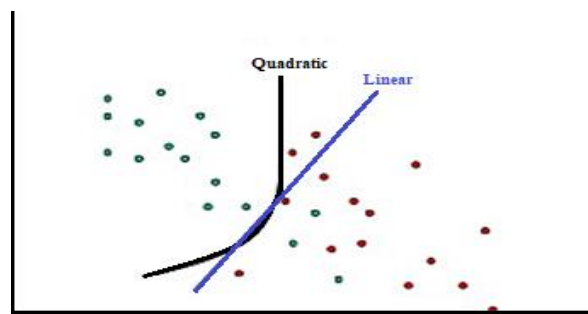


Figure 3.6 Linear vs. quadratic discriminant analysis classifiers.

3.4.3 Logistic regression

Logistic regression is used in the modeling of variables that give binary results. In models with binary status, the result is usually defined as 0 or 1. With the help of a hypothesis in logistic regression, the probability of the situation is estimated. The data extracted from this hypothesis are converted into the logistic function (log function), which creates an S-shaped curve known as "sigmoid" [144, 145].

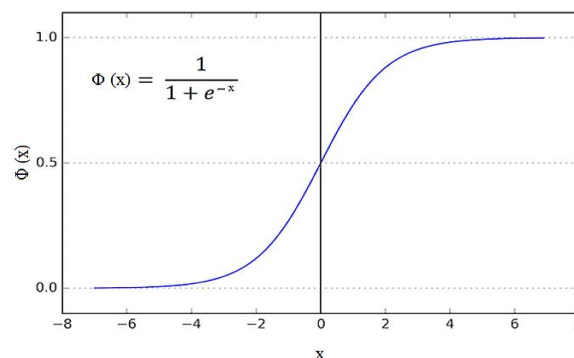


Figure 3.7 Logistic regression model.

The graphic created above is made through this logistic function [144]:

$$f(x) = \frac{1}{1+e^{-x}} \quad (3.36)$$

In this equation, ‘ e ’ represents the sigmoid curve that takes a value between 0 and 1. Accordingly, we write the logistic regression equation as follows:

$$y = \frac{e^{b_0+b_1*x}}{1+(e^{b_0+b_1*x})} \quad (3.37)$$

In this equation, b_0 and b_1 are two coefficients of input x . We estimate these two coefficients using "maximum likelihood estimation" [145].

3.4.4 Support Vector Machines

Support Vector Machines (SVM) is a supervised machine learning algorithm based on statistical learning theory found in 1963 by Vladimir Vapnik and Alexey Chervonenkis [145]. SVM is basically used to optimally separate data from two or more classes. For this, decision boundaries, or in other words, hyperplanes, are determined. SVM is divided into two groups according to whether the data set can be separated linearly or not. In the data that can be separated linearly, the hyperplane must be closest to the two classes' boundary lines for the decision line to give correct results to the new data. Vectors closest to this boundary line are called support vectors. Class labels such as -1, +1 are generally used for classification with support vector machines [80, 144]. The planes on the support vectors shown in dashed lines in Figure 3.8 are called boundary planes. The plane located in the middle of the boundary planes and equidistant from both planes is defined as the hyperplane. Figure 3.8 shows the class labels -1 and +1, the weight vector w (normal of the hyperplane), and b the slope value.

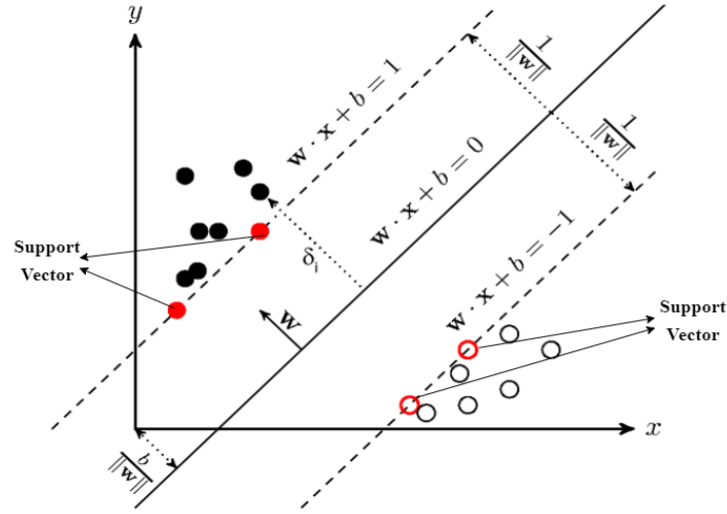


Figure 3.8 Model of SVM algorithm.

In cases where the data set cannot be classified linearly, the mapping of each data with the upper property space and its classification in this new space with the help of a hyperplane is performed using the "Kernel trick". This trick is achieved by indirectly mapping data to another space with much higher dimensions using the kernel function $K(x, y)$. The Kernels commonly used in EEG-based BCI studies are the Gauss or Radial Basic Function (RBF) [80]:

$$K(x, y) = \exp\left(\frac{-\|x-y\|^2}{2\sigma^2}\right) \quad (3.38)$$

In this equation, “ σ ” represents the RBF width.

SVM classifiers are used in many classification problems from face recognition systems to speech analysis.

3.4.5 K-nearest neighbor classifier

K-nearest neighbor (KNN) classifier was proposed in 1967 by T. M. Cover and P. E. Hart [53]. The KNN algorithm is running by using data from a sample set with certain classes. The closeness of the new data to be included in the sample data set is calculated according to the existing data, and the “K” number of neighbors are checked. Whichever of these neighbors is more, the label of the new data consist of the decision of that class [53].

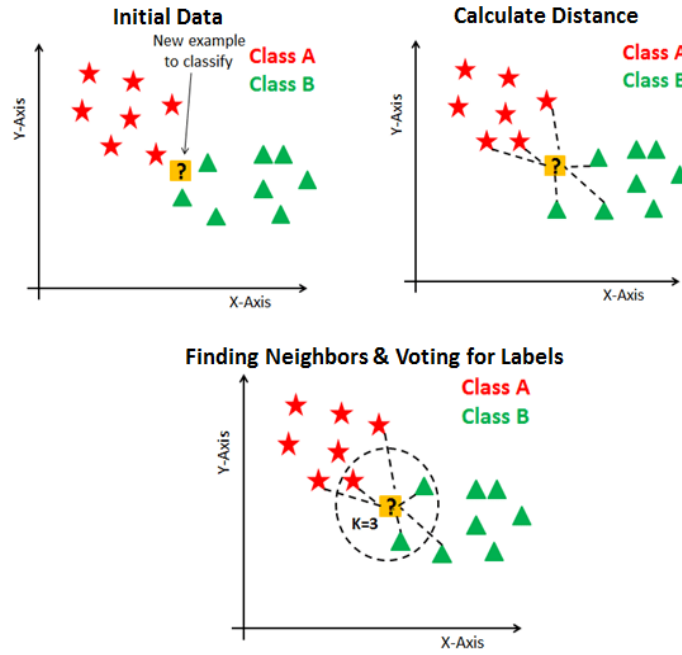


Figure 3.9 KNN step-by-step running scheme.

Generally, 2 types of distance functions are used for distance calculations:

$$Euclidean = \sqrt{\sum_{i=1}^N (x_i - y_i)^2} \quad (3.39)$$

$$Manhattan = \sum_{i=1}^N |x_i - y_i| \quad (3.40)$$

KNN is one of the most popular machine learning algorithms because it is old, simple and resistant to noisy training data. However, it also has disadvantages. The most important of these is that it requires a lot of memory space when used for big data since it stores all the situations when calculating the distance [80, 145].

3.4.6 Naïve bayes classifier

The Naïve Bayes classifier is a probabilistic approach to the pattern recognition problem that can be used with a proposition that seems quite restrictive at first glance. This proposition is that each descriptive feature or parameter to be used in pattern

recognition should be statistically independent. It is a simplified version of Bayes' theorem. Bayes' theorem is expressed by the following equation [53, 144]:

$$P(A|B) = \frac{P(B|A)P(A)}{P(B)} \quad (3.41)$$

$P(A|B)$ = Probability of event A when event B occurs

$P(A)$ = Probability of event A

$P(B|A)$ = Probability of event B when event A occurs

$P(B)$ = Probability of event B

Using the Bayes theorem, we can find the probability of being A given the B formation. Here B is proof and A is hypothesis. The assumption made here is that the predictors / features are independent. This means that the presence of a particular feature does not affect the other. So it is called “naive” [53].

3.4.7 Ensemble Learning

Ensemble learning is meta algorithms that combine multiple machine learning techniques into a single prediction model (classifier) to improve deviation (boosting) and/or predictions (stacking) and also reduce variance (bagging) [53, 144, 169, 170, 171]. According to this algorithm, single classifiers generally cannot achieve a specific and precise classification accuracy due to possible noise in the data, overlapping data distributions, and outliers. The purpose of creating the algorithm is that there is no single model (classifier) that works best for each classification problem. Therefore, ensemble learning methods are needed. An ensemble learning model is generally created in two ways [169, 170]:

- “Sequential ensemble learning methods” in which the basic learners (classifiers at the input) are produced sequentially (e.g., AdaBoost),
- “Parallel ensemble learning methods” in which basic learners are provided in parallel (e.g., Random Forest).

The purpose of the sequential ensemble learning method is to take advantage of the interdependence among the basic learners. Such as, overall performance can be improved by weighing previously mislabelled samples at a higher weight.

The primary motivation of the parallel ensemble learning method is to benefit from the independence among the basic learners. For example, by taking the average in this method, the error can be significantly reduced.

After the models are run sequentially or in parallel, the resulting model outputs are combined according to specific criteria, and the final classification decision is made. The basic framework of ensemble learning modelling is shown in Figure 3.10.

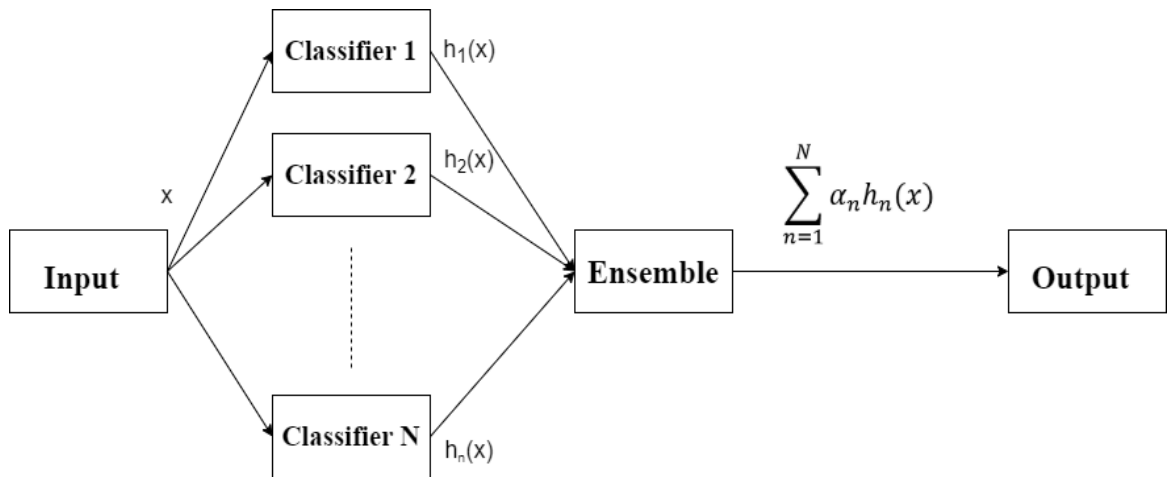


Figure 3.10 The basic model of ensemble learning classification.

Here, x represents the signal presented as an input to the models, $h_n(x)$ represents the model resulting from the classification and α_n represents the combination criteria used based on the sequential or parallel operation of the models.



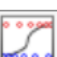
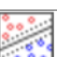



Classifier		Memory Usage	Prediction Speed	Interpretability
Decision Trees		Small	Fast	Easy
Discriminant Analysis		Small for linear Large for quadratic	Fast	Easy
Logistic Regression		Medium	Fast	Easy
Support Vector Machines		Medium for multiclass Large for binary	Medium for linear Slow for others	Easy for linear Hard for all others
Nearest Neighbor Classifiers		Medium	Medium	Hard
Naive Bayes Classifiers		Small for simple distributions Medium for Kernel distributions	Medium for simple distributions Slow for Kernel distributions	Easy
Ensemble Classifiers		Low – High Depending on choice of algorithm	Fast – Medium Depending on choice of algorithm	Hard

Figure 3.11 Summary and some important properties of classifiers used in this thesis.

The classifier properties in Figure 3.11 describe the general characteristics of speed and memory usage for all preset classifiers that cannot be optimized. The classifiers were tested with various data sets (7000 observations, 80 estimators and 50 classes) available in the literature, and the results were defined as follows [172]:

Table 3.5. Speed and memory value definitions of classifiers.

SPEED		MEMORY	
Fast	0.01 second	Small	1 MB
Medium	1 second	Medium	4 MB
Slow	100 seconds	Large	100 MB

3.5. Evaluation of Machine Learning Algorithms Performance

The k -fold cross-validation and confusion matrix evaluation criteria were used to evaluate the performance of the machine learning algorithms used in this thesis.

3.5.1 k-fold cross-validation

The feature set consisting of the features extracted from the data sets used in this thesis is divided into train and test sets. Although the classifier's parameters are adjusted using the train set, the classifier performance is tested using the test set. It is necessary to achieve a good generalization performance for a classifier [53]. One of the most commonly used methods for dividing the data set as a train and test sets is the k -fold cross-validation method [145]. In this method, the data set is randomly divided into k segments. Among these segments, $k-1$ parts are used for the training, and the remaining part is used for the testing. This process is repeated until all parts are used for testing separately. The test errors are recorded each time, and the average of the errors after the last part is reported. The performance of the classifier algorithm used is evaluated in this way [144-148]. In this study, the data set is divided into five equal parts.

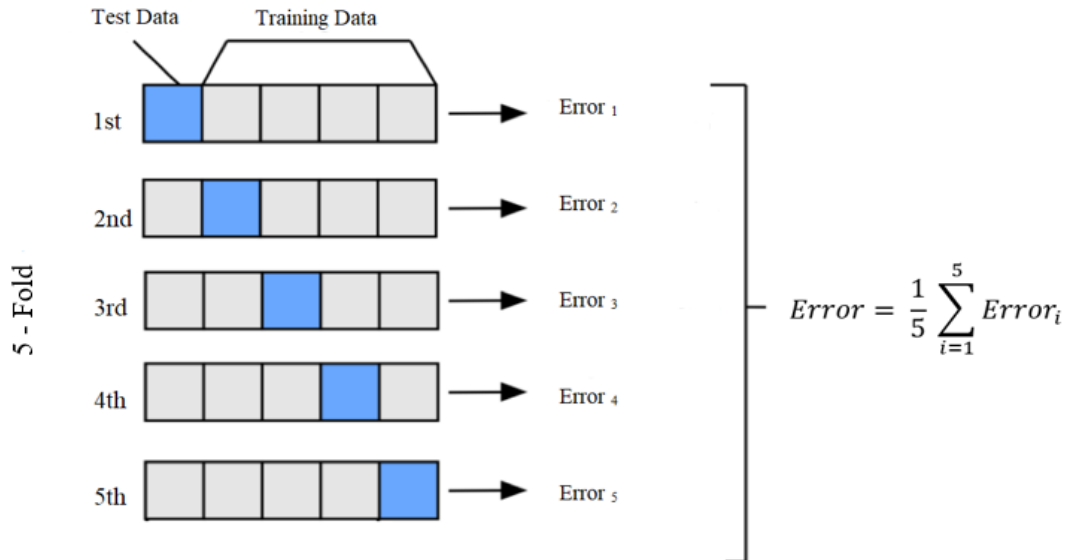


Figure 3.12 k -fold cross-validation model used in the classification of this study with $k=5$.

3.5.2 Confusion Matrix

A confusion matrix shows the number of true and false predictions made by the classification model compared to actual results in the data. The confusion matrix is $N \times N$ sized, and where N is the number of target values (classes). The performance of these models is usually evaluated using the data in the matrix. The table below shows the 2x2 confusion matrix for two classes (Positive and Negative) [144].

Table 3.6 Confusion matrix.

		TARGET (PREDICTIVE)			
		Positive (1)	Negative (0)		
MODEL (ACTUAL)	Positive (1)	a	b	Positive Predictive Value	$a/(a+b)$
	Negative (0)	c	d	Negative Predictive Value	$d/(c+d)$
		Sensitivity	Specificity	Accuracy = $(a+d)/(a+b+c+d)$	
		$a/(a+c)$	$d/(b+d)$		

The model and target values constitute the matrix, and the formulas consisting of these values are as follows:

- a: Actual true and model predicted it true
- b: Actual true and model predicted it false
- c: Actual false and model predicted it true
- d: Actual false and model predicted it false
- ✓ Positive Predictive Value: the proportion of correctly identified positive cases.
- ✓ Negative Predictive Value: the proportion of correctly identified negative cases.
- ✓ Sensitivity or Recall: the proportion of correctly identified true positive cases.
- ✓ Specificity: the proportion of correctly identified true negative cases.
- ✓ Accuracy: the ratio of the total number of correct predictions.

4. RESULTS AND DISCUSSION

The SSVEP data used in this study were obtained through open access from “<https://www.setzner.com/avi-ssvep-dataset/>.” [149] with the permission of the dataset owner. All processing, translation, and performance analyzes were implemented using MATLAB software [172] and IBM SPSS 24 package program [164]. The performance of each machine learning algorithm was evaluated by the accuracy criterion using the confusion matrix.

Characterized as an increase in the amplitude of the stimulating frequency, the photic driver response results in significant baseline and harmonics [21, 102]. Thus, it is possible to determine the stimulus frequency based on the SSVEP measurement. For this purpose, 115 feature vectors were extracted from the SSVEP signals recorded using seven different frequencies: the time domain, the frequency domain, and the time-frequency domain. The extracted feature vectors were run with 25 machine learning algorithms due to 7 basic classifiers and sub-parameters. Simultaneously, the frequencies that constitute the SSVEP data set were evaluated with multiple, selected three-class, and binary classifications. Also, the effect of the increase in the difference between frequencies on the accuracy criterion was investigated, and the results are shown in detail between figures 4.17 – 4.22.

4.1 Time-Domain Features Results

The multiple and binary classification results of 25 feature vectors extracted from SSVEP signals using time domain properties are given below, respectively.

4.1.1 Multiple classification results

According to the results obtained, the highest performance was found in the Ensemble Learning classifier with 52.40%. Considering that time domain properties do not fully reflect the frequency-based SSVEP signal, the results are not low. Because SSVEP signals do not have time-domain features like P300 signals. Also, according to the author's best knowledge, the problem of multiple classifications present in SSVEP signals has not been studied in the literature with seven classes

(commands) so far. The results appear to be relatively good and improved, compared to designs with more than three commands in the literature [173-178].

Table 4.1 Results of multiple classification for time-domain features.

SUBJECTS	ACCURACY (ACC)	CLASSIFIERS
Sub1	25.90	LDA
Sub2	50.00	Ensemble (Bagged Trees)
Sub3	52.40	Ensemble (Subspace Discriminant)
Sub4	42.90	Ensemble (RUSBoosted)
<i>Mean</i>	<i>42.80</i>	

4.1.2 Binary classification results

According to the binary classification results shown in Figure 4.1, the best performance was obtained with an accuracy value of 91.68% in 6-10 frequency pairs based on the average of the subjects. Simultaneously, when the subjects are considered separately, up to 100% results were obtained. In addition, there is no definitive finding related to the increase in the accuracy value parallel to the difference between frequencies for the time domain. When the results are evaluated in terms of classifiers, it is seen in Figure 4.2 that the best performance is in the Ensemble learning classifier.

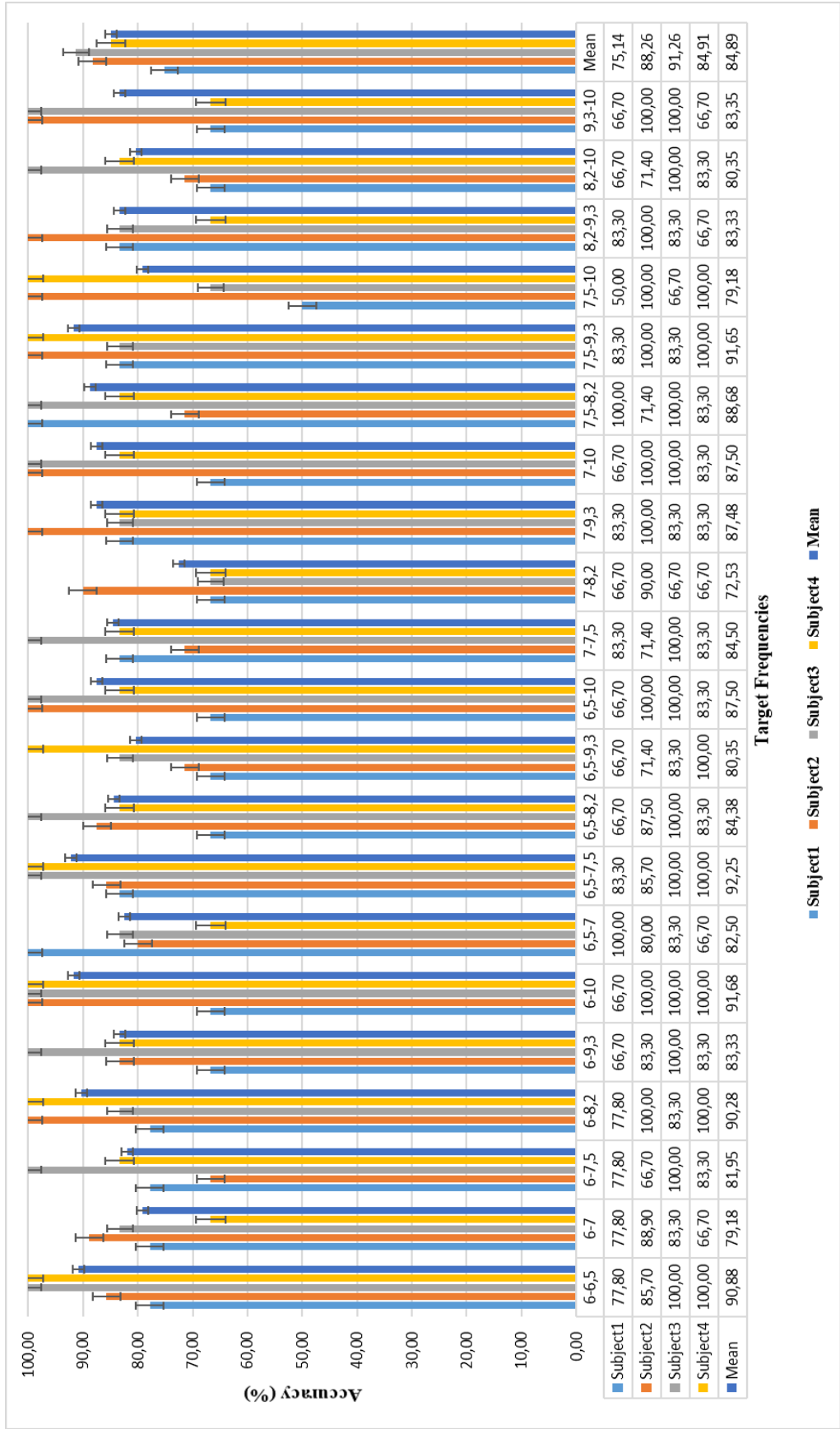


Figure 4.1 Binary classification performance of the time-domain features.

Table 4.2 Results of classification performances in terms of classifiers for time-domain features.

Classes	CLASSIFIERS			
	Subject 1	Subject 2	Subject 3	Subject 4
6-6.5	LDA, SVM (Linear), Ensemble (Subspace Discr.)	Ensemble (Subspace KNN)	LDA, Ensemble (Subspace Discr., Subspace KNN)	LDA, SVM (Linear, Quadratic, Cubic, Medium Gaussian), KNN (Fine, Weighted), Ensemble (Subspace Discr.)
6-7	LDA, Ensemble (Subspace Discr., RUSBoosted)	Ensemble (Bagged Trees)	SVM (Quadratic), Ensemble (Subspace KNN)	Naive Bayes (Kernel), KNN (Fine)
6-7.5	LDA, Logistic Regression	SVM (Linear, Quadratic), Ensemble (Bagged Trees)	Ensemble (Subspace Discr., Subspace KNN)	LDA, SVM (Linear, Cubic), KNN (Fine), Ensemble (Subspace Discr.)
6-8.2	Ensemble (RUSBoosted)	Ensemble (Bagged Trees)	Ensemble (Bagged Trees)	Ensemble (Bagged Trees)
6-9.3	Decision Tree (All), SVM (Gaussian All), KNN (All), Ensemble (Boosted)	LDA, SVM (Linear, Quadratic, Cubic), KNN (Fine)	Ensemble (Subspace KNN)	SVM (Linear, Quadratic, Cubic) KNN (Fine, Weighted)
6-10	Decision Tree (All), SVM (Gaussian All), KNN (All), Ensemble (Boosted)	LDA, SVM (Linear, Quadratic, Cubic, Medium Gaussian), KNN (Fine, Weighted), Ensemble (Subspace Discr.)	LDA, Logistic Regression, SVM (Linear, Quadratic, Cubic), KNN (Fine), Ensemble (Bagged Trees, Subspace KNN)	LDA, SVM (Cubic), KNN (Fine), Ensemble (Subspace Discr., Subspace KNN)
6.5-7	Logistic Regression	Ensemble (Bagged Trees)	Naive Bayes (Kernel)	Ensemble (Bagged Trees)
6.5-7.5	Ensemble (Subspace KNN)	SVM (Linear), Ensemble (Bagged Trees, Subspace KNN)	Ensemble (Subspace KNN)	Logistic Regression, SVM (Cubic), KNN (Fine)
6.5-8.2	Ensemble (Subspace Discr.)	KNN (Weighted), Ensemble (Subspace Discr.)	SVM (Quadratic, Cubic), KNN (Fine)	Ensemble (Subspace KNN)
6.5-9.3	Ensemble (Subspace KNN)	Ensemble (Bagged Trees, Subspace Discr.)	Naive Bayes (Kernel), SVM (Quadratic)	Logistic Regression

Table 4.2 Results of classification performances in terms of classifiers for time-domain features. **Continued.**

Classes	CLASSIFIERS			
	Subject 1	Subject 2	Subject 3	Subject 4
6.5-10	Ensemble (Subspace KNN)	LDA, SVM (Linear, Quadratic, Cubic, Medium Gaussian), KNN (Fine, Weighted), Ensemble (Subspace Discr.)	LDA, Logistic Regression, Ensemble (Subspace Discr., Subspace KNN)	LDA, Naive Bayes (Kernel)
7-7.5	KNN (Fine)	Ensemble (RUSBoosted)	Ensemble (Subspace KNN)	Logistic Regression
7-8.2	SVM (Linear SVM)	Ensemble (Subspace Discr.)	KNN (Fine), Ensemble (Subspace Discr.)	Ensemble (Subspace KNN)
7-9.3	Logistic Regression	Ensemble (Subspace KNN)	Ensemble (Subspace Discr.)	Ensemble (Subspace Discr.)
7-10	SVM (Linear), KNN (Fine), Ensemble (Bagged Trees, Subspace Discr.)	LDA, SVM (Linear, Quadratic, Cubic, Medium Gaussian), KNN (Fine, Weighted), Ensemble (Subspace Discr.)	Ensemble (Subspace KNN)	LDA
7.5-8.2	LDA	SVM (Quadratic), Ensemble (Subspace Discr.)	Ensemble (Subspace KNN)	Logistic Regression, Naive Bayes (Kernel), KNN (Fine)
7.5-9.3	Ensemble (Subspace KNN)	Ensemble (Subspace KNN)	Logistic Regression, SVM (Linear)	Logistic Regression
7.5-10	Ensemble (Subspace KNN, RUSBoosted)	LDA, SVM (Linear, Quadratic, Cubic), Ensemble (Subspace Discr.)	Ensemble (Subspace KNN)	Logistic Regression, Ensemble (Subspace KNN)
8.2-9.3	Ensemble (Subspace Discr.)	Ensemble (Subspace KNN)	LDA, Ensemble (Subspace Discr.)	Ensemble (Bagged Trees)
8.2-10	Ensemble (Bagged Trees)	SVM (Cubic)	LDA, Logistic Regression, Ensemble (Subspace Discr., Subspace KNN)	Naive Bayes (Kernel)
9.3-10	Ensemble (RUSBoosted)	Ensemble (Subspace KNN)	LDA, Ensemble (Subspace Discr.)	Logistic Regression

4.2 Frequency-Domain Features Results

For the frequency domain characteristics used in the problem of determining seven different frequencies, firstly, spectrum analysis was performed to detect the stimulus frequencies more clearly than the signal. This analysis is often used to obtain frequency information in evoked SSVEP responses. The basic idea is always the same: a flashing or moving visual stimulus at a constant frequency (stimulus frequency) reveals a response or even harmonics at the same frequency in the brain [12]. At the same time, the power spectrum of EEG signals was determined by FFT using MATLAB software to calculate its power, entropy, and variance for each band in the frequency range corresponding to the frequencies. For this purpose, the signal received FFT is divided into EEG sub-bands (delta, theta, alpha, beta, gamma), and energy, entropy, and variance values of each band are calculated. A total of 15 feature vectors are generated. The results of evaluating the generated features with machine algorithms are presented in Table 4.2 and Figure 4.4 - 4.6 with accuracy.

4.2.1 Multiple classification results

According to the multiple classification results of the seven frequencies presented in Table 4.3, it was determined that the best performance was in the Ensemble Learning classifier with an accuracy value of 57.10%. Another remarkable finding here is that the results of the classifier from all individuals are the same. This shows us that, like the time-domain, the Ensemble Learning classifier performs better than others. In addition, when multiple classification results of frequency domain features are compared with multiple classification results of time domain features, it has been determined that there is an increase of 4.70% on an individual basis and 3.18% on average.

Table 4.3 Results of multiple classification for frequency-domain features.

SUBJECTS	ACC	CLASSIFIER
Subject 1	29.20	Ensemble (Subspace Discr.)
Subject 2	50.00	Ensemble (Subspace Discr.)
Subject 3	57.10	Ensemble (Subspace Discr.)
Subject 4	47.60	Ensemble (Subspace Discr.)
<i>Mean</i>	<i>45.98</i>	

4.2.2 Selected three class classification results

In this analysis, three frequencies (6Hz - 8.2Hz - 10Hz), which are considered to increase the classification performance, were chosen among the seven frequencies present in the data set, during the feature extraction phase. The reason for choosing these frequencies are the results of the study done in reference [9] [10] and [11]. These frequencies are shown in Figure 4.2.

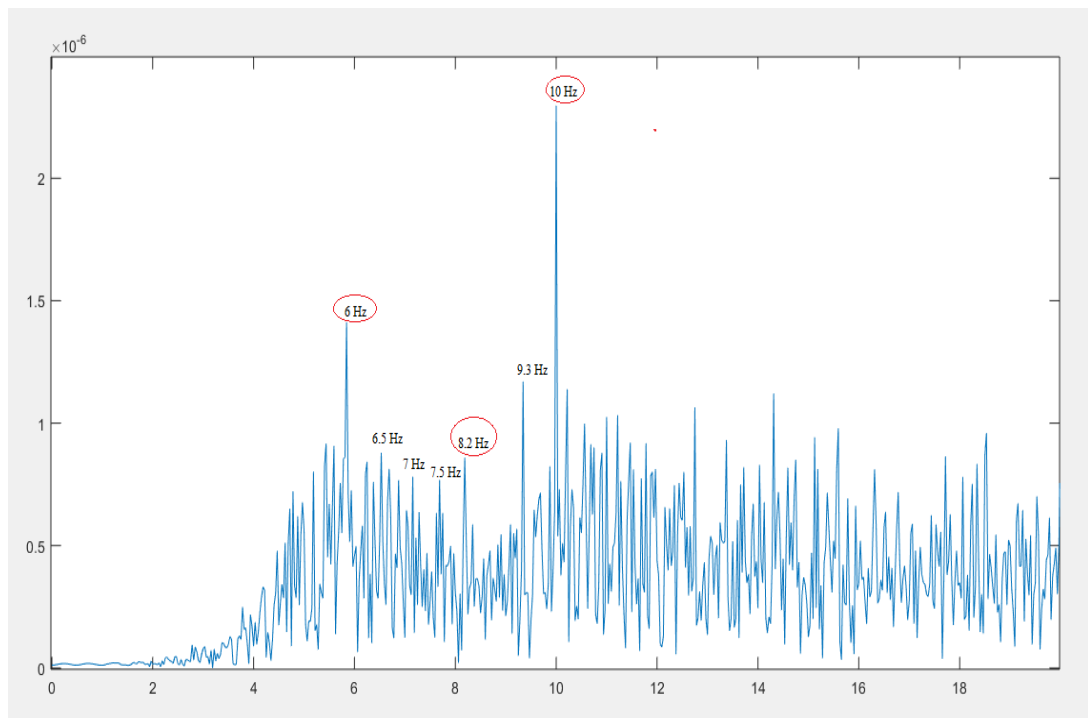


Figure 4.2 Three selected frequencies (6Hz - 8.2Hz - 10 Hz) among the seven frequencies.

In Figure 4.3, the classification results and averages of each of the four participants are presented. According to the results obtained, the highest classification performance for the first participant was 83.30% in the Ensemble Learning classifier, the highest 100% classification performance for the second participant was in the KNN and SVM classifiers, and 88.90% for the third participant in the KNN classifier. Finally, in the fourth participant, it was seen again in the Ensemble Learning classifier with 77.80%.

When the results are evaluated considering the classifiers, the performance of the six different classifiers was calculated by taking the average of the four participants and the highest performance was found in the Ensemble Learning classifier with an accuracy of 79.73%. The second highest classifier following the Ensemble Learning classifier was SVM with 70.85%, whereas k-NN was the third best performing classifier with a very small margin of 70.83%. While LDA and Naive Bayes classifiers give relatively lower results, the Decision Tree classifier appears not to be suitable for SSVEP frequency analysis.

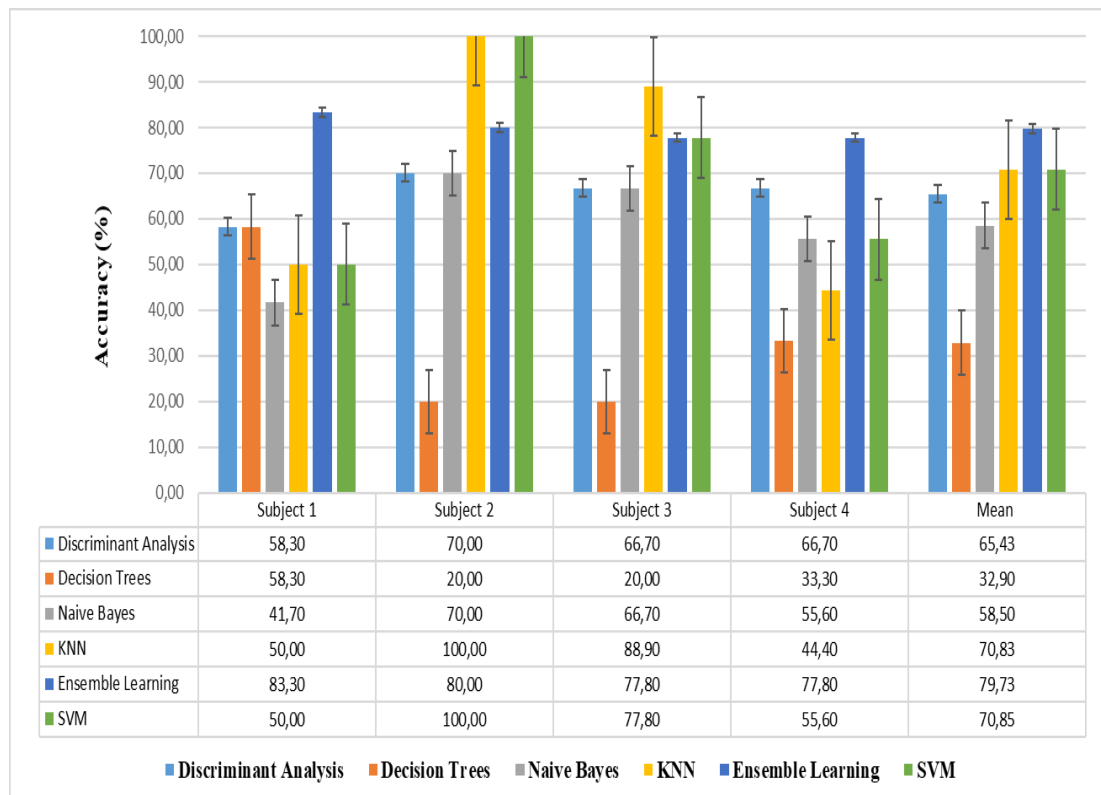


Figure 4.3 Results of selected 3-class classifications for frequency-domain features.

As a result, it has been observed that the methods used are successful by obtaining classification performances up to 100% on the basis of participants and 79.73% when the averages are examined and it can be used in a real time SSVEP based BCI design. At the same time, when comparing classifier performances among themselves, it is seen that Ensemble Learning method gives higher performance compared to other classifiers used in classifying SSVEP signals.

4.2.3 Binary classification results

Considering the averages of the binary classification results of frequency features for four participants, the performances obtained vary between the lowest 70.85% and the highest 100%. Accordingly, the highest performance was determined with 100% accuracy value in 7.5 - 10 frequency pairs. The following six highest performances are 96.43% accuracy in the 6.5 - 9.3 frequency pairs, 95.83% in the 6 - 7.5 frequency pairs, 95.83% in the 6.5 - 7.5 frequency pairs, 95.83% in the 6.5 - 8.2 frequency pairs, 95.83% in the frequency pairs 7 - 8.2, and the last it was obtained with the accuracy values of 95.83% in 7 - 10 frequency pairs. The lowest performance was found in the frequency pair 9.3-10 with an accuracy of 70.85%. It is noteworthy that the highest performance obtained is determined in the frequency pair where the difference between them is relatively high.

When the results are evaluated in terms of classifiers, it is clearly seen in Table 4.4 that the classifier that performs with the highest rate is the Ensemble Learning classifier. Another classifier that follows the Ensemble learning classifier and has obvious success has been the SVM classifier. Other classifiers following Ensemble Learning and SVM were identified as KNN, Logistic Regression and Naive Bayes classifiers, respectively. It is also seen that no successful results have been obtained in the LDA and Decision Tree classifiers.

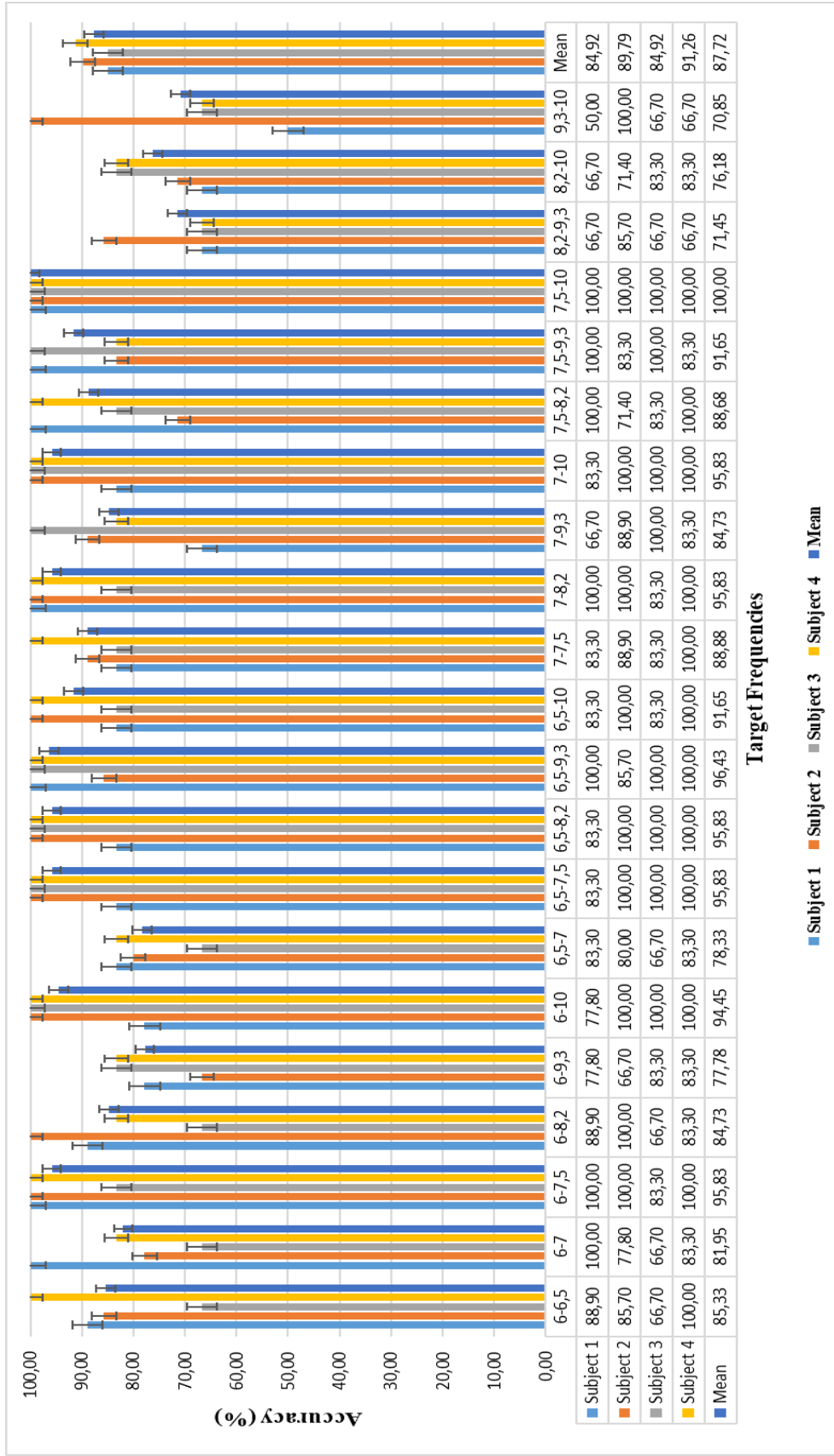


Figure 4.4 Binary classification performance of the frequency-domain features

Table 4.4 Results of classification performances in terms of classifiers for frequency-domain features.

Classes	CLASSIFIERS			
	Subject 1	Subject 2	Subject 3	Subject 4
6-6.5	Ensemble (Subspace Discr.)	Ensemble (Subspace Discr.)	Ensemble (Subspace Discr.)	Logistic Regression, Naive Bayes (Kernel)
6-7	SVM (Quadratic), Ensemble (Subspace Discr.)	Ensemble (Subspace Discr.)	Logistic Regression, Ensemble (Bagged Trees)	Ensemble (Subspace Discr.)
6-7.5	Ensemble (Subspace Discr.)	SVM (Quadratic, Cubic), KNN (Fine)	Logistic Regression, Ensemble (Subspace Discr.)	Logistic Regression, SVM (Quadratic, Cubic), Ensemble (Subspace Discr.)
6-8.2	Logistic Regression, SVM (Cubic)	Logistic Regression	Naive Bayes (Kernel), Ensemble (Subspace Discr., RUSBoosted)	SVM (Linear, Quadratic, Cubic, Medium Gaussian), KNN (Fine), Ensemble (Subspace KNN)
6-9.3	Logistic Regression, Ensemble (Subspace Discr.)	Naive Bayes (All)	Logistic Regression	SVM (Linear, Quadratic, Cubic, Medium Gaussian), KNN (Fine), Ensemble (Subspace KNN)
6-10	Logistic Regression	SVM (Linear, Quadratic, Cubic), KNN (Fine), Ensemble (Subspace Discr.)	SVM (Quadratic, Cubic), Ensemble (Subspace Discr.)	SVM (Linear, Quadratic, Cubic, Medium Gaussian), KNN (Fine)
6.5-7	Ensemble (Bagged Trees, Subspace KNN)	KNN (Fine)	Logistic Regression	SVM (Quadratic), Ensemble (Subspace Discr.)
6.5-7.5	Naive Bayes (Kernel)	Ensemble (Subspace Discr.)	Logistic Regression	Ensemble (Subspace Discr.)
6.5-8.2	SVM (Quadratic, Cubic), Ensemble (Bagged Trees, Subspace KNN)	Ensemble (Bagged Trees)	Ensemble (Subspace Discr.)	Logistic Regression, Ensemble (Subspace Discr.)
6.5-9.3	Ensemble (Subspace Discr.)	Ensemble (RUSBoosted)	Logistic Regression, SVM (Quadratic, Cubic)	Naive Bayes (Kernel), Ensemble (Subspace Discr.)
6.5-10	Ensemble (Subspace Discr.)	SVM (Linear, Quadratic, Cubic, Medium Gaussian), KNN (Fine, Weighted), Ensemble (Subspace Discr.)	Naive Bayes (Kernel), SVM (Linear, Quadratic, Cubic)	SVM (Cubic), KNN (Fine), Ensemble (Subspace Discr.)

Table 4.4 Results of classification performances in terms of classifiers for frequency-domain features. **Continued.**

Classes	CLASSIFIERS			
	Subject 1	Subject 2	Subject 3	Subject 4
7-7.5	Logistic Regression	SVM (Linear, Quadratic)	Logistic Regression, Ensemble (Subspace Discr.)	SVM (Linear, Quadratic, Cubic)
7-8.2	SVM (Quadratic, Cubic), Ensemble (Subspace Discr.)	Naive Bayes (Gaussian), SVM (Medium Gaussian), Ensemble (Subspace Discr.)	SVM (Linear)	Ensemble (Subspace Discr.)
7-9.3	Logistic Regression, Naive Bayes (Kernel), SVM (Quadratic, Cubic), KNN (Fine)	SVM (Linear), Ensemble (Subspace Discr.)	SVM (Linear, Quadratic, Cubic), KNN (Fine), Ensemble (Subspace Discr.)	SVM (Linear)
7-10	SVM (Linear), Ensemble (Subspace Discr.)	SVM (Linear, Quadratic, Cubic, Medium Gaussian), KNN (Fine, Weighted), Ensemble (Bagged Trees)	SVM (Linear, Quadratic, Cubic), Ensemble (Subspace Discr.)	SVM (Linear, Cubic), KNN (Fine), Ensemble (Subspace Discr.)
7.5-8.2	Logistic Regression, SVM (Quadratic, Cubic), KNN (Fine), Ensemble (Subspace Discr.)	Naive Bayes (Kernel), Ensemble (Bagged Trees)	SVM (Linear, Quadratic, Cubic), KNN (Fine, Weighted)	Logistic Regression, Ensemble (Subspace Discr.)
7.5-9.3	Ensemble (Subspace Discr.)	Ensemble (Bagged Trees, Subspace Discr.)	SVM (Linear, Medium Gaussian), KNN (Fine)	SVM (Linear, Quadratic, Cubic, Medium Gaussian), KNN (Fine, Weighted)
7.5-10	Ensemble (Subspace Discr.)	SVM (Quadratic, Cubic)	SVM (Quadratic, Cubic)	Logistic Regression, Ensemble (Subspace Discr., Subspace KNN)
8.2-9.3	Ensemble (RUSBoosted)	SVM (Cubic), KNN (Fine), Ensemble (Bagged Trees)	Ensemble (Subspace Discr., RUSBoosted)	Logistic Regression
8.2-10	SVM (Cubic), KNN (Fine)	Ensemble (RUSBoosted)	KNN (Fine), Ensemble (Subspace Discr.)	SVM (Cubic)
9.3-10	Naive Bayes (Kernel)	SVM (Linear, Quadratic, Cubic), KNN (Fine), Ensemble (Subspace Discr.)	Ensemble (Bagged Trees, Subspace Discr.)	Ensemble (Subspace Discr., RUSBoosted)

4.3 Wavelet Transform Features Results

This section aims to analyse the relationship between mother wavelet selection problem and frequencies by applying the DWT method, which has both time and frequency domain properties to SSVEP signal and has been proven to be successful in EEG signal analysis. For this purpose, three crucial features, such as energy, variance, and entropy, which are frequently used in DWT studies, have been extracted from the sub-bands (delta, theta, alpha, beta, and gamma) of the EEG signal. These features were generated for six different mother wavelets (haar, db4, sym4, coif1, bior3.5, rbio2.8) commonly used in the literature. The results of each were evaluated in detail for multiple, binary, and three selected frequencies.

4.3.1 Multiple classification results (for 8 frequencies)

In this analysis, the results are examined by considering the 12 Hz data available in the data set. The main reason that it was not mentioned before and not used in other analyse is that it is the second harmonic of the 6 Hz signal. In the case of SSVEP signals, the use of the second harmonic of the signal may be deemed unsuitable because it can create an “overlap” [26, 27]. However, this analysis was carried out in order to be present both in the data set and to see its effect on the results.

In this study, the feature selection was also carried out. Feature selection is provided by one-way ANOVA test. There is a prerequisite for the data to be normally distributed to perform this test [29]. For this, the normality test was applied using SPSS software and the statistical significance values (p) obtained were recorded (Table 4.5). Since all the values in this table are greater than the selected 0.05 significance level, all features are considered to have a normal distribution.

Table 4.5 Normality test results of features extracted from SSVEP data.

FETAURES		NORMALITY TEST – SIGNIFICANCE VALUE (P)				
		Delta	Theta	Alfa	Beta	Gamma
Haar	Energy	.200	.258	.179	.191	.166
	Variance	.127	.256	.153	.123	.145
	Entropy	.117	.070	.085	.061	.097
Db4	Energy	.200	.468	.356	.345	.258
	Variance	.082	.143	.124	.263	.066
	Entropy	.200	.259	.149	.179	.109
Sym4	Energy	.140	.091	.119	.413	.234
	Variance	.117	.070	.142	.256	.080
	Entropy	.200	.468	.154	.374	.099
Coif1	Energy	.082	.143	.175	.219	.123
	Variance	.166	.092	.200	.110	.254
	Entropy	.154	.155	.147	.201	.125
Rbio2.8	Energy	.126	.080	.200	.119	.096
	Variance	.200	.138	.169	.104	.200
	Entropy	.069	.094	.086	.073	.051
Bior3.5	Energy	.093	.071	.076	.087	.120
	Variance	.062	.052	.089	.060	.052
	Entropy	.100	.069	.117	.090	.109

While applying the one-way ANOVA test, variance homogeneity test is applied in the second step. For this purpose, the Levene statistics are preferred [29]. Generally, variance homogeneity test results are applied in post-hoc tests and if the significance value is greater than or equal to 0.05 ($p \geq 0.05$), the variance is accepted as homogeneous, otherwise it is considered heterogeneous. According to this result, the post-hoc test to be applied after the ANOVA test is selected. As a result of the test performed on the features in this study, the significance value was found to be 0.62, and variance homogeneity can be mentioned in the groups (Table 4.6).

Tablo 4.6 Variance homogeneity test of normally distributed data.

VARIANCE HOMOGENITY TEST			
Levene statistics	df1	df2	Significance (p)
2.508	7	87	0.62

As a final step in feature selection, differences between groups were determined according to the criterion of significance value ($p \leq 0.05$) with one-way ANOVA test (Table 4.7). The features found statistically significant in the table are shown with “√” according to the EEG frequency bands to which they belong. Accordingly, it is seen that the features of "Haar" and "Bior 3.5" mother wavelets are not selected. It is also seen that the features in the "Beta" and "Gamma" bands are also not selected. Although ANOVA test shows a significant difference between the groups, it does not give which groups are separated from each other and post-hoc tests are recommended for this purpose. However, post-hoc tests were not applied in this study since the purpose of this study was not to separate the groups with ANOVA test and that only a significant difference was found.

Table 4.7 Selected features from EEG frequency bands. The selected features via significance values ($p \leq 0.05$) obtained by ANOVA are indicated by “√”.

FETAURES		EEG FREQUENCY BAND				
		Delta	Theta	Alfa	Beta	Gamma
Haar	Energy					
	Variance					
	Entropy					
Db4	Energy	√	√			
	Variance	√	√			
	Entropy	√	√			
Sym4	Energy	√	√	√		
	Variance	√	√	√		
	Entropy	√	√	√		
Coif1	Energy		√			
	Variance	√	√			
	Entropy					
Rbio2.8	Energy	√	√	√		
	Variance	√	√	√		
	Entropy	√	√	√		
Bior3.5	Energy					
	Variance					
	Entropy					

In the classification phase, the classification algorithms were run using all the features without feature selection and their performances were recorded (Table 4.8). 55.6% performance was achieved with the LDA classifier for the features using Bior3.5 mother wavelet in the first subject. For the second subject, the Ensemble Learner classifier achieved 26.9% performance for the features using Bior3.5 mother wavelet, while the third subject achieved 33.3% performance with the Naive Bayes classifier for the features using the Haar and Db4 mother wavelets. Finally, in the fourth subject, 28.6% classifier performance was obtained with the Naive Bayes - Ensemble Learner classifier for the features using Bior3.5, Db4 and Sym4 mother wavelets. According to this table, it is seen that an average of 36.1% performance is achieved and Bior3.5 mother wavelet generally gives good results but a common wavelet type and classifier cannot be determined for all subjects.

Table 4.8 Multiple classification results of wavelet transform features before the feature selection. (for 8 frequencies).

SUBJECTS	WAVELET FUNCTIONS	BEST PERFORMANCE (%)	CLASSIFIERS
1	Haar	37.0	SVM (Cubic)
	Coif1	25.9	Ensemble (Bagged Trees)
	Db4	29.6	Tree (Fine, Medium, Coarse)
	Bior3.5	55.6	LDA
	Rbio2.8	22.2	Naive Bayes, SVM (Coarse Gaussian), KNN (Coarse)
	Sym4	25.9	KNN (Coarse), SVM (Coarse Gaussian), Ensemble (Boosted Trees)
2	Haar	23.1	SVM (Fine Gaussian), SVM (Coarse Gaussian), KNN (Coarse), Ensemble (Boosted Trees)
	Coif1	23.1	SVM (Coarse Gaussian), KNN (Coarse), Ensemble (Boosted Trees)
	Db4	23.1	SVM (Coarse Gaussian), KNN (Coarse), Ensemble (Boosted Trees)
	Bior3.5	26.9	Ensemble (Subspace KNN)
	Rbio2.8	23.1	SVM (Coarse Gaussian), KNN (Coarse), Ensemble (Boosted Trees)
	Sym4	23.1	SVM (Coarse Gaussian), KNN (Coarse), Ensemble (Boosted Trees)

Table 4.8 Multiple classification results of wavelet transform features before the feature selection. (for 8 frequencies). **Continued.**

SUBJECTS	WAVELET FUNCTIONS	BEST PERFORMANCE (%)	CLASSIFIERS
3	Haar	33.3	Naive Bayes (Kernel), Ensemble (Subspace KNN)
	Coif1	23.8	SVM (Quadratic)
	Db4	33.3	Naive Bayes (Kernel)
	Bior3.5	19.0	KNN (Weighted), Ensemble (Subspace KNN)
	Rbio2.8	19.2	SVM (Coarse Gaussian), KNN (Coarse), Ensemble (Boosted Trees)
	Sym4	19.0	LDA
4	Haar	19.0	KNN (Cubic)
	Coif1	23.8	Naive Bayes (Kernel)
	Db4	28.6	Ensemble (RUSBoosted Trees)
	Bior3.5	28.6	Naive Bayes (Kernel)
	Rbio2.8	19.0	Ensemble (Subspace Discriminant)
	Sym4	28.6	Ensemble (Subspace Discriminant)

Later, the highest classifier performances of the selected features were recorded by running the classification algorithms for four different participants (Table 4.9). In the first subject, 25.9% classifier performance was obtained in the KNN - Ensemble Learner classifier with the features using Coif1 and Sym4 mother wavelets. In the second subject, 23.1% performance was obtained with the KNN - SVM - Ensemble Learner classifiers in all mother wavelet types. In the third subject, 38.1% performance was observed in the LDA classifier with the features using the Sym4 mother wavelet, while in the fourth subject, 38.1% classifier performance was obtained in the Naive Bayes classifier with the features using the Rbio2.8 mother wavelet. According to this table, it is seen that an average performance of 31.3% is obtained and a common wavelet type and classifier, which gives good results for all subjects, as in Table 4.9 in general, could not be determined.

Table 4.9 Multiple classification results of wavelet transform features after the feature selection. (for 8 frequencies).

SUBJECTS	WAVELET FUNCTIONS	BEST PERFORMANCE (%)	CLASSIFIERS
1	Coif1	25.9	Ensemble (Boosted Trees)
	Db4	22.2	SVM (Coarse Gaussian), KNN (Coarse)
	Rbio2.8	22.2	SVM (Coarse Gaussian), KNN (Coarse), Ensemble (Boosted Trees)
	Sym4	25.9	KNN (Coarse), Ensemble (Boosted Trees)
2	Coif1	23.1	Ensemble (Boosted Trees)
	Db4	23.1	SVM (Coarse Gaussian), KNN (Coarse)
	Rbio2.8	23.1	SVM (Fine Gaussian), SVM (Coarse Gaussian), KNN (Coarse), Ensemble (Boosted Trees)
	Sym4	23.1	KNN (Coarse), Ensemble (Boosted Trees)
3	Coif1	9.5	Ensemble (RUSBoosted Trees)
	Db4	33.3	Tree (Fine, Medium, Coarse)
	Rbio2.8	28.6	Ensemble (Subspace KNN)
	Sym4	38.1	LDA
4	Coif1	19.0	Ensemble (RUSBoosted Trees)
	Db4	19.0	Naive Bayes (Gaussian)
	Rbio2.8	38.1	Naive Bayes (Gaussian)
	Sym4	23.8	LDA

Finally, in order to evaluate the SSVEP records of all participants together, the classification algorithms were run both for all the features without the feature selection and after the feature selection was made (Table 4.10). According to these results, when all subjects are evaluated together, the highest average classifier performance is achieved when Rbio2.8 mother wavelet is used in all classifiers. In the table, the classifier performances of the feature selection are shown with an asterisk (*). Accordingly, the data of all subjects with feature selection gives a worse classifier performance in all cases.

Table 4.10 Average success of classifiers before and after feature selection (*).

CLASSIFIERS	WAVELET FUNCTIONS					
	Haar	Db4	Sym4	Coif1	Bior3.5	Rbio2.8
Decision Tree	15.8	15.8	18.9	20.0	22.1	26.3
		14.7*	14.7*	11.6*		21.1*
Discriminant Analysis	18.9	10.5	13.7	18.9	15.8	21.1
		8.4*	14.7*	13.7*		16.8*
Naïve Bayes	15.8	12.6	12.6	14.7	12.6	16.8
		15.8*	16.8*	15.8*		16.8*
Support Vector Machines	20.0	15.8	14.7	14.7	14.7	28.4
		14.7*	24.2*	17.9*		24.2*
k-Nearest Neighbour	21.1	14.7	13.7	14.7	17.9	34.7
		15.8*	15.8*	18.9*		29.5*
Ensemble Learning	23.2	12.6	15.8	21.1	23.2	37.9
		16.8*	16.8*	17.9*		33.7*

Consequently, as a result of the classification procedures performed for each subject individually, the stimulation frequency is estimated with an average accuracy of 36.1% (26.9-55.6) (Table 4.8) when using all the features, and an average of 31.3% (23.1-38.1%) (Table 4.9) when the features were selected, it was determined that the stimulation frequency can be estimated with accuracy. In addition, considering the data of all subjects, it was seen that the stimulation frequency can be estimated with an average of 37.9% (Table 4.10) when using all the features without the selection of the features, and an average of 33.7% (Table 4.10) only if the selected features were used.

Accordingly, when the data of the subjects are evaluated separately, although it is seen that any mother wavelet type and classifier algorithm is not dominant, when the data of the subjects are evaluated together, it is understood that the Ensemble Learning classifier and Reverse Biorthogonal (Rbio2.8) mother wavelet are clearly superior to other classifier and mother wavelet combinations. However, one-way ANOVA, which is used as a statistical based feature selection method, has been shown to give a worse result in BCI control with SSVEP.

4.3.2 Multiple classification results (for 7 frequencies)

In this analysis, unlike section 4.3.1, since the data set contains 6 Hz data, 12 Hz frequency data, which is the second harmonic of 6 Hz, which is not suitable for use in SSVEP analysis and may cause misleading results, was discarded. And the results were evaluated by multiple classification method for 7 frequencies.

According to the results obtained, the highest performance was determined in Subject 1 with the LDA classifier in Bior 3.5 mother wavelet with an accuracy value of 55.60%. In Subject 2, the highest performance was achieved with the Ensemble Learning classifier in Coif 1 mother wavelet with 34.60% accuracy value, and in Subject 3, the highest performance was obtained with the Ensemble Learning and LDA classifiers in Bior 3.5 and Haar wavelets with 42.90% accuracy value. Finally, the highest performance in Subject 4 was determined with the Ensemble Learning and LDA classifiers in Coif1 and Db4 wavelets with 33.30% accuracy.

Considering the mother wavelet selection, Bior3.5 and Coif1 mother wavelets were found to be relatively successful, although there is no dominant wavelet type. However, it is very difficult to suggest an exact mother wavelet type in the multiple classification of SSVEP signals. Experimenting with a larger number of subjects in order to generalize can give precise results. In contrast to the mother wavelet selection, when the classifiers are evaluated, the success of Ensemble learning and LDA classifiers is clearly seen.

Table 4.11 Multiple classification results of wavelet transform features (for 7 frequencies).

SUBJECT	MOTHER WAVELET	ACC	CLASSIFIERS
Subject 1	Coif 1	29.20	KNN (Cosine, Cubic)
	Bior 3.5	55.60	LDA
	Db 4	37.50	SVM (Cubic), KNN (Fine)
	Sym 4	29.20	LDA
	Haar	37.50	KNN (Fine, Weighted)
	Rbio 2.8	33.30	Naive Bayes (Kernel)
Mean		37.05	

Table 4.11 Multiple classification results of wavelet transform features (for 7 frequencies). **Continued.**

SUBJECT	MOTHER WAVELET	ACC	CLASSIFIERS
Subject 2	Coif 1	34.60	Ensemble (Subspace KNN)
	Bior 3.5	23.10	Ensemble (Boosted)
	Db 4	23.10	SVM (Fine Gaussian)
	Sym 4	30.80	Tree (All)
	Haar	23.10	LDA
	Rbio 2.8	23.10	SVM (Coarse Gaussian)
Mean		26.30	
Subject 3	Coif 1	33.30	Ensemble (Subspace KNN)
	Bior 3.5	42.90	Ensemble (Subspace Discr.)
	Db 4	33.30	Naive Bayes (Kernel)
	Sym 4	38.10	Ensemble (Subspace KNN)
	Haar	42.90	LDA
	Rbio 2.8	38.10	Ensemble (Subspace Discr.)
Mean		38.10	
Subject 4	Coif 1	33.30	LDA
	Bior 3.5	28.60	Naive Bayes (Kernel)
	Db 4	33.30	Ensemble (RUSBoosted)
	Sym 4	28.60	LDA
	Haar	23.80	LDA
	Rbio 2.8	28.60	Ensemble (Subspace Discr.)
Mean		29.37	

4.3.3 Classification results for three selected frequencies

In this analysis, as in the classification of frequency domain features (section 4.2.2), multiple classification was made by selecting 3 selected frequencies (6 Hz - 8.2 Hz – 10 Hz) where the differences between the frequencies were higher among the seven frequencies. However, unlike the analysis made in the frequency domain, the selected features are classified and evaluated when they are used together, that is, when energy, variance and entropy features are used as a single feature vector, and when they are used as separate features. Thus, detailed information about the power, irregularity and bias of the signal was obtained. At the same time, it is learned how to

use these three features, which have the indispensable properties of the signal, more effectively. And the contribution of these features, which are frequently used in the literature, as a new form of features is wanted to be shown.

In Figure 4.5, the accuracy values obtained by classification of the energy, entropy, and variance features extracted using each wavelet family for 4 people are presented. Mean, minimum and maximum values of the classification results of 4 people were also shown. According to these results, the values given by the Haar wavelet function for energy, entropy, and variance feature groups, which yield more successful results than other wavelet functions, were 75.85%, 73.08%, and 73.75%, respectively. There were no major differences between the mean values of the 3 features extracted based on the Haar wavelet. However, it was seen that the entropy feature group had a 100% success rate compared to the others. Success performance values following Haar wavelet family were as follows: bior3.5 mother wavelet with 65.71%, 69.62% and 65.34%, db4 mother wavelet with 52.35%, 54.85%, 54.85%, rbio2.8 mother wavelet with 52.35%, 51.95%, 52.65%, 46.93%, 48.88%, 49.58% with coif1 mother wavelet, and 42.23%, 39.43%, 41.50% were obtained in sym4 mother wavelet.

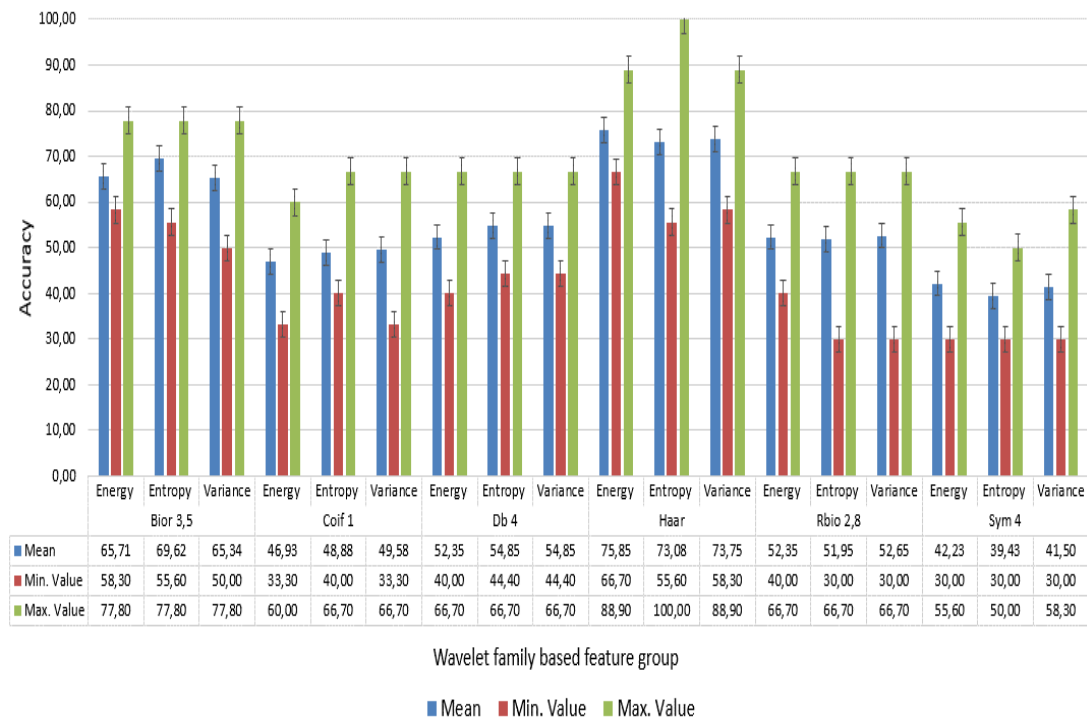


Figure 4.5 Classification performance of energy, entropy, and variance as separate features.

In Figure 4.6, the extracted features based on wavelet were used as a feature set, and the successful performances of the wavelet families were compared in this way. According to the results obtained, it was seen that the most successful wavelet family was the Haar wavelet function. The ranking of success in other wavelet families has not changed. The accuracy values are as follows: 75.85% with Haar mother wavelet, 67.53% with bior3.5 mother wavelet, 60.85% with db4 mother wavelet, 56.25% with coif1 mother wavelet, 52.35% with rbio2.8 mother wavelet and 44.73% with sym4 mother wavelet obtained. It was seen that some mother wavelet performances increased when compared with the accuracy values in which the features in Figure 4.5 were handled separately. Mean values of coif1, db4, and sym4 mother wavelet functions increased.

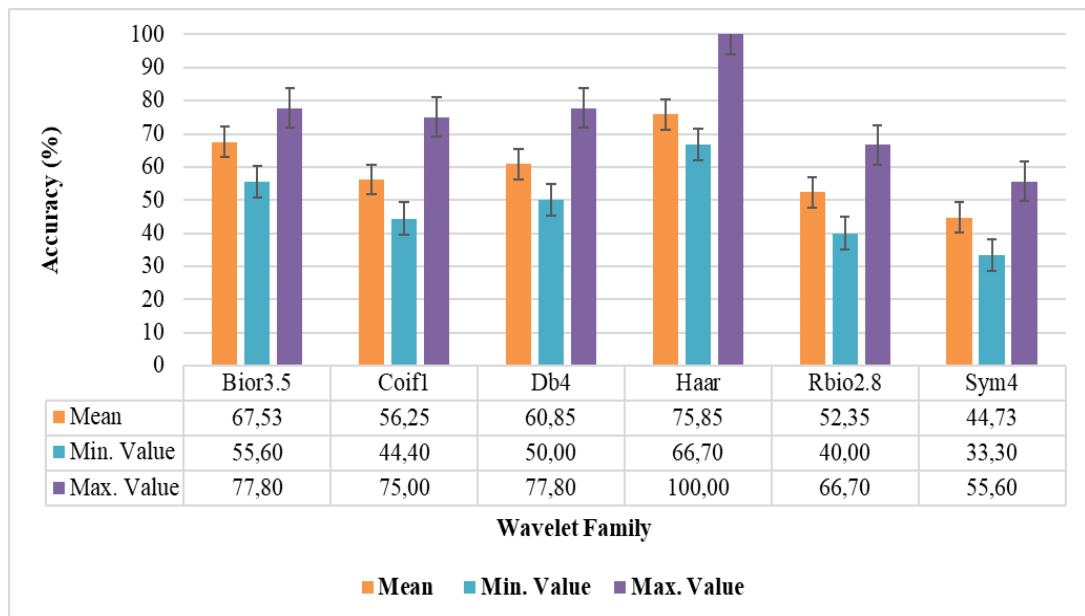


Figure 4.6 Classification performance of energy, entropy, and variance together as a feature set.

In Table 4.12, classifier performances of each participant of energy, entropy and variance as separate features are presented. These results indicate the highest accuracy values obtained in each wavelet function and the classifier with the most successful performance. The six basic classifiers used in classification are compared to decide the most successful classifiers among themselves. In addition to the six basic classifiers used, the ones specified in parentheses refer to the sub-parameters of the classifiers.

Table 4.12 Classification performance of energy, entropy, and variance as separate features for selected three frequencies.

Features with wavelet functions	CLASSIFIERS			
	Subject 1	Subject 2	Subject 3	Subject 4
bior3.5_energy	Ensemble Learning (Subspace Discriminant)	SVM (Quadratic), KNN (Fine), Ensemble Learning (Subspace KNN)	Ensemble Learning (Subspace KNN)	Ensemble Learning (Subspace KNN)
bior3.5_entropy	LDA	SVM (Quadratic), KNN (Weighted), Ensemble Learning (Bagged Trees)	Ensemble Learning (Subspace KNN)	Ensemble Learning (Subspace KNN)
bior3.5_variance	LDA	Naive Bayes (Kernel), KNN (Weighted), Ensemble Learning (Subspace Disc. & KNN)	Ensemble Learning (Subspace KNN)	Ensemble Learning (Bagged Trees, Subspace KNN)
coif1_energy	SVM (Fine, Medium, Coarse), KNN (All), Ensemble Learning (Boosted Trees)	LDA	LDA	Naive Bayes (Kernel)
coif1_entropy	Ensemble Learning (Subspace Discriminant)	LDA, Naive Bayes (Kernel)	LDA	Naive Bayes (Gaussian, Kernel)
coif1_variance	SVM (Quadratic), DesicionTree (All)	LDA, Ensemble Learning (Bagged Trees, Subspace Discr.)	LDA	KNN (Fine), Ensemble Learning (Bagged Trees)
db4_energy	Ensemble Learning (Subspace Discriminant)	SVM (Cubic), Ensemble Learning (Subspace KNN)	Ensemble (Subspace KNN)	Naive Bayes (Kernel)
db4_entropy	Ensemble Learning (Subspace Discriminant), SVM (Cubic)	Ensemble Learning (Subspace KNN)	SVM (Cubic), Naive Bayes (Kernel)	Ensemble Learning (Bagged Trees)
db4_variance	Ensemble Learning (Subspace Discriminant)	Ensemble Learning (Subspace KNN)	Naive Bayes (Kernel), Ensemble Learning (Subspace KNN)	Naive Bayes (Kernel)

Table 4.12 Classification performance of energy, entropy, and variance as separate features for selected three frequencies. **Continued.**

Features with wavelet functions	CLASSIFIERS			
	Subject 1	Subject 2	Subject 3	Subject 4
haar_energy	Decision Tree (All)	Ensemble Learning (Bagged Trees)	LDA	Ensemble Learning (Subspace KNN)
haar_entropy	Decision Tree (All)	Ensemble Learning (Bagged Trees)	LDA	Ensemble Learning (Subspace KNN)
haar_variance	Naive Bayes	Ensemble Learning (Bagged Trees)	LDA	Ensemble Learning (Subspace KNN)
rbio2.8_energy	SVM (Linear SVM)	Ensemble Learning (RUSBoosted Trees)	LDA, Ensemble Learning (Subspace Discriminant)	Ensemble Learning (Subspace KNN)
rbio2.8_entropy	LDA	Naive Bayes (Kernel)	Ensemble Learning (Subspace Discriminant)	LDA
rbio2.8_variance	SVM (Linear SVM)	Ensemble Learning (RUSBoosted Trees)	Ensemble Learning (Subspace Discriminant)	Ensemble Learning (Subspace KNN)
sym4_energy	SVM (Fine, Gaussian, Coarse), KNN (All), Ensemble Learning (Boosted Trees, Subspace Discriminant)	Ensemble Learning (Subspace Discriminant)	LDA, SVM (Quadratic, Cubic)	Ensemble Learning (Bagged Trees, Subspace KNN)
sym4_entropy	SVM (Fine, Gaussian, Coarse), KNN (All), Ensemble Learning (Boosted Trees)	LDA	SVM (Quadratic, Cubic)	Ensemble Learning (RUSBoosted Trees)
sym4_variance	SVM (Linear SVM), Ensemble Learning (Subspace Discriminant)	LDA, Ensemble Learning (Subspace Discriminant)	SVM (Quadratic)	Ensemble Learning (Subspace KNN)

The results to be expressed in the pie chart in Figure 4.7 are the number of hits of the classifiers obtained in Table 4.12. These numbers were obtained by running all algorithms 240 times in total. With reference to results obtained (Figure 4.7), it is obvious that the most successful and also the most frequent classifier in the classification was obtained as the Ensemble classifier. Other classifiers following the Ensemble Learning classifier can be ranked as Discriminant Analysis, SVM, Naive Bayes, KNN, and Decision Tree.

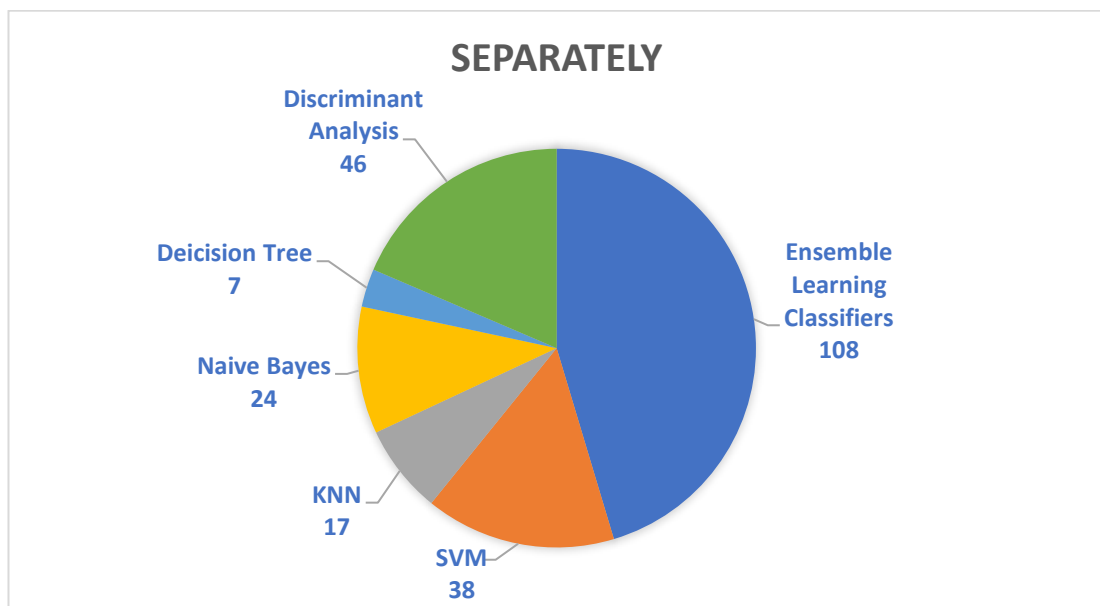


Figure 4.7 Percentage of classifier where the best result is the most often obtained as a result of running the algorithms 240 times in total. (Energy, entropy, and variance as separate features).

In Table 4.13, the classifier performances where the feature group is evaluated as feature set is presented, and also, in Figure 4.8, the number of hits of the obtained results in terms of classifiers are shown. According to the results obtained (Figure 4.8 and Table 4.13), the most frequent and also most successful classifier has been again Ensemble Learning classifier. The ranking of the classifier achievements has been obtained in the same order as in Figure 4.7. In other words, other classifiers following the Ensemble Learning classifier can be ranked as Discriminant Analysis, SVM, Naive Bayes, KNN, Decision Tree.

Table 4.13 Classification performance of energy, entropy, and variance as a feature set for selected three frequencies.

Features with wavelet functions	CLASSIFIERS			
	Subject 1	Subject 2	Subject 3	Subject 4
bior3.5	LDA	KNN (Weighted KNN)	Ensemble Learning (Subspace KNN)	Ensemble Learning (Subspace KNN)
coif1	LDA, Ensemble Learning (Subspace Discriminant)	Naive Bayes (Kernel), Ensemble Learning (Subspace Discriminant)	LDA, Ensemble Learning (Subspace Discriminant)	Naive Bayes (All)
db4	SVM (Fine, Quadratic, Coarse), KNN (All), Ensemble Learning (Boosted Trees)	Ensemble Learning (Subspace KNN)	Naive Bayes (Kernel)	LDA
haar	LDA	Ensemble Learning (RUSBoosted Trees)	LDA	Ensemble Learning (Subspace KNN)
rbio2.8	SVM (Linear)	LDA, Naive Bayes (Gaussian), Ensemble Learning (All)	Ensemble Learning (Subspace Discriminant)	Ensemble Learning (Bagged Trees, Subspace KNN)
sym4	SVM (Fine, Coarse), KNN (All), Ensemble Learning (Boosted Trees)	LDA	SVM (Cubic)	Ensemble Learning (RUSBoosted Trees)

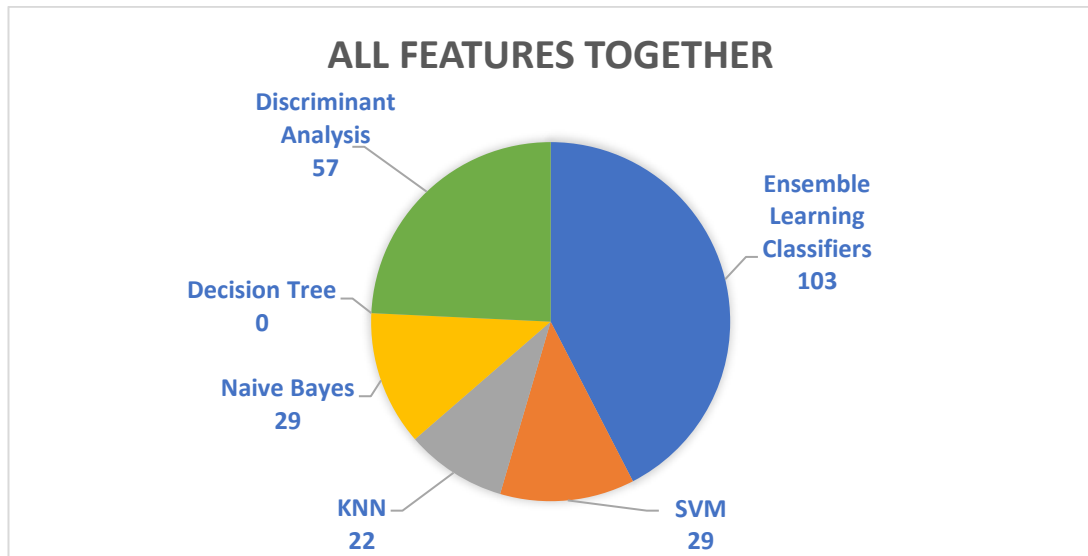


Figure 4.8 Percentage of classifier where the best result is the most often obtained as a result of running the algorithms 240 times in total. (Energy, entropy, and variance as a feature set).

As a result of the classification processes performed separately for each subject, when the performances of both feature groups were examined, the most successful wavelet function was found as the Haar wavelet. When the average accuracy values of the feature groups are examined, the results in the case that the three features are used as a single feature vector gave higher results for all wavelet functions than the other feature group. Although there is no dominant result in the comparison of energy, entropy, and variance features among themselves, the highest result was seen in the entropy feature in Subject 3 with 100%. When the machine learning algorithms have been examined, it has seen that the Ensemble learning algorithm classifiers with the highest performance compared to the others [179].

4.3.4. Binary classification results

In this analysis, feature vectors are treated as a single feature vector and individual feature vectors, similar to those in Section 4.2.3. The resulting feature vectors were then evaluated by binary classification in order to analyze frequencies in detail. As the results of the first part of the experimental design, the classification performances are obtained for:

- three features separately (energy, entropy and variance),
- average of the three features separately (Mean),
- the extracted features were grouped as a single feature set (All features together).

Each feature (energy, entropy, variance and all features together) extracted using each wavelet family for 4 participants. All values of the classification results are presented in Figure 4.9- 4.14 for each mother wavelet, respectively.

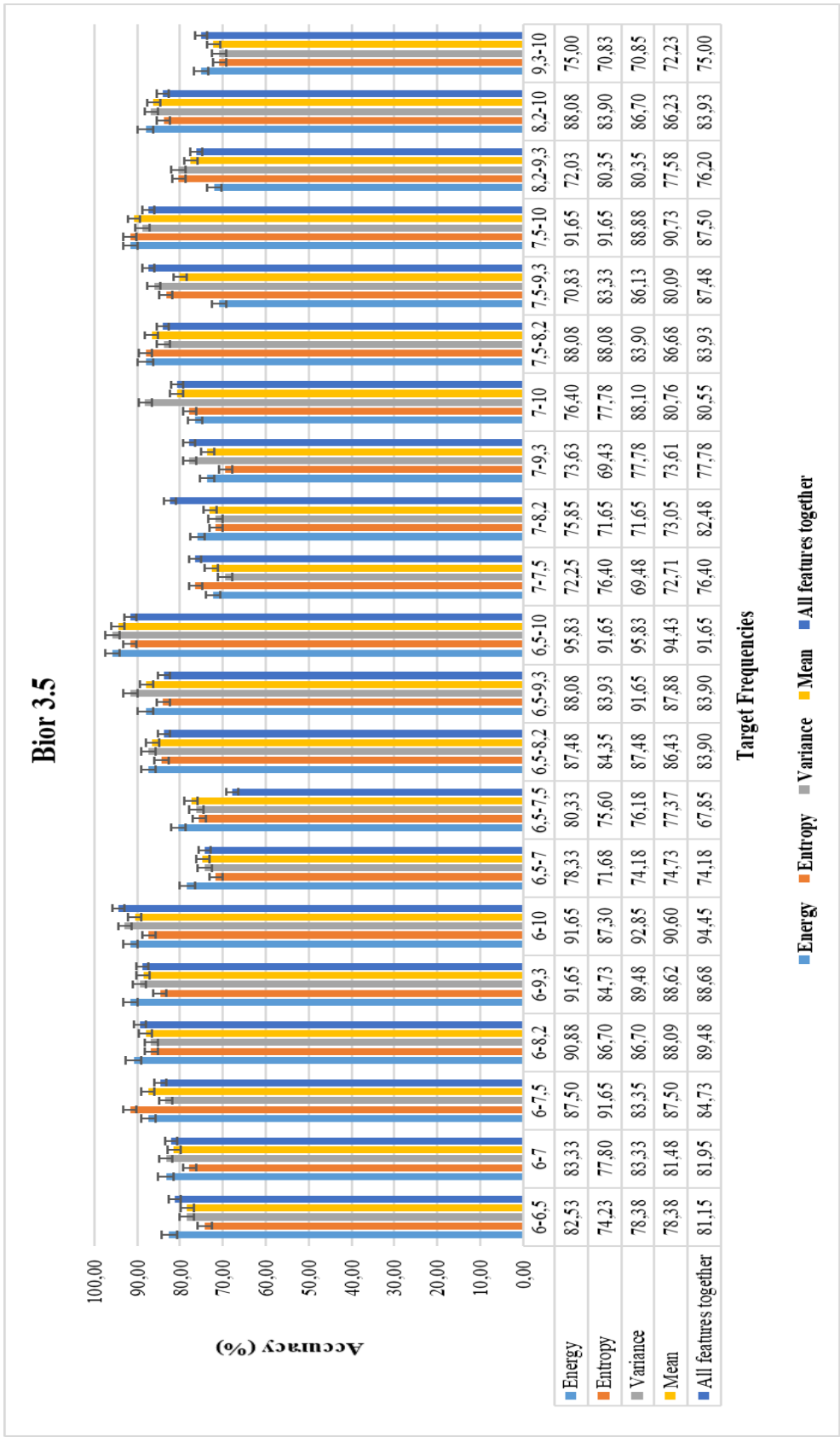


Figure 4.9 Binary classification performance of the features for Bior 3.5 mother wavelet function.

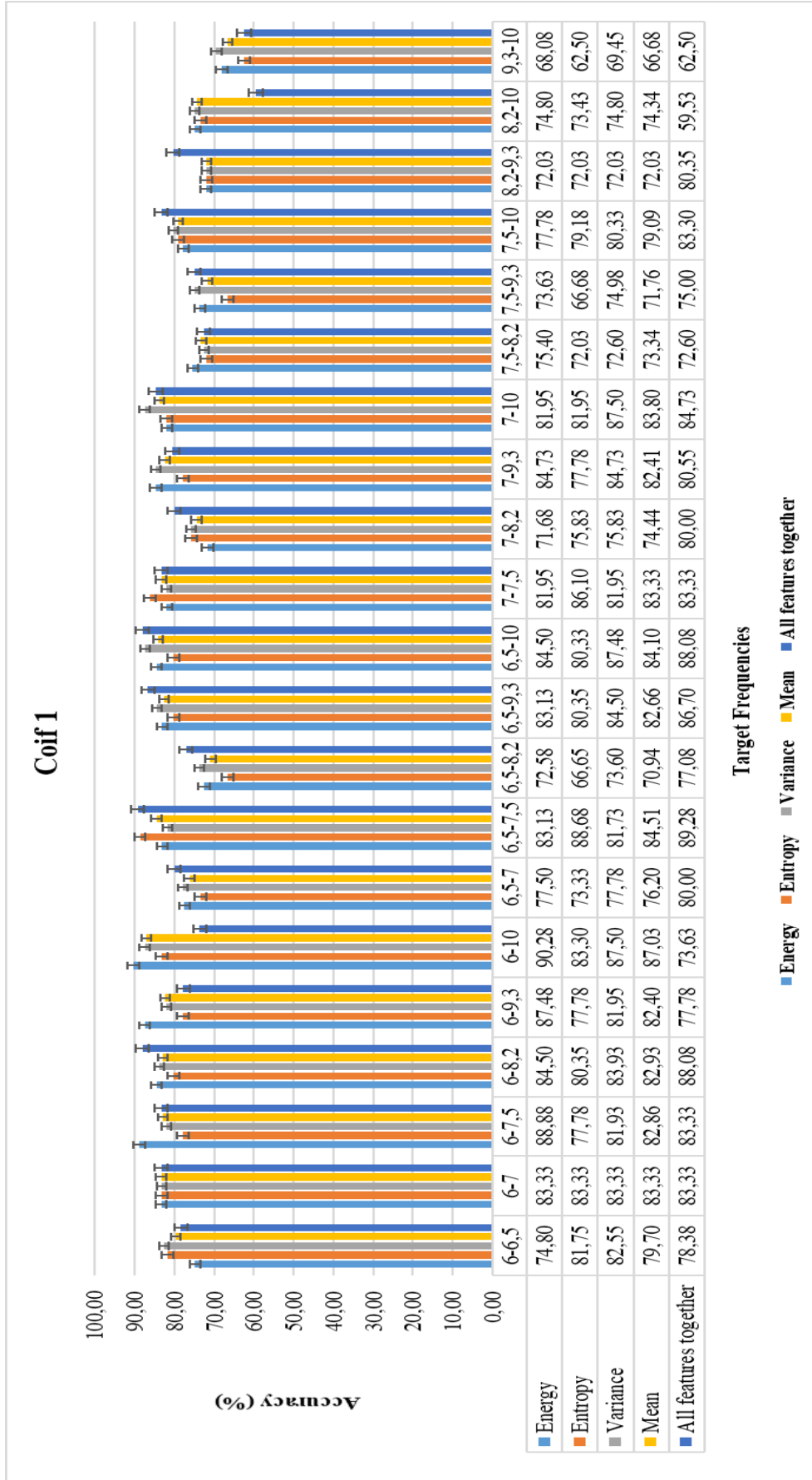


Figure 4.10 Binary classification performance of the features for Coif 1 mother wavelet function.

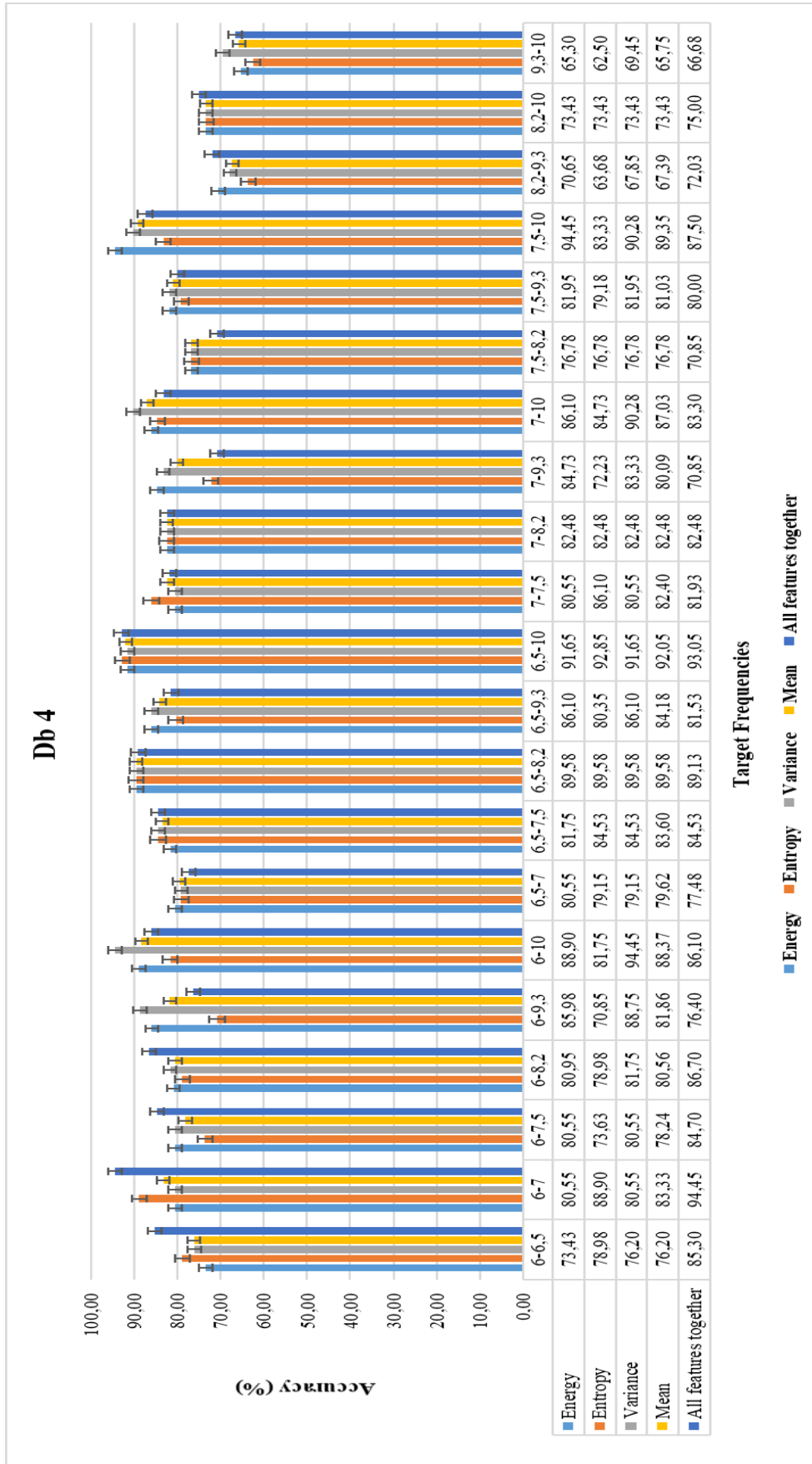


Figure 4.11 Binary classification performance of the features for Db 4 mother wavelet function.

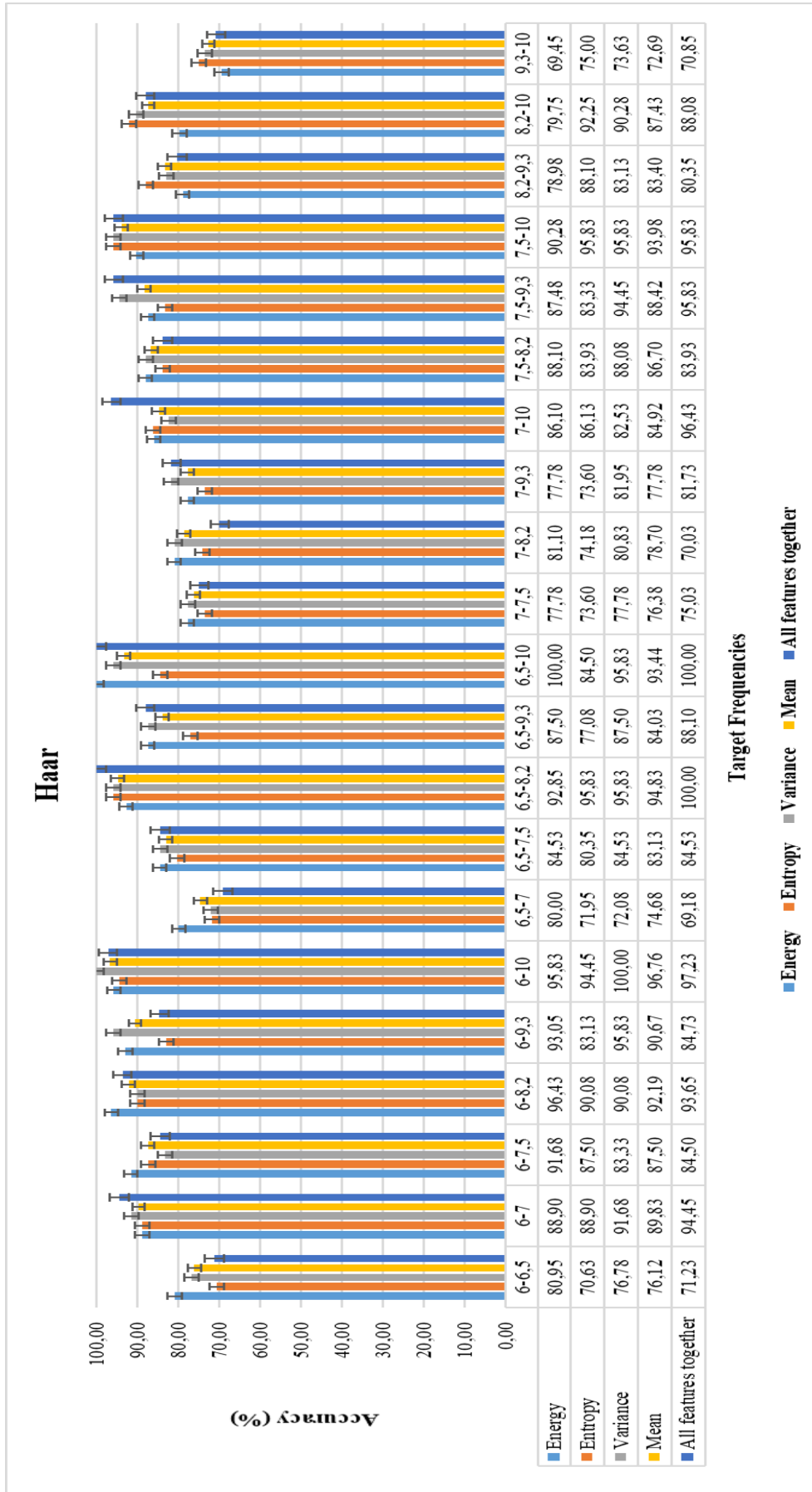


Figure 4.12 Binary classification performance of the features for Haar mother wavelet function.

Rbio 2.8

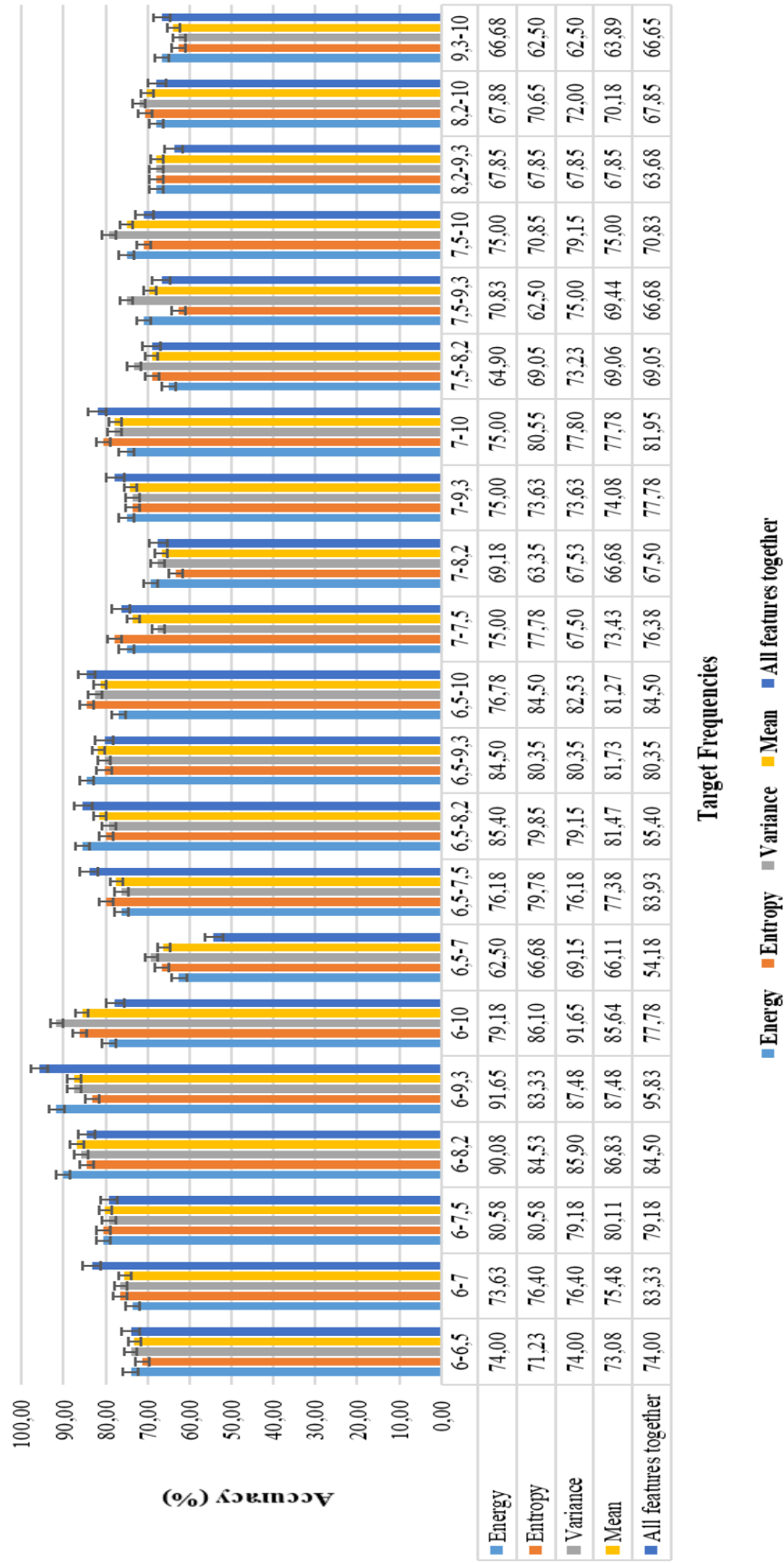


Figure 4.13 Binary classification performance of the features for Rbio 2.8 mother wavelet function.

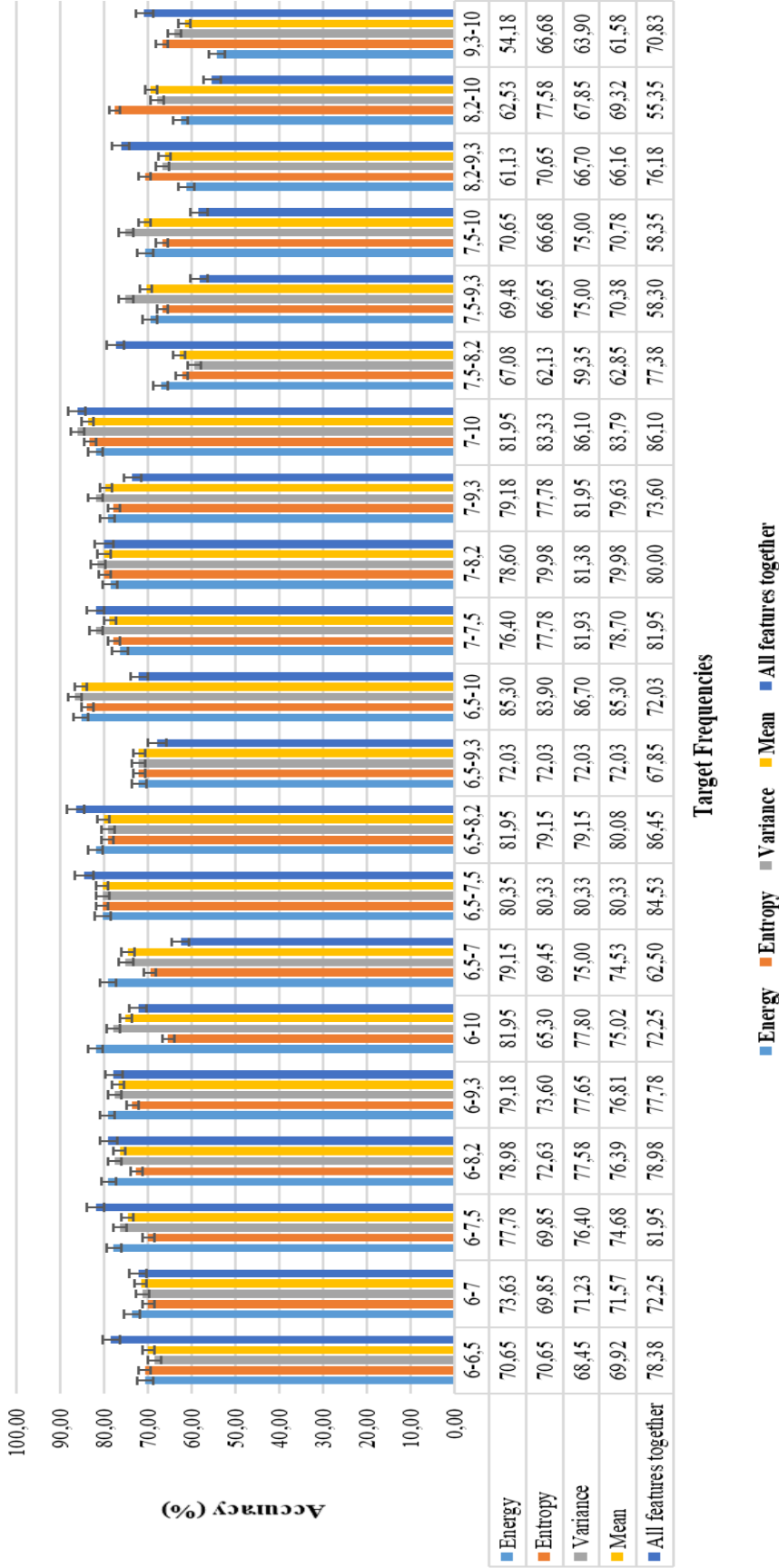


Figure 4.14 Binary classification performance of the features for Sym 4 mother wavelet function.

According to these results, features obtained from the Haar wavelet function yielded higher accuracies than those obtained from the other wavelet functions. Maximum accuracy performances were obtained in the frequency pairs "6-10", "6.5-8.2", "6.5-10" in the Haar wavelet (Table 4.14). When the features are evaluated, it is realized that the "All features together" feature generally has better results for all mother wavelet functions.

Table 4.14 Classification results of the most successful frequency pairs of the Haar mother wavelet.

FREQUENCY PAIR	ENERGY	ENTROPY	VARIANCE	MEAN	ALL FEATURES TOGETHER
6 - 10	95.83	94.45	100.00	96.76	97.23
6.5 – 8.2	92.85	95.83	95.83	94.83	100.00
6.5 - 10	100.00	84.50	95.83	93.44	100.00

And another researched hypothesis results are presented in Figure 4.15 – 4.20 for each mother wavelet, respectively. The purpose here is to show the change in the accuracy value according to the increase in the difference between the frequencies.

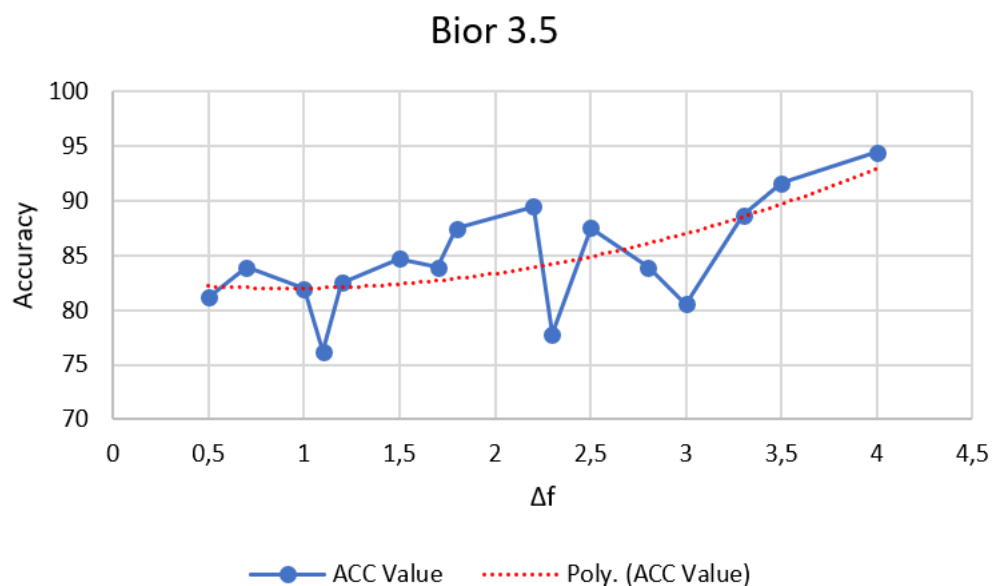


Figure 4.15 Change of accuracy value according to the differences between frequencies for Bior 3.5 mother wavelet.

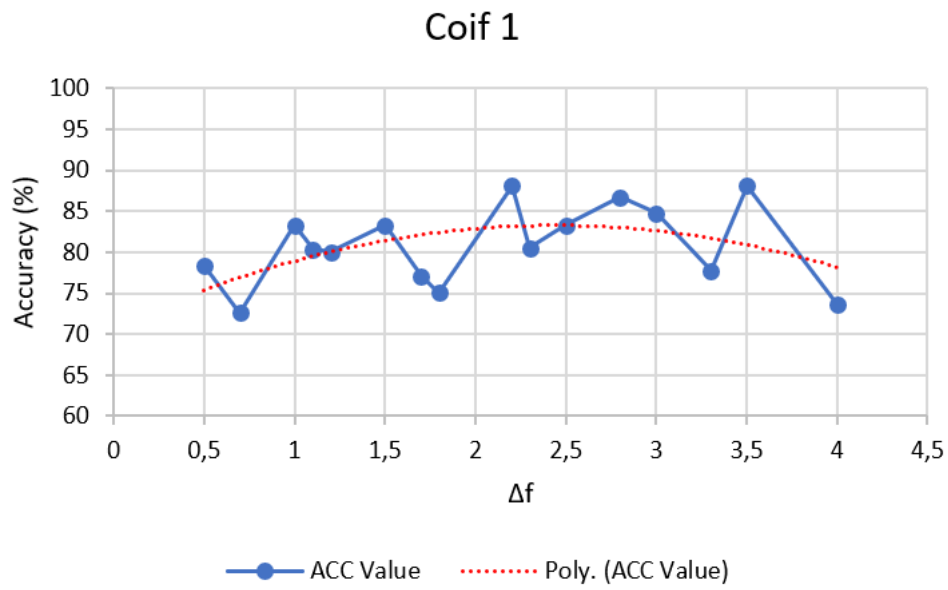


Figure 4.16 Change of accuracy value according to the differences between frequencies for Coif 1 mother wavelet.

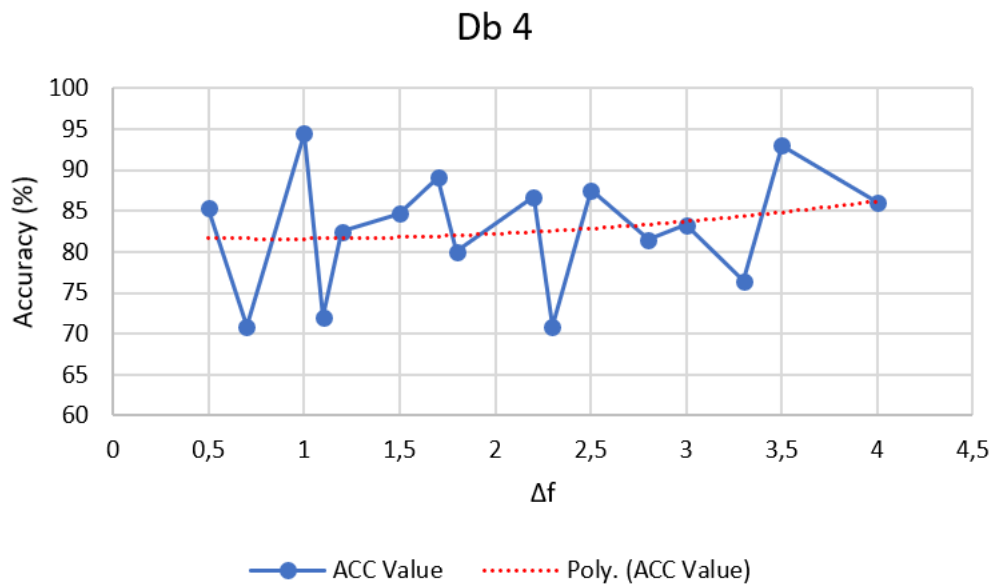


Figure 4.17 Change of accuracy value according to the differences between frequencies for Db 4 mother wavelet.

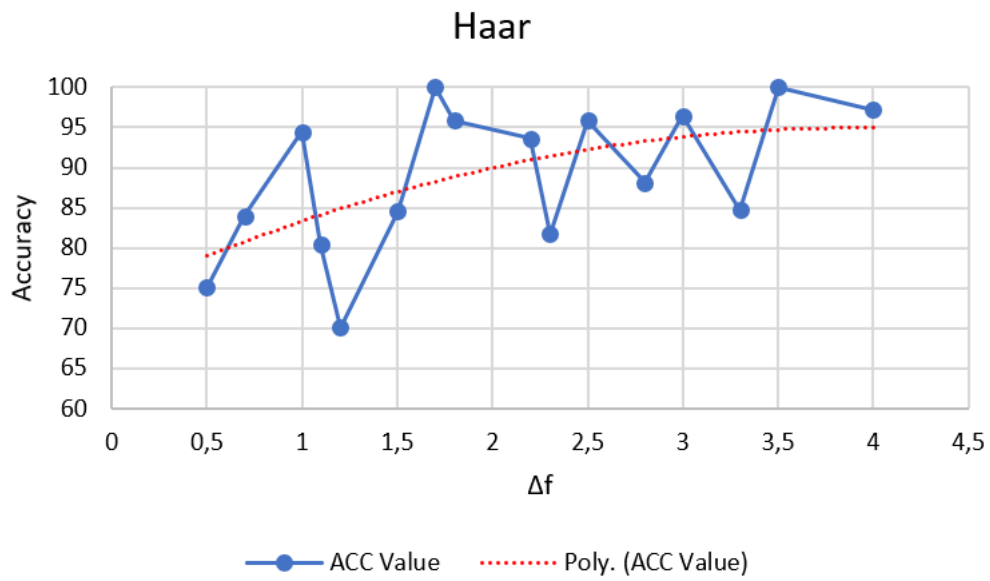


Figure 4.18 Change of accuracy value according to the differences between frequencies for Haar mother wavelet.

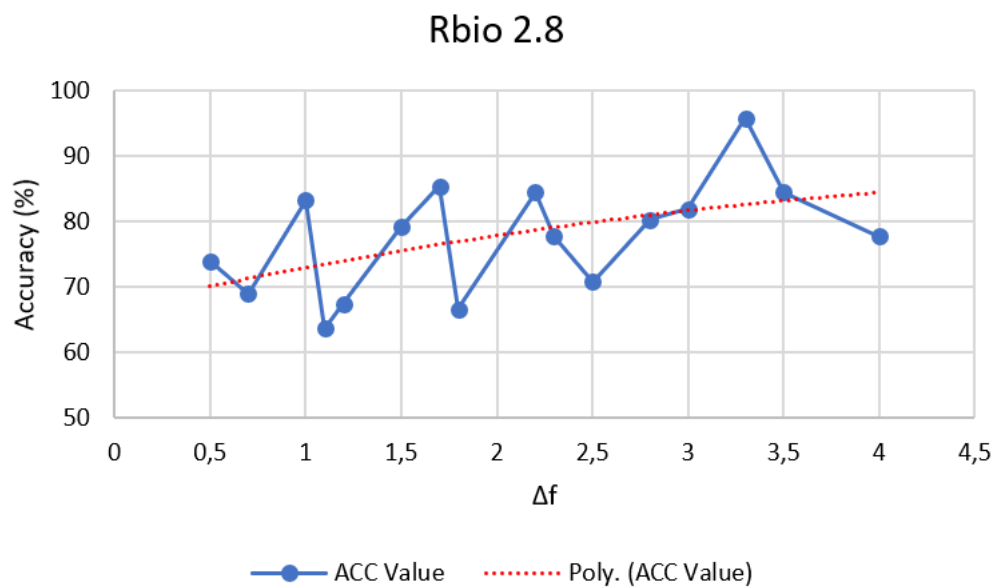


Figure 4.19 Change of accuracy value according to the differences between frequencies for Rbio 2.8 mother wavelet.

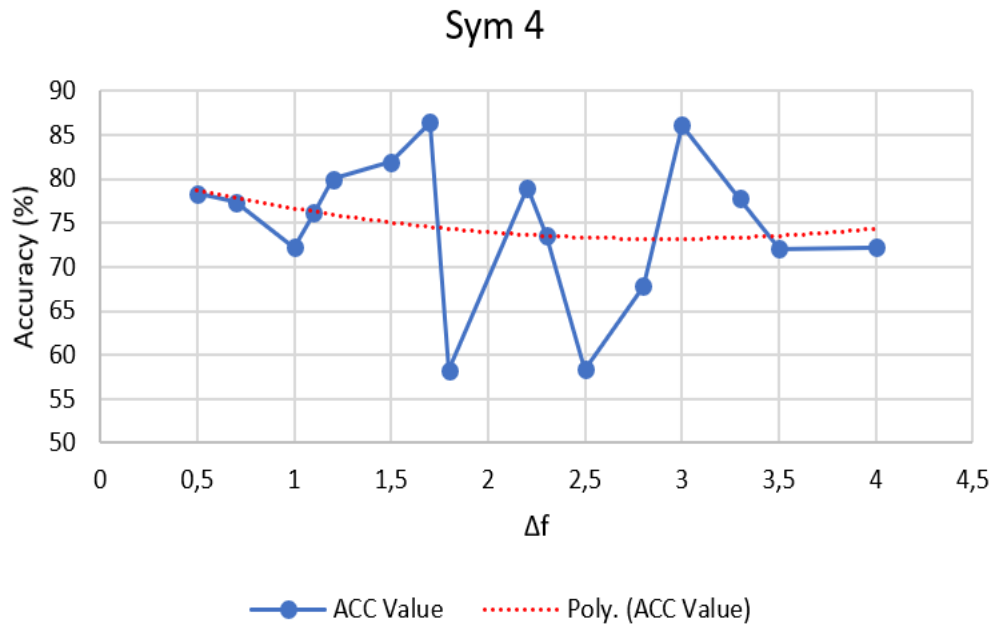


Figure 4.20 Change of accuracy value according to the differences between frequencies for Sym 4 mother wavelet.

As a result of the classification, when the seven basic classifiers are compared among themselves according to their percentage accuracy performance, the result obtained is presented in Table 4.15. Since the classification results of all the features ranking are similar for all the wavelet functions, the classification result of the "All features together" for Haar wavelet function is presented. According to these results, the most successful classifier was obtained as the Ensemble classifier.

Table 4.15 Classification performance of energy, entropy, and variance as a feature set (All features together) for Haar wavelet.

Classes	CLASSIFIERS			
	Subject 1	Subject 2	Subject 3	Subject 4
6-6.5	Ensemble Learning (RUSBoosted)	Ensemble Learning (Subs. KNN), KNN (Fine, Weighted), SVM (Cubic, Fine Gaussian)	LDA, SVM (Quadratic), KNN (Fine)	Ensemble Learning (Subs. Ditr.)
6-7	Logistic Regression	Ensemble Learning (RUSBoosted)	Logistic Regression	Ensemble Learning (Subs. Ditr.)
6-7.5	SVM (Medium Gaussian), Ensemble Learning (Subs. KNN, RUSBoosted)	Ensemble Learning (RUSBoosted)	LDA, Logistic Regression, Ensemble Learning (Subs. KNN)	LDA, Logistic Regression
6-8.2	LDA, Ensemble Learning (RUSBoosted)	KNN (Weighted)	Logistic Regression	Ensemble Learning (Subs. KNN)
6-9.3	Ensemble Learning (RUSBoosted)	Naive (Gaussian), Ensemble Learning (Subs. KNN)	LDA, Logistic Regression, Naive Bayes (Kernel)	LDA, Logistic Regression
6-10	Ensemble Learning (RUSBoosted)	Ensemble Learning (Subs. Discr.)	Logistic Regression	LDA, Logistic Regression, SVM (Quadratic, Cubic), Ensemble Learning (Subs. KNN)
6.5-7	Logistic Regression	Naive Bayes (Gaussian)	Naive Bayes (Kernel), Ensemble Learning (Subs. KNN)	Ensemble Learning (Subs. Discr.)
6.5-7.5	SVM (All), KNN (Fine, Weighted)	Ensemble Learning (Bagged, RUSBoosted)	SVM (Linear, Quadratic, Cubic), Ensemble Learning (Bagged)	Ensemble Learning (Subs. Discr.)
6.5-8.2	KNN (Fine)	Ensemble Learning (Subs. KNN)	Ensemble Learning (Bagged)	LDA, Ensemble Learning (Subs. Discr., Subs. KNN)
6.5-9.3	Logistic Regression, SVM (Linear, Quadratic, Cubic), KNN (Fine, Weighted), Ensemble Learning (Subs. Discr.)	Ensemble Learning (Bagged)	Ensemble Learning (Bagged)	Naive Bayes (Kernel)
6.5-10	LDA	Ensemble Learning (Subs. KNN)	Ensemble Learning (RUSBoosted)	Logistic Regression, Ensemble Learning (Subs. KNN)
7-7.5	Ensemble Learning (Bagged)	Decision Tree (All), Naive (Gaussian), SVM (Fine, Coarse), KNN (All), Ensemble Learning (Boosted, Subs. KNN)	Naive Bayes (Kernel, Gaussian), Ensemble Learning (Subs. KNN)	Naive Bayes (Kernel)
7-8.2	LDA, Logistic Regression	Naive Bayes (Gaussian), SVM (Quadratic, Cubic), KNN (Fine)	LDA, Logistic Regression	Naive Bayes (Kernel), LDA, Logistic

Table 4.15 Classification performance of energy, entropy, and variance as a feature set (All features together) for Haar wavelet. **Continued.**

Classes	CLASSIFIERS			
	Subject 1	Subject 2	Subject 3	Subject 4
7-9.3	Ensemble Learning (Subs. KNN)	Ensemble Learning (RUSBoosted)	SVM (Linear), Ensemble Learning (Bagged Trees)	Logistic Regression
7-10	Logistic Regression	Ensemble Learning (Bagged)	SVM (Linear)	Logistic Regression
7.5-8.2	Ensemble Learning (Subs. KNN)	KNN (Fine)	Ensemble Learning (Subs. KNN)	KNN (Fine)
7.5-9.3	LDA, Logistic Regression, Ensemble Learning (Subs. KNN)	Ensemble Learning (Bagged)	Ensemble Learning (Subs. KNN)	LDA
7.5-10	SVM (Medium Gaussian), Ensemble Learning (Bagged Trees)	Logistic Regression	SVM (Linear), Ensemble Learning (Subs. Discr.)	Ensemble Learning (Subs. KNN)
8.2-9.3	Ensemble Learning (Subs. Discr., KNN)	Naive Bayes (Gaussian)	Ensemble Learning (RUSBoosted)	LDA, Ensemble Learning (Subs. Discr.)
8.2-10	Logistic Regression	Ensemble Learning (Subs. Discr.)	Logistic Regression	LDA, Ensemble Learning (Subs. Discr.)
9.3-10	LDA, Logistic Regression	Naive Bayes (Kernel)	Ensemble Learning (Bagged)	Ensemble Learning (RUSBoosted)

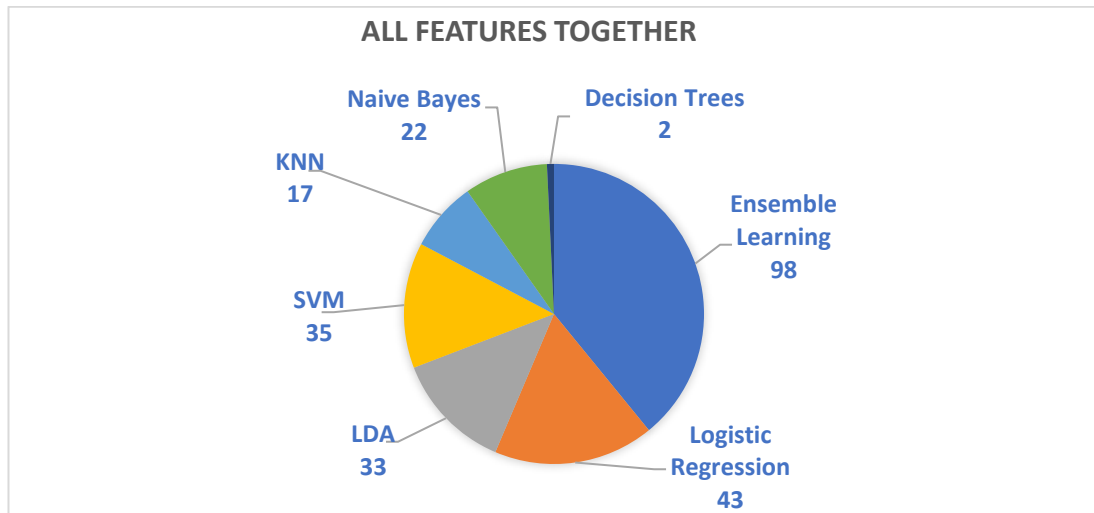


Figure 4.21 Percentage of classifier where the best result is the most often obtained as a result of running the algorithms 250 times in total. (Energy, entropy, and variance as a feature set).

5. CONCLUSION

The study presented in this thesis aimed to achieve significant optimization of cortical visual responses, signal processing methods, and machine learning algorithms, as well as the accuracy and reliability of the superior multi-command SSVEP-based BCI system, which is lacking in the literature. New approaches have been explored using existing methods to develop an accurate, reliable, comfortable SSVEP-based BCI that can offer people with severe motor neuron diseases a communication alternative using attention modulation without requiring neuromuscular activities or eye movements.

In this study, a total of 115 different feature vectors, namely time-domain, frequency domain and time-frequency domain, were extracted from SSVEP (AVI SSVEP Dataset) data obtained through open access. These feature vectors are classified by a total of 25 different classification processes due to the sub-parameters of the seven basic machine learning algorithms. In addition, in the classification step, whether the frequency of the visual stimulus presented to the subjects can be determined with the same frequency in the occipital lobe of the brain was evaluated with multiple, three selected frequencies and binary classification methods. Classification evaluation is presented with 5-fold cross validation method and accuracy values obtained from confusion matrix.

As a result, the following research objectives were achieved in this study:

- When the results of the time domain features are evaluated first, it can be seen that these features give usable (noteworthy) results in the classification of SSVEP signals. However, given the natural structure of the SSVEP signal, it is a fact that the results obtained are not sufficient for a real-time SSVEP-based BCI design, since the time domain properties do not reflect the characteristics of the signal alone.
- When the classification results of the frequency domain features, another feature group, were evaluated alone, satisfactory results were obtained.

Higher accuracy values were obtained in both multi-classification and binary classification compared to time domain.

- And when the last feature group time-frequency domain features are used, using mother DWT functions (Haar, Db2, Sym4, Coif1, Bior3.5, Rbior2.8), SSVEP signals are divided into frequency subbands (delta, theta, alpha, beta, gamma) and energy, entropy and variance values of each band are calculated. In this way, feature vectors were created and feature vectors were used as, both separately and also together. In other words, four different features were used in total. Extracted feature vectors were tested with a binary, multiple and three selected classes classification method to see the relationship between seven different classifiers and each frequency in detail.
- Although multiple classification results seem to be low for all feature groups, there is no study with 7 frequencies (by command) when the literature is searched according to the best knowledge of the author, but high results were obtained compared to studies with 3 and 4 frequencies.
- For stimulation frequency detection in the SSVEP signal, a new form has been proposed that has been proven to be more effective with respect to the use of energy, entropy and variance features than the properties derived from the frequency domain and time-frequency domain. According to this form, instead of the energy, entropy and variance properties used separately, the feature vector, which is all together (All features together), gave better results than the others.
- As a result of the feature selection made with the one-way ANOVA test, it was seen that it reduces the classification accuracy and it is not recommended to use the method in SSVEP signals.
- By conducting detailed research on stimulation frequencies, frequency pairs estimated with the highest accuracy were determined. Although this result showed small differences between the mother wavelet functions, the highest performance was obtained in the frequency pairs in which the difference was generally high (6-10, 6.5-10, 7-10, and 7.5-10).

- In the literature, the performances of the classifier types that were not compared before were evaluated in terms of SSVEP detection and the most successful classifier was found to be the Ensemble Classifier.
- Also, does system performance increase in parallel with the differences between frequencies? Based on this hypothesis, the relationship between frequencies was investigated in pairs. The results obtained confirmed the hypothesis, as can be seen from the figures in Figure 4.17 – 4.22. A decrease in “Sym4” function was observed, where only the lowest performances were obtained (Figure 4.22).
- Finally, the most successful mother wavelet selection was made. Accordingly, it was the Haar wavelet function that gave the best results compared to others.

REFERENCES

1. Griffin E. *A first look at communication theory* (6th edition): McGraw-Hill; 2006.
2. Ruben BD, Stewart LP. *Communication and Human Behavior* (5th edition): Pearson Education; 1998.
3. Vidal JJ. Toward direct brain-computer communication. *Annual Review of Biophysics and Bioengineering*. 1973;2(1): 157-180.
4. Wolpaw JR, Birbaumer N, McFarland DC, Pfurtscheller G, Vaughan TM. Brain-computer interfaces for communication and control. *Clinical Neurophysiology*. 2002;113(6): 767-791.
5. Mak JN, Wolpaw JR. Clinical applications of brain-computer interfaces: current state and future prospects. *IEEE Reviews in Biomedical Engineering*. 2009;2: 187-199.
6. McFarland DJ, Wolpaw JR. Brain-computer interfaces for communication and control. *Communication of ACM*. 2011;54(5): 60-66.
7. Wolpaw JR, Birbaumer N, Heetderks WJ, McFarland DJ, Peckham PH, Schalk G, Donchin E, Quatrano LA, Robinson CJ, Vaughan TM. Brain-computer interface technology: a review of the first international meeting. *IEEE Transactions on Rehabilitation Engineering*. 2000;8: 164-173.
8. Vaughan TM, Heetderks WJ, Trejo LJ, Rymer WZ, Weinrich M, Moore MM, Kubler A, et al. Brain-computer interface technology: a review of the second international meeting. *IEEE Transactions on Neural Systems and Rehabilitation Engineering*. 2003;11(2): 94-109.
9. Schalk G, McFarland DJ, Hinterberger T, Birbaumer N, Wolpaw JR. BCI2000: a general-purpose brain-computer interface (BCI) system. *IEEE Transactions on Biomedical Engineering*. 2004;51(6): 1034-1043.
10. Allison BZ, Wolpaw EW, Wolpaw JR. Brain-computer interface systems: progress and prospects. *Expert Review of Medical Devices*. 2007;4(4): 463-74.
11. Nicolas-Alonso LF, Gomez-Gil J. Brain computer interfaces, a review. *Sensors*. 2012;12(2): 1211-1279.
12. Vidal JJ. Real-time detection of brain events in EEG. *Proceedings of the IEEE*. 1977;65(5): 633-641.
13. Vaid S, Singh P, Kaur C. EEG signal analysis for BCI interface: a review. 2015 *Fifth International Conference on Advanced Computing & Communication Technologies, Haryana*. 2015. p. 143-147.
14. Wolpaw JR, Boulay CB. *Brain-computer interfaces*: Springer; 2010.
15. Graimann B, Allison B, Pfurtscheller G. *Brain-computer interfaces: a gentle introduction*. Brain-computer interfaces: Springer; 2010.
16. Mason SG, Birch GE. A general framework for brain-computer interface design. *IEEE Transactions on Neural Systems and Rehabilitation Engineering*. 2003;11(1): 70-85.
17. Abdulkader SN, Atia A, Mostafa MSM. Brain computer interfacing: applications and challenges. *Egyptian Informatics Journal*. 2015;16(2): 213-230.
18. Ramadan RA, Vasilakos AV. Brain computer interface: control signals review. *Neurocomputing*. 2017;223: 26-44.

19. Abiri R, Borhani S, Sellers E, Jiang Y, Zhao X. A comprehensive review of EEG-based brain-computer interface paradigms. *Journal of Neural Engineering*. 2019;16 011001.
20. Wang YJ, Wang RP, Gao XR, Hong B, Gao S. A practical VEP-based brain-computer interface. *IEEE Transactions on Neural Systems and Rehabilitation Engineering*. 2006;14(2): 234-239.
21. Wang Y, Gao X, Hong B, Jia C, Gao S. Brain-computer interfaces based on visual evoked potentials. *IEEE Engineering in Medicine and Biology Magazine*. 2008;27(5): 64-71.
22. Gao X, Xu D, Cheng M, Gao S. A BCI-based environmental controller for the motion-disabled. *IEEE Transactions on Neural Systems and Rehabilitation Engineering*. 2003;11(2): 137-140.
23. Gao S, Wang Y, Gao X, Hong B. Visual and auditory brain-computer interfaces. *IEEE Transactions on Biomedical Engineering*. 2014; 61(5): 1436–1447.
24. Basar E. *EEG-brain dynamics: relation between EEG and brain evoked potentials*: Brain Lang Elsevier; 1980.
25. Regan D. *Human brain electrophysiology: evoked potentials and evoked magnetic fields in science and medicine*: Elsevier;1989.
26. Regan D. Comparison of transient and steady-state methods. *Annals of the New York Academy of Sciences*. 1982;388: 45–71.
27. Regan D. Some characteristics of average steady-state and transient responses evoked by modulated light. *Electroencephalography and Clinical Neurophysiology*. 1966a;20(3): 238–248.
28. Regan D. An effect of stimulus colour on average steady-state potentials evoked in man. *Nature* 1966b;210: 1056–1057.
29. Sutter EE. The brain response interface-communication through visually induced electrical brain responses. *Journal of Microcomputer Applications*. 1992;15(1): 31-45.
30. Wang Y, Wang YT, Jung TP. Visual stimulus design for high-rate SSVEP BCI. *Electronics Letters*. 2010;46(15): 1057-1058.
31. Mohamed EA, Yusoff MZK, Selman NK, Malik AS. Enhancing EEG signals in brain computer interface using wavelet transform. *International Journal of Information and Electronics Engineering*. 2014;4(3): 234-238.
32. Zhang Z, Li X, Deng Z. A CWT-based SSVEP classification method for brain-computer interface system. *International Conference on Intelligent Control and Information Processing, Dalian*. 2010. p. 43-48.
33. Varuneshkumar M, Anil K, Jaiswal AK. Performance comparison of daubechies, biorthogonal and haar transform for grayscale image compression. *International Journal of Computer Applications*. 2015;126(9): 40-42.
34. Sonia S, David PS, Poulouse J. A comparative study of wavelet-based feature extraction techniques in recognizing isolated spoken words. *International Journal of Signal Processing Systems*. 2013;1(1): 49-53.
35. Gandhi T, Panigrahi KB, Anand S. A comparative study of wavelet families for EEG signal classification. *Neurocomputing*. 2011;74(17): 3051-3057.
36. Kousarrizi MRN, Ghanbari AA, Teshnehlal M, Shorehdeli MA, Gharaviri A. Feature extraction and classification of EEG signals using wavelet transform, SVM and artificial neural networks for brain computer interfaces. *2009 International Joint*

Conference on Bioinformatics, Systems Biology and Intelligent Computing, Shanghai. 2009. p. 352-355.

37. Bian Y, Li H, Zhao L, Yang G, Geng L. Research on steady state visual evoked potentials based on wavelet packet technology for brain-computer interface. *Procedia Engineering*. 2011;15: 2629-2633.

38. Mumtaz M, Afzal M, Mushtaq A. Sensorimotor cortex EEG signal classification using hidden markov models and wavelet decomposition. *IEEE Symposium on Signal Processing and Information Technology (ISSPIT), Louisville, Kentucky*. 2018. p. 375-381.

39. Salyers JB, Dong Y, Gai Y. Continuous wavelet transform for decoding finger movements from single-channel EEG. *IEEE Transactions on Biomedical Engineering*. 2019;66(6): 1588-1597.

40. Poorna SS, Raghav R, Nandan A, Nair GJ. EEG based control - a study using wavelet features. *2018 International Conference on Advances in Computing, Communications and Informatics (ICACCI), Bangalore*. 2018. p. 550-553.

41. Alomari MH, Awada EA, Samaha A, Alkamha K. Wavelet-based feature extraction for the analysis of EEG signals associated with imagined fists and feet movements. *Computer and Information Science*. 2014;7(2): 17-27.

42. Ebrahimpour R, Babakhani K, Mohammad-Noori M. EEG-based motor imagery classification using wavelet coefficients and ensemble classifiers. *The 16th CSI International Symposium on Artificial Intelligence and Signal Processing (AISP 2012), Fars*. 2012. p. 458-463.

43. Sunny S, David Peter S, Jacob KP. Performance analysis of different wavelet families in recognizing speech. *International Journal of Engineering Trends and Technology (IJETT)*. 2013;4(4): 512-517.

44. Wijayanto I, Rizal A, Hadiyoso S. Multilevel wavelet packet entropy and support vector machine for epileptic EEG classification. *4th International Conference on Science and Technology (ICST), Yogyakarta, Indonesia*. 2018. p.1-6.

45. Gupta N, Sood N, Saini I. Statistical feature-based comparison of EEG in meditation for various wavelet. *2018 First International Conference on Secure Cyber Computing and Communication (ICSCCC), India*. 2018. p. 73-77.

46. Xu B, Zhang L, Song A, Wu C, Li W, Zhang D, Xu G, et al. Wavelet transform time-frequency image and convolutional network-based motor imagery EEG classification. *IEEE Access*. 2019;7: 6084-6093.

47. Uyulan C, Erguzel TT. Comparison of wavelet families for mental task classification. *The Journal of Neurobehavioral Sciences*. 2016;3(2): 59-64.

48. Dogra A, Goyal B, Agrawal S. Performance comparison of different wavelet families based on bone vessel fusion. *Asian Journal of Pharmaceutics*. 2016;10(4): S791-S795.

49. Garg G. A signal invariant wavelet function selection algorithm. *Medical & Biological Engineering & Computing*. 2016;54: 629-642.

50. Abo-Zahhad M, Al-Ajlouni AF, Ahmed SM, Schilling RJ. A new algorithm for the compression of ECG signals based on mother wavelet parameterization and best-threshold levels selection. *Digital Signal Processing*. 2013;23(3): 1002-1011.

51. Singh R, Mehta R, Rajpal N. Efficient wavelet families for ECG classification using neural classifiers. *Procedia Computer Science*. 2018;132: 11-21.

52. Hariharan M, Fook CY, Sindhu R, Ilias B, Yaacob S. A comparative study of wavelet families for classification of wrist motions. *Computers & Electrical Engineering*. 2012;38(6): 1798-1807.
53. Duda RO, Hart PE, Stork DG. *Pattern Classification*: John Wiley & Sons;2001.
54. Isler Y, Kuntalp M. Combining classical HRV indices with wavelet entropy measures improves to performance in diagnosing congestive heart failure. *Computers in Biology and Medicine*. 2007;37(10): 1502-1510.
55. Isler Y, Narin A, Ozer M, Perc M. Multi-stage classification of congestive heart failure based on short-term heart rate variability. *Chaos, Solitons & Fractals*. 2019;118: 145-151.
56. Narin A, Isler Y, Ozer M, Perc M. Early prediction of paroxysmal atrial fibrillation based on short-term heart rate variability. *Physica A: Statistical Mechanics and its Applications*. 2018;509: 56-65.
57. Isler Y. Discrimination of Systolic and Diastolic Dysfunctions using Multi-Layer Perceptron in Heart Rate Variability Analysis. *Computers in Biology and Medicine*. 2016;76: 113-119.
58. Khushaba RN, Kodagoda S, Lal S, Dissanayake G. Driver drowsiness classification using fuzzy wavelet-packet-based feature-extraction algorithm. *IEEE Transactions on Biomedical Engineering*. 2011;58(1): 121-131.
59. Devi A, Misal A, Sinha GR. Performance analysis of DWT at different levels for feature extraction of PCG signals. *2013 Annual International Conference on Emerging Research Areas and 2013 International Conference on Microelectronics, Communications and Renewable Energy, Kanjirapally*. 2013. p. 1-5.
60. Hu X, Wang Z, Ren X. Classification of surface EMG signal using relative wavelet packet energy. *Computer Methods and Programs in Biomedicine*. 2005;79(3): 189-195.
61. Wang G, Wang Z, Chen W, Zhuang J. Classification of surface EMG signals using optimal wavelet packet method based on Davies-Bouldin criterion. *Medical & Biological Engineering & Computing*. 2006;44(10): 865-872.
62. Lv Z, Wu X, Li M, Zhang D. A novel eye movement detection algorithm for EOG driven human computer interface. *Pattern Recognition Letters*. 2010;31(9): 1041-1047.
63. Rahman MM, Bhuiyan MIH, Hassan AR. Sleep stage classification using single-channel EOG. *Computers in Biology and Medicine*. 2018;102(2018): 211-220.
64. Rosso OA, Blanco S, Yordanova J, Kolev V, Figliola A, Basar E. Wavelet entropy: a new tool for analysis of short duration brain electrical signals. *Journal of Neuroscience Methods*. 2001;105: 65-75.
65. Goksu H. BCI oriented EEG analysis using log energy entropy of wavelet packets. *Biomedical Signal Processing and Control*. 2018;44(2018): 101-109.
66. Shi L, Jiao Y, Lu B. Differential entropy feature for EEG-based vigilance estimation. *2013 35th Annual International Conference of the IEEE Engineering in Medicine and Biology Society (EMBC), Osaka*. 2013. p. 6627-6630.
67. Bian H, Wang J, Li N, Deng B, Wei X, Li H. Wavelet packet energy entropy analysis of EEG signals evoked by acupuncture. *2010 3rd International Conference on Biomedical Engineering and Informatics, Yantai*. 2010. p. 1089-1093.
68. Zhang Y, Xu P, Cheng K, Yao D. Multivariate synchronization index for frequency recognition of SSVEP-based brain-computer interface. *Journal of Neuroscience Methods*. 2014;221: 32-40.

69. Tarafdar KK, Pradhan BK, Nayak SK, Khasnobish A, Chakravarty S, Ray SS, Pal K. Data mining based approach to study the effect of consumption of caffeinated coffee on the generation of the steady-state visual evoked potential signals. *Computers in Biology and Medicine*. 2019;115: 103526.
70. Hazarika J, Kant P, Dasgupta R, Laskar SH. Neural modulation in action video game players during inhibitory control function: an EEG study using discrete wavelet transform. *Biomedical Signal Processing and Control*. 2018;45(2018): 144-150.
71. Sayilgan E, Isler Y. Medical devices sector in medical industry 4.0. *2017 Medical Technologies National Congress (TIPTEKNO), Trabzon*. 2017. p. 1-4.
72. Russell S, Norvig P. *Artificial intelligence—a modern approach* (3rd edition): Prentice Hall; 2018.
73. Mudgal SK, Sharma SK, Chaturvedi J, Sharma A. Brain computer interface advancement in neurosciences: applications and issues. *Interdisciplinary Neurosurgery*. 2020;20(2020): 100694.
74. Pasqualotto E, Federici S, Belardinelli MO. Toward functioning and usable brain-computer interfaces (BCIs): a literature review. *Disability and Rehabilitation: Assistive Technology*. 2012;7(2): 89-103.
75. Parent A, Carpenter MB. *Carpenter's human neuroanatomy*: Williams & Wilkins; 1995.
76. Ackerman S. *Discovering the brain*: National Academy Press; 1992.
77. Bigos KL, Hariri A, Weinberger D. *Neuroimaging genetics: principles and practices*: Oxford University Press; 2015.
78. Authored by: Boundless.com. *Functional systems of the cerebral cortex*. Available from: <https://courses.lumenlearning.com/boundless-ap/chapter/functional-systems-of-the-cerebral-cortex/> [Accessed 15th March 2020].
79. Başar E, Güntekin B. Chapter 19 - Review of delta, theta, alpha, beta, and gamma response oscillations in neuropsychiatric disorders. *Supplements to Clinical Neurophysiology*. 2013;62: 303-341.
80. Lotte F. *Study of electroencephalographic signal processing and classification techniques towards the use of brain-computer interfaces in virtual reality applications*. Human-Computer Interaction [cs.HC]. INSA de Rennes, 2008.
81. Scherer R, Schloegl A, Lee F, Bischof H, Jansa J, Pfurtscheller G. The self-paced graz brain-computer interface: methods and applications. *Computational Intelligence and Neuroscience*. 2007;2007: 79826.
82. Waziri A, Claassen AJ, Stuart RM, Arif H, Schmidt JM, Mayer SA, Badjatia N, et al. Intracortical electroencephalography in acute brain injury. *Annals of Neurology*. 2009;66(3): 366–77.
83. Lauer RT, Peckham PH, Kilgore KL, Heetderks WJ. Applications of cortical signals to neuroprosthetic control: A critical review. *IEEE Transactions on Neural Systems and Rehabilitation Engineering*. 2000;8: 205–208.
84. Chao ZC, Nagasaka Y, Fujii N. Long-term asynchronous decoding of arm motion using electrocorticographic signals in monkeys. *Frontiers in Neuroengineering*. 2010;3.
85. Baillet S, Mosher JC, Leahy RM. Electromagnetic brain mapping. *IEEE Signal Process. Mag.* 2001;18: 14–30.
86. Kauhanen L, Nykopp T, Lehtonen J, Jylanki P, Heikkonen J, Rantanen P, Alaranta H, Sams M. EEG and MEG brain-computer interface for tetraplegic

- patients. *IEEE Transactions on Neural Systems and Rehabilitation Engineering*. 2006;14: 190–193.
87. Weiskopf N, Mathiak K, Bock SW, Scharnowski F, Veit R, Grodd W, Goebel R, Birbaumer N. Principles of a brain-computer interface (BCI) based on real-time functional magnetic resonance imaging (fMRI). *IEEE Transactions on Biomedical Engineering*. 2004;51: 966–970.
 88. Shirley C, Ward T, Markham C, McDarby G. On the suitability of near-infrared (NIR) systems for next-generation brain-computer interfaces. *Physiological Measurement*. 2004;25: 815.
 89. Sitaram R, Zhang H, Guan C, Thulasidas M, Hoshi Y, Ishikawa A, Shimizu K, Birbaumer N. Temporal classification of multichannel near-infrared spectroscopy signals of motor imagery for developing a brain-computer interface. *Neuroimage*. 2007;34: 1416–1427.
 90. Chugani HT, Phelps ME, Mazziotta JC. Positron emission tomography study of human brain functional development. *Annals of Neurology*. 1987;22: 487–497.
 91. Caton Richard MD. The electrical currents of the brain. *British Medical Journal*. 1875;2: 278.
 92. Haas LF. Hans Berger (1873-1941), Richard Caton (1842-1926), and electroencephalography. *Journal of Neurology, Neurosurgery & Psychiatry*. 2003;74(1): 9.
 93. Jasper H. The ten-twenty electrode system of the international federation. *Electroencephalography and Clinical Neurophysiology*. 1958;10(2): 371–375.
 94. Garcia Molina G. *Direct Brain-Computer Communication Through Scalp recorded EEG Signals*. PhD Thesis, Swiss Federal Institute of Technology, Lausanne. 2014.
 95. Gursel Ozmen N, Durmus E, Sadreddini Z. Can music classification be an alternative for brain computer interface applications. *Uludağ University Journal of The Faculty of Engineering*. 2017;22(2): 11-22.
 96. Sadreddini Z, Durmuş E, Özmen NG. EEG verilerinden farklı müzik türü ve zihinsel görevlerin ayırt edilmesi. *Akıllı Sistemlerde Yenilik ve Uygulamaları (ASYU)*, 9-10 Ekim 2014, İzmir, Türkiye. 2014. p. 44-48.
 97. Wang M, Daly I, Allison BZ, Jin J, Zhang Y, Chen L, Wang X. A new hybrid BCI paradigm based on P300 and SSVEP. *Journal of Neuroscience Methods*. 2015;244(2015): 16-25.
 98. Hong KS, Khan MJ. Hybrid brain-computer interface techniques for improved classification accuracy and increased number of commands: a review. *Frontiers in Neurorobotics*. 2017;11(35).
 99. Hoffman LD, Polich J. P300, handedness, and corpus callosal size: gender, modality, and task. *International Journal of Psychophysiology*. 1999;31(2): 163-174.
 100. Takano K, Komatsu T, Hata N, Nakajima Y, Kansaku K. Visual stimuli for the P300 brain-computer interface: A comparison of white/gray and green/blue flicker matrices. *Clinical Neurophysiology*. 2009;120: 1562–1566.
 101. Vialatte FB, Maurice M, Dauwels J, Cichocki A. Steady-state visually evoked potentials: focus on essential paradigms and future perspectives. *Progress in Neurobiology*. 2010;90(4): 418-438.
 102. Bin G, Gao X, Wang Y, Hong B, Gao S. VEP-based brain-computer interfaces: time, frequency, and code modulations. *IEEE Computational Intelligence Magazine*. 2009;4(4): 22-26.

103. Liu Y, Wei Q, Lu Z. A multi-target brain-computer interface based on code modulated visual evoked potentials. *PLoS ONE*. 2018;13(8): e0202478.
104. Middendorf M, McMillan G, Calhoun G, Jones KS. Brain-computer interfaces based on the steady-state visual-evoked response. *IEEE Transactions on Rehabilitation Engineering*. 2000;8(2): 211-214.
105. Norcia AM, Appelbaum LG, Ales JM, Cottareau BR, Rossion B. The steady-state visual evoked potential in vision research: A review. *Journal of Vision*. 2015;15(6): 1-46.
106. Allison BZ, McFarland DJ, Schalk G, Zheng SD, Jackson MM, Wolpaw JR. Towards an independent brain-computer interface using steady state visual evoked potentials. *Clinical Neurophysiology*. 2008;119(2): 399-408.
107. Friman O, Volosyak I, Graser A. Multiple channel detection of steady-state visual evoked potentials for brain-computer interfaces. *IEEE Transactions on Biomedical Engineering*. 2007;54(4): 742-750.
108. Muller-Putz GR, Scherer R, Neuper C, Pfurtscheller G. Steady-state somatosensory evoked potentials: suitable brain signals for brain-computer interfaces?. *IEEE Transactions on Neural Systems and Rehabilitation Engineering*. 2006;14(1): 30-37.
109. Muller-Putz GR, Pfurtscheller G. Control of an electrical prosthesis with an SSVEP-based BCI. *IEEE Transactions on Biomedical Engineering*. 2008;55(1): 361-364.
110. Singla R. *SSVEP-based BCIs, Evolving BCI Therapy - Engaging Brain State Dynamics*: IntechOpen; 2018.
111. Bakardjian H. *Optimization of steady state visual responses for robust brain computer interface*. Doctor of Philosophy. Department of Electronic and Information Engineering. Tokyo University of Agriculture and Technology. 2011.
112. Allison BZ, Luth T, Valbuena D, Teymourian A, Volosyak I, Graser A. BCI demographics: how many (and what kinds of) people can use an SSVEP BCI?. *IEEE Transactions on Neural Systems and Rehabilitation Engineering*. 2010;18(2): 107-116.
113. Volosyak I, Valbuena D, Lüth T, Malechka T, Graser A. BCI Demographics II: how many (and what kinds of) people can use a high-frequency SSVEP BCI?. *IEEE Transactions on Neural Systems and Rehabilitation Engineering*. 2011;19(3): 232-239.
114. Kuś R, Duszyk A, Milanowski P, Łabęcki M, Bierzyńska M, Radzikowska Z, et al. On the quantification of SSVEP frequency responses in human EEG in realistic BCI conditions. *PLoS ONE*. 2013;8(10): e77536.
115. Li B. Effectiveness of flickering video clips as stimuli for SSVEP-based BCIs. *TENCON 2015 - 2015 IEEE Region 10 Conference, Macao*. 2015. p. 1-4.
116. Singla R, Khosla A, Jha R. Influence of stimuli colour in SSVEP-based BCI wheelchair control using support vector machines. *Journal of Medical Engineering & Technology*. 2014;38(3): 125-134.
117. Diez PF, Müller SMT, Mut VA, Laciár E, Avila E, Bastos-Filho TF, Sarcinelli-Filho M. Commanding a robotic wheelchair with a high-frequency steady-state visual evoked potential based brain-computer interface. *Medical Engineering & Physics*. 2013;35(8): 1155-1164.

118. Shao L, Zhang L, Belkacem AN, Zhang Y, Chen X, Li J, Liu H. EEG-controlled wall-crawling cleaning robot using SSVEP-based brain-computer interface. *Journal of Healthcare Engineering*. 2020;6968713.
119. Lin Z, Zhang C, Wu W, Gao X. Frequency recognition based on canonical correlation analysis for SSVEP-based BCIs. *IEEE Transactions on Biomedical Engineering*. 2007;54(6): 1172-1176.
120. Kotlewska I, Wójcik MJ, Nowicka MM, Marczak K, Nowicka A. Present and past selves: a steady-state visual evoked potentials approach to self-face processing. *Scientific Reports*. 2017;7(16438).
121. Chen X, Wang Y, Nakanishi M, Gao X, Jung T, Gao S. High-speed spelling with a noninvasive brain-computer interface. *Proceedings of the National Academy of Sciences of the United States of America*. 2015;112(44): E6058-E6067.
122. Chiang K, Wei C, Nakanishi M, Jung T. Cross-Subject Transfer Learning Improves the Practicality of Real-World Applications of Brain-Computer Interfaces. *2019 9th International IEEE/EMBS Conference on Neural Engineering (NER), San Francisco*. 2019. p. 424-427.
123. Zhu D, Bieger J, Molina GG, Aarts RM. A survey of stimulation methods used in SSVEP-based BCIs. *Computational Intelligence and Neuroscience*. 2010;2010: 702357.
124. Bieger J, Garcia-Molina G, Zhu D. Effects of stimulation properties in steady-state visual evoked potential based brain-computer interfaces. *2010 Annual International Conference of the IEEE Engineering in Medicine and Biology Engineering in Medicine and Biology Society (EMBC)*. 2010. p. 3345-3348.
125. Wittevrongel B, Van Hulle MM. Frequency- and phase encoded SSVEP using spatiotemporal beamforming. *PLoS ONE*. 2016;11(8): e0159988.
126. <https://www.britannica.com/science/human-eye/Extraocular-muscles>
127. National Eye Institute. *Diagram of the Eye*. Available from: <http://www.nei.nih.gov/health/eyediagram/eyeimages3.asp>. [Accessed 3rd October 2019].
128. Wu CH. *A distance adaptable brain-computer interface based on steady-state visual evoked potential*. Degree of Doctor of Philosophy in Biomedical Engineering, Biomedical Engineering Department University of Strathclyde Glasgow, UK. 2017.
129. Zemon V, Gordon J. Luminance-contrast mechanisms in humans: visual evoked potentials and a nonlinear model. *Vision research*. 2006;46(24): 4163–4180.
130. Nakanishi M, Wang Y, Wang YT, Mitsukura Y, Jung TP. Generating visual flickers for eliciting robust steady-state visual evoked potentials at flexible frequencies using monitor refresh rate. *PLoS ONE*. 2014;9(6): e99235.
131. Wu Z, Lai Y, Xia Y, Wu D, Yao D. Stimulator selection in SSVEP-based BCI. *Medical Engineering and Physics*. 2008;30: 1079–1088.
132. Bashashati A, Fatourehchi M. A survey of signal processing algorithms in brain-computer interfaces based on electrical brain signals. *Journal of Neural Engineering*. 2007;4: 32-57.
133. Khosla A, Khandnor P, Chand T. A comparative analysis of signal processing and classification methods for different applications based on EEG signals. *Biocybernetics and Biomedical Engineering*. 2020;40(2): 649-690.
134. Liu Q, Chen K, Qingsong A, Xie S. Review: recent development of signal processing algorithms for SSVEP-based brain computer interfaces. *Journal of Medical and Biological Engineering*. 2014;34(4): 299-309.

135. Makeig S, Kothe C, Mullen T, Bigdely-Shamlo N, Zhang Z, Kreutz-Delgado K. Evolving signal processing for brain–computer interfaces. *Proceedings of the IEEE*. 2012;100(Special Centennial Issue): 1567-1584.
136. Lotte F. *A Tutorial on EEG Signal-processing Techniques for Mental-state Recognition in Brain–Computer Interfaces*: Springer; 2014.
137. Oikonomou VP, Liaros G, Georgiadis K, Chatzilari E, Adam K, Nikolopoulos S, Kompatsiaris I. Comparative Evaluation of State-of-the-Art Algorithms for SSVEP-Based BCIs. *ArXiv*. 2016; 1-33.
138. Başar E, Demilrap T, Schürmann M, Başar-Eroğlu C, Ademoğlu A. Oscillatory brain dynamics, wavelet analysis, and cognition. *Brain Lang*. 1999;66: 146-183.
139. Lotte F, Bougrain L, Cichocki A, Clerc M, Congedo M, Rakotomamonjy A, Yger F. A review of classification algorithms for EEG-based brain-computer interfaces: a 10-year update. *Journal of Neural Engineering*. 2018;15(3): 55.
140. Herman P, Prasad G, McGinnity TM, Coyle D. Comparative analysis of spectral approaches to feature extraction for EEG-based motor imagery classification. *IEEE Transactions on Neural Systems and Rehabilitation Engineering*. 2008;16(4): 317-326.
141. Hoodgar M, Mehrani M, Amin M, Forootan F. Proposing an effective feature extraction model for EEG signals to enhance quality of hand's motion detection. *Journal of Academic and Applied Studies*. 2013;3(2): 1-19.
142. Sun S, Zhou J. A review of adaptive feature extraction and classification methods for EEG-based brain-computer interfaces. *2014 International Joint Conference on Neural Networks (IJCNN), Beijing*. 2014. p. 1746-1753.
143. Liuand H, Motoda H. *Feature selection for knowledge discovery and data mining*: Kluwer Academic Publishers; 1998.
144. Alpaydin E. *Introduction to Machine Learning*: MIT Press; 2004.
145. James G, Witten D, Hastie T, Tibshirani R. *An Introduction to Statistical Learning*: Springer; 2013.
146. Jung Y, Hu J. A k-fold averaging cross-validation procedure. *Journal of Nonparametric Statistics*. 2015;27: 1-13.
147. Jiao Y, Du P. Performance measures in evaluating machine learning based bioinformatics predictors for classifications. *Quantitative Biology*. 2016;4(4): 320–330.
148. Narin A, İşler Y, Özer M. Konjestif kalp yetmezliği teşhisinde kullanılan çapraz doğrulama yöntemlerinin sınıflandırıcı performanslarının belirlenmesine olan etkilerinin karşılaştırılması. *DEÜ Mühendislik Fakültesi Mühendislik Bilimleri Dergisi*. 2014;16(48): 1-8.
149. Vilic A. AVI steady-state visual evoked potential (SSVEP) signals dataset 2013. Available from: <https://www.setzner.com/avi-ssvep-dataset/>. [Accessed 15th August 2018].
150. Geethanjali P, Mohan YK, Sen J. Time domain feature extraction and classification of EEG data for brain computer interface. *2012 9th International Conference on Fuzzy Systems and Knowledge Discovery, Sichuan*. 2012. p. 1136-1139.
151. Boubchir L, Daachi B, Pangracious V. A review of feature extraction for EEG epileptic seizure detection and classification. *2017 40th International Conference on Telecommunications and Signal Processing (TSP), Barcelona*. 2017. p. 456-460.

152. Sayilgan E, Yuce YK, Isler Y. Prediction of evoking frequency from steady-state visual evoked frequency. *Natural and Engineering Sciences*. 2019;4(3): 91-99.
153. Durmuş E, Sadreddini Z, Gürsel Özmen N. Beyin-bilgisayar arayüzü sistemleri için uygun öznitelik ve sınıflandırıcı seçimi. *Otomatik Kontrol Ulusal Toplantısı (TOK), Kocaeli, Türkiye*. 2014. p. 651-656.
154. Sayilgan E, Yuce YK, Isler Y. Determining gaze information from steady-state visually-evoked potentials. *Karaelmas Science and Engineering Journal*. ACCEPTED. 2020.
155. Mallat SG. A theory for multiresolution signal decomposition: the wavelet representation. *IEEE Transactions on Pattern Analysis and Machine Intelligence*. 1989;11(7): 674-693.
156. Akansu N, Tazebay MV, Medley MJ, Das PK. Wavelet and subband transforms: fundamentals and communication applications. *IEEE Communications Magazine*. 1997;35(12): 104-115.
157. Abbate A, Decusatis CM, Das PK. *Wavelets and subbands: fundamentals and application*: Birkhäuser Boston; 1995.
158. Chen D, Wan S, Xiang J, Bao FS. A high-performance seizure detection algorithm based on Discrete Wavelet Transform (DWT) and EEG. *PLoS ONE*. 2017;12(3): e0173138.
159. Gao Z, Li S, Cai Q, Dang W, Yang Y, Mu C, Hui P. Relative wavelet entropy complex network for improving EEG-based fatigue driving classification. *IEEE Transactions on Instrumentation and Measurement*. 2019;68(7): 2491-2497.
160. Amin HU, Malik AS, Ahmad RF, Badruddinb N, Kamel N, Hussain M, Chooi WT. Feature extraction and classification for EEG signals using wavelet transform and machine learning techniques. *Australasian Physical & Engineering Sciences in Medicine*. 2015;38(2015): 139–149.
161. Al-Fahoum AS, Al-Fraihat AA. Methods of EEG signal features extraction using linear analysis in frequency and time-frequency domains. *ISRN Neuroscience*. 2014;7(730218).
162. Heidari H, Einalou Z. SSVEP extraction applying wavelet transform and decision tree with Bayes classification. *International Clinical Neuroscience Journal (ICNSJ)*. 2017;4(3): 91-97.
163. Sayilgan E, Yuce YK, Isler Y. Evaluation of wavelet features selected via statistical evidence from steady-state visually-evoked potentials to predict the stimulating frequency. *Gazi University Journal of Engineering and Architecture*. 2020;Accepted.
164. IBM. *IBM SPSS Statistics*. Available from: <https://www.ibm.com/tr-tr/products/spss-statistics>. [Accessed 2nd September 2018].
165. Lotte F, Congedo M, Lecuyer A, Lamarche F, Arnaldi B. A review of classification algorithms for EEG-based brain–computer interfaces. *Journal of Neural Engineering*. 2007;4(2): R1-R13.
166. Dey A. Machine learning algorithms: a review. *International Journal of Computer Science and Information Technologies*. 2016;7(3): 1174-1179.
167. Sayilgan E, Yuce YK, Isler Y. Durağan durum görsel uyaran potansiyellerinden fourier dönüşümü ile üç farklı frekansın kestirimi. *Düzce Üniversitesi Bilim ve Teknoloji Dergisi*. 2020;Accepted.
168. Sayilgan E, Yuce YK, Isler Y. Determining seven different brain-computer interface commands using fourier transform and machine learning methods from

- SSVEP. *2nd International Conference of Applied Sciences, Engineering and Mathematics (IBU-ICASEM 2020)*, June 4-6, Skopje/North, Macedonia. 2020.
169. Rokach L. Ensemble-based classifiers. *Artificial Intelligence Review*. 2010;33: 1–39.
170. Polikar R. Ensemble learning. *Scholarpedia*. 2009;4(1): 2776.
171. Necati Demir. *Ensemble methods: Elegant techniques to produce improved machine learning results*. Available from: <https://www.toptal.com/machine-learning/ensemble-methods-machine-learning>. [Accessed 3rd May 2019].
172. MATLAB and Machine Learning and Deep Learning Toolbox Release 2019a. The MathWorks. Inc., Natick, Massachusetts, United States.
173. Sharma K, Kar S. Extracting multiple commands from a single SSVEP flicker using eye-accommodation. *Biocybernetics and Biomedical Engineering*. 2019;39(3): 914-922.
174. Oojha MK, Rajotiya RN, Tyagi N. Frequency detection of single channel steady state visual evoked potential using canonical correlation analysis approach. *ICRAMSTEL-2019 at: JIMS Engineering Management Technical Campus, Greater Noida*. 2019.
175. Diez PF, Mut VA, Avila Perona EM, Leber EL. Asynchronous BCI control using high-frequency SSVEP. *Journal of NeuroEngineering and Rehabilitation*. 2011;8: 39.
176. Nakanishi M, Wang Y, Wang YT, Jung TP. A comparison study of canonical correlation analysisbased methods for detecting steady-state visual evoked potentials. *PLoS ONE*. 2015;10(10): e0140703.
177. Sayilgan E, Yuce YK, Isler Y. Discriminating the gaze among five boxes from EEG signals using machine learning. *International Conference on Artificial Intelligence towards Industry 4.0 (ICAI4.0)*, 14-16 November 2019, Iskenderun, Hatay, Turkey. 2019. p. 391-398.
178. Sayilgan E, Yuce YK, Isler Y. Classification of hand movements from EEG signals using machine learning. *Innovations in Intelligent Systems and Applications Conference, 31 October-2 November 2019, Izmir, Turkey*. 2019.
179. Sayilgan E, Yuce YK, Isler Y. Evaluation of mother wavelets and wavelet-based features on steady-state visually-evoked potentials for triple-command brain-computer interfaces. *Biomedical Signal Processing and Control*. 2020;Under Review.

CURRICULUM VITAE

Ebru Sayilgan

Education:

- 2016 – 2020 **Izmir Katip Celebi University**
PhD in Biomedical Technologies
- 2013 – 2016 **Karadeniz Technical University**
M.Sc. in Mechanical Engineering
- 2008 – 2013 **Karadeniz Technical University**
B.Sc. in Mechanical Engineering



Projects:

- 2017 - 2018 TUBITAK 1512 - 2170241 nolu TEYDEB BIGG “Prosthetic Hand Design with Electronic Control Adjustable to Amputation Degree”, R&D Engineer, (Ege University – Science and Technology Centre).
- 2015 - 2016 TUBITAK 1512 - 2140021 nolu TEYDEB BIGG “Chemical Tempered High Mechanical Strength Glasses with Ion Exchange Process”, R&D Enginner, (Yildiz Technical University - TechnoPark).

List of Journal Papers:

1. **Sayilgan E.**, Yuce Y.K., Isler Y., “Investigating the Effect of Flickering Frequency in Steady-State Visually-Evoked Potentials on Dichotomic Brain-Computer Interfaces”, Computers in Biology and Medicine, SUBMITTED, 2020, (SCI).
2. **Sayilgan E.**, Yuce Y.K., Isler Y., “Evaluation of Mother Wavelets and Wavelet-Based Features on Steady-State Visually-Evoked Potentials for Triple-Command Brain-Computer Interfaces”, Biomedical Signal Processing and Control, UNDER REVIEW, 2020, (SCI).
3. **Sayilgan E.**, Yuce Y.K., and Isler Y., “Evaluation of Wavelet Features from Different Mother Wavelets on Steady-State Visually-Evoked Potentials to Predict the Stimulating Frequency”, Gazi University Journal of Engineering and Architecture, ACCEPTED, 2020, (SCI-E, TR-INDEX).

4. **Sayilgan E.**, Yuce Y.K., Isler Y., “Estimation of Three Distinct Commands Using Fourier Transform of Steady-State Visual-Evoked Potentials”, *Düzce University Journal of Science and Technology*, ACCEPTED, 2020, (TR-INDEX).
5. **Sayilgan E.**, Yuce Y.K., Isler Y., Determining Gaze Information from Steady-State Visually-Evoked Potentials, *Karaelmas Science and Engineering Journal*, ACCEPTED, 2020, (TR-INDEX).
6. **Sayilgan E.**, Yuce Y.K., Isler Y., “Prediction of Evoking Frequency from Steady-State Visual Evoked Frequency”, *Natural and Engineering Sciences*, 4(3), 91-99, 2019, (INTERNATIONAL OTHER INDEX).
7. Gürsel Özmen N., **Durmus E.**, Sadreddini Z. “Can Music Classification be an Alternative for Brain Computer Interface Applications?”, *Uludağ University Journal of The Faculty of Engineering*, 22(2), 11-22, 2017, (TR-INDEX).

List of Conference Proceedings:

1. **Sayilgan E.**, Yuce Y.K., Isler Y., “Determining Seven Different Brain-Computer Interface Commands using Fourier Transform and Machine Learning Methods from SSVEP”, 2nd International Conference of Applied Sciences, Engineering and Mathematics (IBU-ICASEM 2020), June 4-6, Skopje/North Macedonia, 2020.
2. **Sayilgan E.**, Yuce Y.K., Isler Y., “Discriminating the Gaze among Five Boxes from EEG Signals using Machine Learning”, *International Conference on Artificial Intelligence towards Industry 4.0 (ICAII4.0)*, Conference Proceedings Book (ISBN: 9978-605-68970-3-0), 391-398, Iskenderun / Hatay / Turkey, 14-16 November 2019.
3. **Sayilgan E.**, Yuce Y.K., Isler Y., “Prediction of Evoking Frequency from Steady-State Visual Evoked Frequency”, *International Conference on Artificial Intelligence towards Industry 4.0 (ICAII4.0)*, Conference Proceedings Book (ISBN: 978-605-68970-3-0), 366-373, Iskenderun / Hatay / Turkey, 14-16 November 2019.
4. Karabiber Ö., **Sayilgan E.**, Isler Y., “Arrhythmia Classification Using Fuzzy C-Means Clustering”, *International Conference of Applied Sciences, Engineering and Mathematics (IBU-ICASEM 2017)*, May 5-7, Struga-Ohrid/Macedonia, Book of Abstracts (ISBN: 978-608-65137-5-7), 98, 2017.
5. **Sayilgan E.**, Yuce Y.K., Isler Y., “Classification of Hand Movements from EEG Signals using Machine Learning”, *Innovations in Intelligent Systems and Applications Conference (ASYU)*, Izmir, Turkey, 31 October-2 November (2019).
6. **Sayilgan E.**, Sahin S., “Feature Extraction of ECG Signals using NI LabVIEW Biomedical Workbench and Classification with Artificial Neural Network”, *Innovations in Intelligent Systems and Applications Conference (ASYU)*, Antalya, Turkey, (2017).
7. **Sayilgan E.**, Isler Y., “Medical Devices Sector in Medical Industry 4.0”, *Medical Technologies Congress (TIPTEKNO)*, Trabzon, Turkey, (2017).

8. **Sayilgan E.**, Karabiber O., Isler Y., “Use of Clustering Algorithms and Extreme Learning Machine in Determining Arrhythmia Types”, 25th IEEE Signal Processing and Communications Applications Conference (SIU), Antalya, Turkey, (2017).
9. **Durmus E.**, Gürsel Ozmen N., “Selection of Proper Electrodes and Improving Performance in Brain Computer Interfaces”, 23rd IEEE Signal Processing and Communications Applications Conference (SIU), Malatya, Turkey, (2015).
10. **Durmus E.**, Sadreddini Z., Gürsel Ozmen N., “Selection of Appropriate Feature and Classifier for Brain Computer Interface Systems”, International Federation of Automatic Control (TOK), Kocaeli, Turkey, (2014).
11. Sadreddini Z., **Durmus E.**, Gürsel Ozmen N., “Distinctive Music Type and Mental Tasks from EEG Data”, Innovations in Intelligent Systems and Applications Conference (ASYU), Izmir, Turkey, (2014).